On Motor Learning and Force Fields: Encoding and Decoding

A DISSERTATION
SUBMITTED TO THE FACULTY OF THE GRADUATE SCHOOL
OF THE UNIVERSITY OF MINNESOTA
BY

Rahul Gupta

IN PARTIAL FULFILLMENT OF THE REQUIREMENTS
FOR THE DEGREE OF
Doctor Of Philosophy

Professor James Ashe (Adviser)

November, 2008

Acknowledgements

I am grateful to my adviser Dr James Ashe for his time, encouragement and support throughout my graduate career. I would also like to thank the members of the Brain Sciences Center, especially Dean Evans for his help with everything and anything related to the monkeys and Dale Boeff for his help with the hardware set-up.

This research was supported by a Merit Review grant from the Department of Veterans Affairs, NS42278 from the NIH and partially by a Doctoral Dissertation Fellowship from the Graduate School, University of Minnesota.

On Motor Learning and Force Fields: Encoding and Decoding

by Rahul Gupta

ABSTRACT

The control of motor behavior is essential for us to interact with our environment. We possess an almost infinite variety of motor behaviors and acquire new ones with great facility. How the brain can control such a great number of behaviors and easily learn new ones remains something of a mystery. A recent theory based on the concept of 'internal models' of motor behavior has been proposed as a unifying approach to the understanding of motor control and learning. In this theory, internal models are defined as models of the motor periphery of an organism and the surrounding contextual environment, such that they can predict the sensory consequences of an intended movement and the forces required to generate that movement.

While much of the data from behavioral experiments in human subjects can be interpreted in the context of internal models, as yet we do not have a clear understanding of the neural mechanisms that might support such models. In this dissertation my primary focus is on the neural mechanisms of the learning of internal models and on the neural processes that enable us to rapidly switch from one model to another. To study this, I trained monkey subjects to learn to adapt their arm movements in the presence of a perturbing force field and recorded neural signals (single cell and local field potentials) from the motor cortex and the dorsal premotor cortex during the learning. We then studied how the subjects adapted when a force field in the opposite direction was introduced and the neural basis of this adaptation. This last manipulation was meant to simulate how we can acquire multiple internal models of behavior and dynamically switch between them. Our main result was that internal models are learned through gradual changes in the relative weighting of the motor parameters (direction, position, velocity and force) in single cells. In addition switching between models was accompanied by rapid and dramatic shifts in the parameter weighting. Interestingly, changes in the direction tuning of single cells seemed to have little to do with internal models. We also found systematic changes in the local field potentials associated with the models, though these data are somewhat preliminary. Finally, we did not find large differences between the neural activity in motor cortex and dorsal premotor cortex during learning or model switching.

In addition to the main experiment outlined above we performed two ancillary studies: one on the acquisition of multiple internal models in human subjects and the other in which

we applied a decoding algorithm to the neural data collected in the primary experiment to predict the end point forces exerted by the monkey subjects.

Table of Contents

Acknowledgements i

Abstract ii

List of Tables vii

List of Figures viii

1 Introduction 1

1.1 The problem . . . 1
1.2 Historical experimental approaches to motor control . . . 2
1.3 Behavioral paradigms to study motor learning . . . 4
1.3.1 Learning of visuomotor perturbations . . . 4
1.3.2 Learning of force perturbations . . . 5
1.4 Internal model theory of motor learning . . . 8
1.5 Behavioral studies of sensorimotor interference and consolidation: Arm movements in force fields . . . 11
1.6 Acquisition of multiple internal models . . . 14
1.7 Neurophysiological studies of force-field learning . . . 17
1.8 Comments on our experiments . . . 19
1.9 Summary . . . 21

2 Experimental Methods 22

2.1 Behavioral experiment with human subjects . . . 22
2.1.1 Robotic manipulandum . . . 22
2.1.2 Experimental set-up . . . 22
2.1.3 Task design . . . 23
2.1.4 Generation of the force field . . . 24
2.1.5 Data analysis . . . 25

2.2 Neural recordings in monkeys . . . 25
2.2.1 Basic task design . . . 26
2.2.2 Design of the force fields . . . 27
2.2.3 Sequence of the force fields during neural recordings . . . 28
2.2.4 Implantation of chronic electrode arrays . . . 29
2.2.5 Data collection . . . 30
2.2.6 Data pre-processing . . . 31

3 Lack of Adaptation to Random Conflicting Gaussian-Distributed Force Fields 34
3.1 Results . . . 35
3.1.1 Time course of adaptation . . . 35
3.1.2 Variation of hand-path errors with the applied forces . . . 37
3.1.3 Another independent measure of performance . . . 38
3.2 Discussion . . . 39

4 Neural correlates of force-field learning in single cells 44
4.1 Evidence of adaptation from the behavior . . . 45
4.2 Rotation of the preferred directions of muscles . . . 49
4.3 Direction tuning of single cells . . . 52
4.3.1 Task-related cells . . . 52
4.3.2 Direction tuning: Variation in the number of tuned cells across sessions 56
4.3.3 Direction tuning: Changes in the quality of fit . . . 56
4.3.4 Comparison of tuning between different force fields . . . 58
4.4 Changes in the relative weightings of kinematic and kinetic variables related to changes in force fields . . . 62
4.4.1 Learning modulates the number of cells actively engaged in the task 63
4.4.2 Adaptive changes in the relative weights of different task variables in different force conditions . . . 64
4.4.3 Time lag with the best R^2 of the regression . . . 66
4.5 Summary . . . 67

5 Neural Correlates of Force-field Learning in Local Field Potentials 70
5.1 Characteristics of the LFP power spectra . . . 71
5.2 Characteristics of the LFP coherence spectra . . . 72
5.3 Correlates of learning and interference in the LFP power . . . 76

6 Off-line Decoding of End-Point Forces Using Neural Ensembles: Application to a Brain-Machine Interface **83**

6.1 Analysis methods . . . 84

6.1.1 Prediction algorithms . . . 85

6.1.2 Performance evaluation . . . 87

6.2 Results . . . 87

6.2.1 Optimum lag and filter width . . . 89

6.2.2 Effect of the number of cells . . . 90

6.2.3 Predictive performance of M1 versus PMd . . . 91

6.2.4 Generalization to novel force-fields . . . 92

6.2.5 Simultaneous prediction of the trajectory and the forces . . . 94

6.2.6 Is it really kinetics or just scaled kinematics? . . . 96

6.3 Discussion . . . 98

6.3.1 Decoding performance and choice of parameters . . . 98

6.3.2 Decoding using different brain areas . . . 99

6.3.3 Generalizability of the decoding algorithms . . . 100

7 Discussion **102**

7.1 Methodological issues . . . 102

7.2 Behavioral evidence of learning and interference . . . 104

7.3 Lack of systematic changes in the direction-tuning properties of single cells 106

7.4 Weighting of task parameters by single cells and their dynamic switching . 108

7.5 Reflection of adaptation in the LFP signal . . . 110

7.6 Conclusions . . . 111

References **113**

List of Tables

2.1 List of sessions for the first subject 29
2.2 List of sessions for the second subject 30
4.1 Direction-tuning results for the muscles 55
6.1 Description of the data sets 85
6.2 Results for the linear regression and Kalman filter methods 88

List of Figures

1.1 Forward and inverse models . . . 9
1.2 Multiple paired forward-inverse internal models . . . 16
2.1 Time course of a trial . . . 26
2.2 Temporal sequence of forces introduced . . . 28
2.3 Location of the array electrodes . . . 31
3.1 Hand-paths of a typical subject . . . 36
3.2 Average performance of the subjects . . . 37
3.3 Hand-path error varies linearly with viscosity . . . 40
3.4 Subject performance improved with time . . . 41
4.1 Temporal sequence of forces introduced . . . 46
4.2 Changes in the hand path as a subject learns the force field . . . 47
4.3 Hand paths during the force trials and the catch trials . . . 48
4.4 Summary of the behavioral performance of both subjects . . . 49
4.5 Catch-trial deviations for both subjects . . . 50
4.6 Long-term learning . . . 50
4.7 Example of trial-average EMG signal . . . 51
4.8 Example of EMG direction-tuning curves . . . 53
4.9 Number of cells analyzed for each subject . . . 54
4.10 Fraction of task-related cells . . . 54
4.11 Fraction of tuned cells . . . 57
4.12 Change per day in R^2 of cosine fit to the tuning curves of M1 cells . . . 60
4.13 Change per session in R^2 of cosine fit to the tuning curves of M1 cells for second subject . . . 60
4.14 Changes in the tuning properties of single cells within each day . . . 61
4.15 Percentage of cells with significant regression coefficients, across sessions . . . 64
4.16 Percentage of cells with significant regression coefficients, across time lags . . . 65
4.17 Percentage of cells with most contribution from a particular state variable, across sessions . . . 66

4.18 Percentage of cells with most contribution from a particular state variable, across time lags 67
4.19 Multiple regression: differences between M1 and PMd 68
4.20 Time lag with the maximum R^2 69
5.1 Examples of LFP average power spectra for first subject 73
5.2 Examples of LFP average power spectra for second subject 74
5.3 Example of LFP power spectrum for each channel 74
5.4 Examples of LFP average coherence spectra for both subjects 75
5.5 Example of LFP coherence spectra for each channel 77
5.6 Example of average LFP power in beta band in the CUE period across the sessions 78
5.7 Variation in the beta band power around the introduction of forces 80
5.8 Variation in the gamma band power around the introduction of stiffness interference 81
6.1 Actual and predicted value of x-forces 88
6.2 Variation of filter performance with time lag and filter width 89
6.3 Variation in decoding performance with number of cells 91
6.4 Comparison of the decoding performance of M1 and PMd 92
6.5 Generalization across force fields 93
6.6 Performance metrics for generalization across force fields 95
6.7 Position decoding 96
6.8 Performance metrics for simultaneous decoding of position and force 97

Chapter 1

Introduction

The ability of humans and animals to learn and make highly skilled movements has intrigued scientists and philosophers for centuries. The fundamental questions people are trying to answer are how does an organism *control* its body to generate a large variety of coordinated motions and how does it *learn* to do so. The focus of this dissertation is on the mechanisms of learning new motor behaviors. A study of motor learning has the potential to also offer insights into motor control as the two phenomena are highly inter-related.

1.1 The problem

The issue of the control of motor behavior, in general, has been a difficult one because of a *large number of degrees of freedom* in the motor apparatus of humans and animals. This problem was elegantly exposited by Bernstein as early as 1935 (published in English in 1967; Bernstein, 1967), whose ideas have had a tremendous influence on subsequent thinking and research in this area. The large number of degrees of freedom allows an organism to accomplish any particular movement in myriad ways. For example, it can take different paths to reach a goal; for a fixed path, it can use different motions of the joints to move its limbs along the path; for a fixed pattern of joint motion, it can use multiple combinations of muscles and different patterns of muscle activation. Thus, there is a high level of redundancy in the motor system making the solution to the control problem non-unique. The problem is then how the motor controller decides the best way to move, i.e., how does it place constraints on the degrees of freedom to come up with a solution for generating desired coordinated motion. Note that it is not necessary that the solution has to be completely unique– variability in human and animal motion is indeed observed; however, the general patterns have usually been observed to be remarkably stereotyped (e.g. straight-line hand paths and bell shaped hand-velocity profiles observed in point-to-point reaching movements under a lot of different conditions; Morasso, 1981; Shadmehr and Mussa-Ivaldi, 1994).

A recent influential theory of motor control and learning, known as the Internal Model theory, proposes viewing the motor system as a cascade of a central controller (residing in the nervous system) and the controlled object (the motor periphery). The controller then uses combinations of models of the motor periphery and the surrounding contextual environment to learn and direct appropriate motor performance. While the theory has been successful in explaining a lot of behavioral data, neural correlates of internal models (or the so-called controller) have remained largely elusive. An important direction of current research in motor control and learning is therefore to discover these neural correlates and derive insights into the mechanisms of motor control and learning.

In this dissertation I describe results from two experiments that we conducted to investigate the mechanisms of learning new motor behaviors in the context of reaching movements of the arm. The first, a behavioral study, focused on the efficacy of contextual cues in enabling subjects to simultaneously learn two conflicting force fields, and subsequently switch between them. In the second study, we focused on the changes in the response properties of single cells in the motor cortices of non-human primates, as the subjects learnt different novel force fields and switched between them. We interpret our results in the context of internal models and suggest specific neural mechanisms via which different internal models can be acquired and switched.

1.2 Historical experimental approaches to motor control

The history of motor control extends as far back as at least the early nineteenth century. Ragnar Granit (Granit, 1981) provides a good review on the subject. It was generally understood from the beginning of physiology that we are capable of anticipatorily adjusting our commands to the motoneurons in proportion to the requirements of the expected performance. Neurologists were constantly reminded in their clinics of the importance of the influence of spinal and supraspinal structures on movement. Hughlings Jackson, in mid-nineteenth century, proposed a cortical focus for the origin of epilepsy (commonly called Jackson's epilepsy) (Jackson, 1932). However, an experimental approach to brain control was not possible until the discovery of the motor area by electrical stimulation of the cortex of dogs in 1870 by Fritsch and Hitzig (Fritsch and Hitzig, 1870). Their findings were confirmed in a patient by Bartholow in 1874 (Bartholow, 1874), and in a more thorough manner in the monkey by Ferrier in 1873 (Ferrier, 1873; also his book, *The Functions of the Brain*, in 1876; see Evarts, 1981, for more references).

The earliest quantitative approach in this field was addressed to the notion of "muscle sense", a "centripetal" idea. The two components of muscle sense– sensation of force (described in 1826 by Bell; Bell, 1826) and sensation of movement (studied by Goldscheider around 1887-1898; Goldscheider, 1898) – were studied through psychophysical experiments

on perception thresholds. The "centrifugal" aspect was emphasized, for instance, when Duchenne (Duchenne, 1867) pointed out in 1867 that locomotor ataxia could exist despite normal performance of all the testable senses.

Reflex action provided an important early theoretical framework and a lot of important contributions were made in that direction by Sir Charles Sherrington. The contributions of Sherrington are compiled by Denny-Brown in the *Selected Writings of Sir Charles Sherrington* (Sherrington, 1939). Liddell's *Discovery of Reflexes* (Liddell, 1960) provides a historical account. Probably the best final summary is found in the 1932 book by Sherrington and co-workers, *Reflex Activity of the Spinal Cord* (Creed et al., 1932). Around the 1880s the era of histology rose to prominence (Liddell, 1960) and structural knowledge gradually became available as needed. The Golgi silver chromate stain was introduced in 1875 and Cajal developed the reduced silver methods in the eighties.

Amplification and other kinds of timing and recording electronics were beginning to be used in neurophysiological laboratories in 1930s and, combined with microelectrodes, this allowed detailed extracellular and intracellular recordings from muscle fibers and motoneurons. Intracellular microrecordings allowed investigation of the cellular operations and synaptic microphysiology, and allowed differentiation of the concepts of facilitation, disinhibition, inhibition and disfacilitation.

The development of ideas and techniques in cortical control of movement from the days of Fritch and Hitzig to the era of microeletrodes and electronic instrumentation has been described by Phillips and Porter in their 1977 book *Corticospinal Neurones: Their Role in Movement* (Phillips and Porter, 1977). A major theme in cortical localization originated with Jackson's question of whether muscles or movements are represented in the motor area. The debate still goes and the current general understanding can be summarized by Jackson's own answer that the motor area is an organization for joining muscles into movements "in thousands of different combinations", and by the words of Leyton and Sherrington (Leyton and Sherrington, 1917), that "the motor cortex is a labile organ" and "the upbuilding of larger combinations (*of movements*) varied in character ... is one of the main offices performed by the motor cortex" (cited from Ashe, 1997).

Following the introduction of the technique of extracellular single cell recording in awake behaving animals in the late 1950s by Jasper (Ricci, Doane, and Jasper, 1957) and independently by Hubel (Hubel, 1959), Evarts (1968) was the first to apply it to the study of motor function (see Evarts, 1981; for a review). Significant advances have been made since then, but due to considerations of space it is not possible to talk about them in this thesis. However, I would like to mention the work of Georgopoulos and colleagues in the context of reaching movements as that directly relates to our experiments. In a series of studies Georgopolous and colleagues introduced the concept of direction tuning of single cells, the notion of *preferred direction* and how the activity of the cells in a population

could be combined using a *population vector* (Georgopoulos et al., 1982; Georgopoulos et al., 1983; Georgopoulos, Schwartz, and Kettner, 1986; Georgopoulos, Kettner, and Schwartz, 1988; see Georgopoulos, 1995; for a review). Recent studies (Scott et al., 2001; Cisek and Scott, 1999) have raised doubts on the generality of population vector analysis, but the concepts still remain a strong influence on a lot of current studies, not only in motor control but also in some sensory systems.

1.3 Behavioral paradigms to study motor learning

The experimental approaches to study motor learning in the context of reaching movements fall into two broad categories– learning of new *motor kinematics* or learning of new *motor dynamics* (sometimes also called *kinetics*). Below, I review separately the results from behavioral studies of learning new kinematics and dynamics.

1.3.1 Learning of visuomotor perturbations

Kinematics of reaching refers to the trajectory of the movement. "Trajectory" here means how the state of the arm evolves with time, and it includes not just position but also other variables, like velocity and acceleration, which can be used to describe the state of the arm. It has been typically found to be mathematically convenient, and behaviorally appropriate, to describe the state in either of two coordinate systems: a cartesian coordinate system, which gives the (x, y, z) components of the state variable, and is used when we want to describe the motion in terms of the state of the end-point (the part of the limb, usually the hand/fingers, directly involved in manipulating the external device at the point of contact); or, a polar coordinate system, which gives the coordinates as a set of (r, ϕ, θ), when we want to describe the motion in terms of the state of the joints (shoulder and/or elbow). These are referred to as *end-point based* or *extrinsic* coordinates and *joint based* or *intrinsic* coordinates, respectively.

A number of studies have shown that for reaching movements in various directions the hand-paths taken by subjects are almost always straight-lines (straight in the general shape, that is; of course, some noise around the straight line is expected, as for any biological system), with bell-shaped velocity profiles (Morasso, 1981; Shadmehr and Mussa-Ivaldi, 1994). For every adult, this straight-line movement is an extremely common and overly well-learned movement, having been learned during growing-up. This "simple" movement has become the *de facto* standard through the years to probe the learning of motor kinematics as well dynamics of reaching. Studies of kinematics introduce artificial perturbations in kinematic aspects of these natural movements and observe how the subjects react to that. In one very common experimental paradigm, subjects are asked to make two-dimensional reaching movements in various directions while they cannot see

their hand. The only visual feedback about the movement that is available to them is via an artificially generated cursor, either on a surface in the plane of the movement or on a facing computer screen. This cursor tracks the position of the subject's hand. To introduce artificial perturbations, the experimenters rotate the position of the cursor by various angles about the starting point, so that when the subject moves, say, in a 90 degree direction, the cursor follows the hand but, say, in a 120 degree direction– a counter clockwise (CCK) rotation of 30 degrees in this case. This results in the subject reaching in a different direction and he/she is then required to modify the kinematics of the movement so as to direct it in the desired direction. This paradigm is referred to as *visuo-motor rotation* (e.g. Krakauer, Ghez, and Ghilardi, 2005; Miall, Jenkinson, and Kulkarni, 2004; Wise et al., 1998; Krakauer et al., 2000). Note that studies of visuomotor rotation have not been limited to reaching movements; other tasks like tracking a target and drawing different shapes have also been employed (e.g., Bock, Schneider, and Bloomberg, 2001; Tong and Flanagan, 2003).

Another important paradigm for studying visuomotor adaptation, and one which probably predates visuomotor rotations, involves the use of displacing prisms to create visuomotor distortions (Flook and McGonigle, 1977; McGonigle and Flook, 1978; Roller et al., 2001; Goedert and Willingham, 2002). The principle is the same as above, viz. the subject has to adapt to the altered visual feedback regarding the kinematics of his movements. Typically the subject is asked to put on a pair of prism-goggles or look through slots that can house prisms, and then point or throw objects at certain targets. Initial movements of the subjects are displaced from the desired direction but subjects are gradually able to adapt to the imposed distortions and produce normal movements.

Such studies of kinematic adaptation have demonstrated over and over again that human and animal subjects are able to modify their kinematics to achieve the desired behavior. This phenomenon is what we formally refer to as *motor learning of kinematics* or *motor adaptation of kinematics*– a change in the kinematics of a movement in response to the altered environmental conditions so as to achieve the original desired goal. Most studies of visuomotor rotations have also demonstrated that the acquired learning is retained, without the need for further exposure (Krakauer, Ghez, and Ghilardi, 2005; Caithness et al., 2004), for periods sometimes as long as a month (Bock, Schneider, and Bloomberg, 2001). This retention is behaviorally manifested in terms of improved performance on the second exposure to the same altered environment as compared to the performance when the alteration was first introduced.

1.3.2 Learning of force perturbations

It is clear that to perform any movement, forces need to be applied to the appropriate body part. These force are generated by muscular contractions, which form the lowest

rung in the hierarchy of motor control. The *dynamics of reaching* refers to the aspects of reaching movements related to force generation. Specifically, dynamics involves how the forces required to move the limb along a particular trajectory are generated in the precise temporal sequence, and coordinated so as to produce the desired movement.

To probe motor learning in the context of reaching movement dynamics, novel perturbing forces are applied to the arm of a subject (at the hand, elbow or shoulder) while he/she is reaching in various directions, and the subsequent behavior is studied. These forces are applied via a torqueable robotic manipulandum, which typically houses two/three motors that apply the desired torques in two/three dimensions (the exact details may vary from system to system, but the basic principle is the same). Subjects make reaching movements while holding with one of their hands (usually the dominant arm) a handle attached to the device, with the arm supported or free. In studies of bimanual adaptation, of course, both hands may be used to perform the task. Forces can be applied at the hand (the end-point in this case) via the handle (e.g. Shadmehr and Mussa-Ivaldi, 1994; Gandolfo, Mussa-Ivaldi, and Bizzi, 1996), or at the elbow or shoulder via appropriate connectors (e.g. Gribble and Scott, 2002). This simplistic arrangement attempts to model real-world situations where novel forces might be exerted on your limbs as you attempt to carry out various movements in different unfamiliar environments. As in the case of kinematics, drawing tasks have also been employed for studying dynamic adaptation (Conditt, Gandolfo, and Mussa-Ivaldi, 1997; Fukushi and Ashe, 2003).

From a number of such studies it has been established that the sudden application of novel forces, that are state-dependent, during the reach perturbs the arm of the subjects in the direction of the force. However, with time (and practice) the subjects are able to "learn" the structure and magnitude of the applied forces and are able to compensate for them in such a way as to be able to move with trajectories not different from the ones observed in the absence of any applied force (as mentioned above, these normal trajectories are straight-line paths for reaching movements). This adaptation is what we formally refer to as *motor learning of dynamics* or *motor adaptation of dynamics*– a change in the pattern of forces produced by the motor system in response to the altered environmental conditions so as to still be able to perform the original desired movement. As for the case of kinematics, learning of novel dynamics has been found to be retained for periods as long as 5 months (Shadmehr and Brashers-Krug, 1997). However, not all patterns of forces have been found to be learnable. Examples of these are forces depending only on time (vs. state of the limb; Conditt and Mussa-Ivaldi, 1999; Karniel and Mussa-Ivaldi, 2003) and simultaneously presented forces producing oppositely-directed perturbations (see Chapter 3; Gupta and Ashe, 2007).

Design of force fields

At this point it is helpful to have a general idea of the structure of force fields used in the experiments to study dynamics. The forces are typically designed to depend on some state variable that describes the current state of the moving limb. Typically these variables are either the instantaneous position (for *elastic/stiffness forces*), velocity (for *viscous forces*) or acceleration (for *inertial forces*). Theoretically, a combination of these could also be used, but that is not very common. The forces are applied in the form of *force fields*, wherein the instantaneous value of the force depends on the instantaneous value of a state variable (position, velocity or acceleration), and thus defines a field over the state-space of that variable. For example, for a two-dimensional movement, the instantaneous velocity of the hand forms a two-dimensional state space, the two dimensions typically being the cartesian x- and y-components of the velocity vectors, v_x and v_y, respectively (theoretically any two orthogonal vectors in the space can be used). Then a viscous force field can be defined simply as

$$\begin{aligned} F_x = &\quad A \times v_x + B \times v_y \\ F_y = &\quad C \times v_x + D \times v_y \end{aligned} \tag{1.1}$$

which can be written in matrix form as

$$\begin{bmatrix} F_x \\ F_y \end{bmatrix} = \begin{bmatrix} A & B \\ C & D \end{bmatrix} \begin{bmatrix} v_x \\ v_y \end{bmatrix} \tag{1.2}$$

Viscous force fields have been the most popular paradigm and a large number of studies, both behavioral experiments with humans (Shadmehr and Mussa-Ivaldi, 1994; Gandolfo, Mussa-Ivaldi, and Bizzi, 1996; Shadmehr and Brashers-Krug, 1997; Scheidt, Dingwell, and Mussa-Ivaldi, 2001; Karniel and Mussa-Ivaldi, 2002; Osu et al., 2004) and neural recordings in monkeys (Gandolfo et al., 2000; Gribble and Scott, 2002; Li, Padoa-Schioppa, and Bizzi, 2001; Padoa-Schioppa, Li, and Bizzi, 2002; Fukushi and Ashe, 2003; Padoa-Schioppa, Li, and Bizzi, 2004), have provided evidence of learning in these fields. Only a limited number of studies have used elastic (Caithness et al., 2004; Tong, Wolpert, and Flanagan, 2002; Fukushi and Ashe, 2003) or inertial force (Krakauer, Ghilardi, and Ghez, 1999; Fukushi and Ashe, 2003; Sergio, Hamel-Paquet, and Kalaska, 2005) but have again provided similar results. [Note that although Krakauer, Ghilardi, and Ghez (1999) applied an inertial perturbation, it was in the form of an inertial load attached to the forearm rather than in the form of an explicit state-dependent force field.] A particularly useful special case of force fields that has been used very often is called a *curl field* where the forces are perpendicular to the instantaneous value of the independent variable (e.g velocity

for viscous fields) (Li, Padoa-Schioppa, and Bizzi, 2001; Donchin, Francis, and Shadmehr, 2003). One of the advantages of using curl fields is that they provide an isotropic (rotation-invariant) perturbation such that the direction of the force is always perpendicular to the movement for all directions. This, for one thing, causes the preferred direction of *all* the muscles that are directionally tuned during the task to rotate predictably in the direction of the applied force, irrespective of their initial preferred direction (Li, Padoa-Schioppa, and Bizzi, 2001). In the above equations, making A and D equal to zero results in a curl field; usually B is taken to be equal and opposite (in sign) to C to have same field strengths in both dimensions.

Other dynamic perturbations that have been used include time-dependent force fields (Conditt and Mussa-Ivaldi, 1999; Karniel and Mussa-Ivaldi, 2003), where the instantaneous value of the applied force depends predictably on time (i.e., the force is a function of time), and is independent of the state of the moving limb. For example, Karniel and Mussa-Ivaldi (2003) applied forces that varied sinusoidally as a function of time, independent of the position or velocity of the moving arm.

1.4 Internal model theory of motor learning

Motor learning is ubiquitous in the animal kingdom. Nevertheless, the underlying mechanisms remain elusive. Over the years, a number of theories have been proposed to explain motor control and learning, but at the moment none of them can be called complete. Some of the major theories include the *reflex-chain hypothesis* in the early twentieth century (Sherrington, 1939), the *dynamical systems* idea (Saltzman and Kelso, 1987; Schöner, 1990), the *equlibrium point theory* (Feldman et al., 1998;Mussa-Ivaldi and Bizzi, 2000) and the *internal model* (IM) theory in more recent times (Kawato, 1999, and Wolpert and Ghahramani, 2000). Our experimental design is similar to that used by researchers investigating the IM theory and so our results can be directly compared to those experiments. I briefly explain the concept of IMs below.

The task of performing a goal-directed movement can be broadly divided into three sequential steps: making the decisions about the intention to move and processing sensory stimuli; planning kinematics, like the trajectory to follow; and, calculating the required forces to move the limb along the desired trajectory. This requires a sequence of sensorimotor transformations (Soechting and Flanders, 1992; Soechting and Flanders, 1995; Kalaska et al., 1997). According to the IM theory, learning of motor tasks involves acquisition of IMs, which encode the sensorimotor transformations that map sensory inputs into desired motor outputs. An IM can be considered as a model of the motor system along with the external environment in which the organism has to perform. It can be used to predict sensory consequences of intended motor commands (*forward model*– the predictor)

or to predict the motor commands required to produce a desired motor behavior (*inverse model*– the controller) (see Fig 1.1).

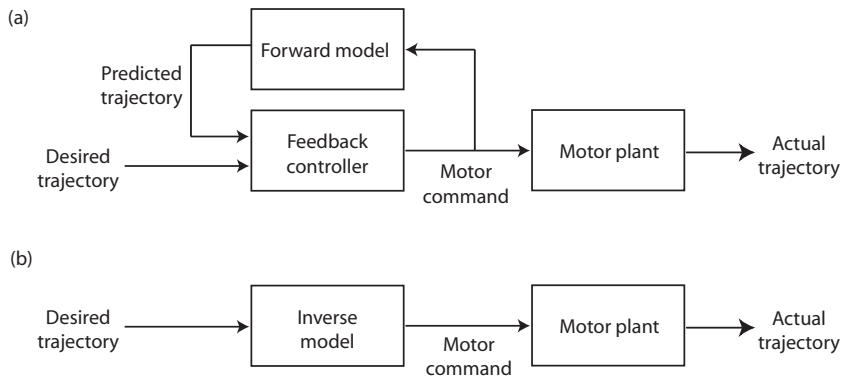

Figure 1.1: The use of forward and inverse models in two control architectures applied to the case of reaching movements. **(a)** Forward models predict the consequences of motor commands. **(b)** In contrast, inverse models calculate the required motor command to produce desired results. Figure reproduced from Kalaska et al. (1997).

In studies of motor learning, after a subject has adapted to the altered environment, sometimes the experimenters turn off the perturbation on randomly selected trials, called *catch trials*. On such catch trials, the subjects' movement trajectories have been found to deviate in a direction opposite to that observed when the perturbation was initially introduced. This behavior is termed *after-effects* and is thought to occur because, having learnt the new conditions, the subjects were still compensating for them when the perturbations was unexpectedly turned off. This, therefore, caused overcompensation and deviated their movement in the opposite direction. The presence of aftereffects suggests that subjects form a model of the altered conditions and use that model to appropriately compensate for the conditions. This is particularly interesting for force-field learning experiments as this implies that subjects do not merely stiffen their arms to counter the perturbing force (Shadmehr and Mussa-Ivaldi, 1994).

Further evidence for formation of models comes from studies demonstrating that learning can generalize across certain tasks. For example, Conditt, Gandolfo, and Mussa-Ivaldi (1997) showed that adapting to a force field during reaching improved subjects' performance in a circle drawing task in the same workspace under the same field. This suggests that subjects learned a structured model of the state-dependent force field and did not use rote memory of previously experienced patterns of forces. Furthermore, generalization of learning of dynamics has also been observed to varying extents between different workspaces (Shadmehr and Mussa-Ivaldi, 1994), different directions (Gandolfo, Mussa-Ivaldi, and Bizzi, 1996) and from dominant to nondominant arm (but not *vice versa*; Criscimagna-Hemminger et al., 2003). Generalization has also been reported for visuomotor adaptation tasks, for example between a left-right reversal and an up-down

reversal (Bock, Schneider, and Bloomberg, 2001).

According to the definitions, the evidence cited above supports the presence of inverse models in that these models guide the motor system in producing the required motor commands to effect the desired movement trajectories. In contrast, forward models are used to predict the sensory consequences of motor actions. An important paradigm that has helped researchers study the role of forward models has been the relationship between grip-force (GF) and load-force (LF) (Flanagan and Wing, 1997). Studies of Johansson and colleagues (Johansson and Westling, 1984; Johansson et al., 1992; Johansson and Cole, 1992) showed that when lifting objects or pulling on fixed loads, GF is adjusted in parallel with changes in LF such that it is always slightly greater than the minimum required to prevent slip. This anticipation of the LF was seen only when it is self-generated and not when it is applied by an external agent. Without going into too much detail here, a number of studies by Witney and colleagues (Witney, Goodbody, and Wolpert, 1999; Witney, Vetter, and Wolpert, 2001; Witney and Wolpert, 2003) and the one by Flanagan and Wing (1997) have shown that humans are able to predict self-generated LFs under a variety of load conditions, suggesting the presence of forward internal models. In addition, Flanagan et al. (2003) showed that while adapting to novel dynamic environments, subjects could predict the consequences of their actions before they could generate appropriate actions for control. Wolpert, Ghahramani, and Jordan (1995) and Miall and Wolpert (1996) provide a good introduction to forward models.

An interesting model of motor control and learning, called the MOSAIC model, was recently proposed by Wolpert and Kawato (1998). The authors proposed a modular approach to motor control and learning and describe a novel scheme in which multiple forward and inverse internal models are integrated and work together to provide control and adaptation. One of the sections below carries a brief discussion of this model (see Fig 1.2 and Section 1.6).

There are still a number of open questions in the IM theory. It is not very well understood where and how the models are acquired and where they get stored for later use. There is some evidence suggesting that the cerebellum may be involved in the acquisition and storage of IMs (see Wolpert, Miall, and Kawato (1998) for a review). An important issue is to understand how the decisions to choose between different internal models are made and what roles do sensory cues play in that decision. Another important issue relates to the capacity of the nervous system to acquire and store multiple models. During normal daily-life, humans and animals interact with an immensely wide variety of environments and are able to learn to perform movements in various different conditions. Furthermore, re-exposure to an environment usually doesn't necessitate complete re-learning, suggesting that we are able to store most of what we learn. One wonders if there is any fundamental limit to what a human or an animal can learn, when given sufficient practice. It is easy

to imagine that if an organism is required to learn more than it has the capacity to, or if it is exposed to tasks that require conflicting models to be learned, one would observe some kind of interference or competetion between multiple, possibly conflicting, models and the nervous system has to somehow decide what is best ("optimum") for the organism in that situation. Numerous behavioral and some imaging studies have explored learning and interference in the human motor system; however, neural recordings (in monkeys) have been very limited. The concepts of consolidation and interference are discussed in greater detail below.

Finally, it should be pointed out that to the best of my knowledge, there has been no direct neurophysiological evidence demonstrating the existence of internal models in the nervous system. The primary difficulty in this regard is that it is still not clear what aspects of the movement and the environment are important enough for the organism to model. Thus far, internal models have remained an elegant computational framework awaiting physiological support. Our experiments are aimed at exploring how the brain reacts to altered environments, and, whether or not our results fit in with the IM theory, we hope that they would bring us a step closer to understanding the mechanism of motor learning and interference.

1.5 Behavioral studies of sensorimotor interference and consolidation: Arm movements in force fields

An interesting observation that came out of the studies of motor learning was that of *interference*. To understand interference it is important to understand the (currently believed) physiological correlates of learning. In most systems, learning is thought to result from modifications of the synapses between the neurons. This modification can be in terms of the number (and, possibly, location) of the synapses (*anatomical/structural modification*), as well as in terms of the strength of pre-existing synapses (long-term potentiation, long-term depression; *functional modification*). A recent study showed that axons and dendrites of neocortical pyramidal cells have a large number of points of physical contact which are not functional synapses (Kalisman, Silberberg, and Markram, 2005). These points of contacts have the potential to give rise to new synapses "on demand". It is believed that the knowledge of a new motor skill is most likely acquired in terms of modification of synapses in the "motor areas". However, it is not certain exactly where this acquisition takes place and where the memory gets stored for the long-term.

Now, in studies of motor learning during reaching it was observed that if subjects were exposed to anti-correlated environments (commonly referred to as *conflicting* in literature) in close temporal proximity, performance of subjects in the second environment was impaired as compared to naïve subjects, and the retention of the learning of the

first environment was dramatically reduced. Generically, environments requiring opposite error-corrections (adaptations) have been called conflicting (Bock, Schneider, and Bloomberg, 2001). Such *interference* between conflicting environments has been observed for the learning of kinematics as well as dynamics. A typical experiment requires subjects to adapt to one kind of kinematics/dynamics (environment A; Task A1) in the first session, then to the opposite kind (environment B; Task B1) in a second session. The subject is then tested on the original environment (Task A2; third session). We refer to this as the "A-B-A paradigm". Sometimes there are subsequent sessions depending on the exact purpose of the study. Varying amounts of time separation have been employed between consecutive sessions, and that has been found to be critically important in some studies (but, significantly, not so in others). From these studies, two behavioral forms of interference have been distinguished– *anterograde* and *retrograde*. For the paradigm described above, anterograde interference, as the name suggests, refers to the (interfering) effects of task A1 on task B1, while retrograde interference is the name given to the effect of B1 on A2 (when compared with A1). Generically speaking, interference is thought to involve unlearning of previous adaptation and its replacement by the adaptation to the new environment.

Consolidation of motor skills, on the other hand, refers to the gradual storage of the memory of the acquired skill, with some degree of stability conferred on it, such that the skill can be recalled at a later date. Therefore, in essence, consolidation is what should be observed when there is no interference. A number of studies have demonstrated that when subjects adapt to velocity-dependent force fields, initial performance when re-exposed to the same field is better than that during the first exposure and the re-learning is more rapid (Brashers-Krug, Shadmehr, and Bizzi, 1996; Shadmehr and Brashers-Krug, 1997). This suggests that the learning during the first exposure got stored (consolidated) and was available for recall/use later. Such consolidation has been shown to persist for as long as 5 months without further training (Shadmehr and Brashers-Krug, 1997). However, the improvement in performance is abolished if subjects are exposed soon after to another force field that perturbs in the opposite direction (*retrograde interference*). Furthermore, the performance of these subjects in the second force field is worse than that of naive subjects exposed to that field suggesting the presence of *anterograde interference* as well. Lack of consolidation is observed both when opposite rotary fields are presented in sequential blocks (e.g. Brashers-Krug, Shadmehr, and Bizzi, 1996) or when presented on alternating trials (Karniel and Mussa-Ivaldi, 2002). However, if practice in the two conflicting fields is separated in time by more than 6 hrs, both forms of interferences are absent and normal consolidation is seen; furthermore, within that period of 6 hrs, the amount of interference was observed to proportionately decrease with time (Brashers-Krug, Shadmehr, and Bizzi, 1996; Shadmehr and Brashers-Krug, 1997). To explain this interference and consolidation,

it has been suggested that when two opposite fields are learned close together in time, they compete for the same resources in the short-term memory and thus interfere with each other; this causes "unlearning" of the first field and replacement by the memory of the second environment. Gradually, the learning of any environment is consolidated and converted into a long-term form that is resistant to modification. Thus, no interference is observed if the learning is allowed to consolidate. From the above two studies, the time for this consolidation to occur appears to be 5-6hrs. This is viewed by some researchers as a two-stage model of motor learning: an initial stage involving *acquisition* of learning and its retention in short-term memory, and a second stage involving more gradual *consolidation* of the learning in long-term memory. Our experiments focus on the acquisition stage of motor learning.

This consolidation theory was however called into question in a recent study by Caithness et al. (2004). They provided strong evidence that interference occured even if exposures to the conflicting fields were separated by 24hrs or even 1 week. Interference was shown to occur for velocity-dependent force fields under different conditions, one of which quite closely replicated the experimental set-ups of the studies by Shadmehr and colleagues mentioned above. Furthermore, intereference was also found to occur between conflicting position-dependent force fields, indicating that the phenomenon is not specific to viscous fields. Two other important points made by the study were: first, interference was observed even when the effect of the previous day's learning was washed out with practice on force-free ("washout") trials at the start of the day, indicating that the inteference was of a retrograde, rather than anterograde, nature (Miall, Jenkinson, and Kulkarni, 2004; Krakauer, Ghez, and Ghilardi, 2005); and second, that interference was seen not only when subjects perfomed in an opposite force field, but also when they performed the task without any forces. This second observation is contradictory to what Gandolfo, Mussa-Ivaldi, and Bizzi (1996) observed and once again calls into question exactly what aspects of the task interfere in memory (Bock, Schneider, and Bloomberg, 2001; Tong and Flanagan, 2003).

Tong, Wolpert, and Flanagan (2002), in a study of interference between visuomotor rotation and force fields, proposed that two environments can be learned independently if they depend on different kinematic parameters of movement. In a direct test of this hypothesis, Bays, Flanagan, and Wolpert (2005) have shown this not to be the case in general, by demostrating retrograde as well as anterograde interference between a CW position-dependent force field and velocity-dependent force field (performed with an interval of 5 min), which, however, was less than the interference between CW and CCW position-dependent fields. These authors explained their results through a "motor-adjustment hypothesis", according to which "the amount of interference between two perturbations depends on the extent to which the required adjustments to ... motor command conflict,

with complete interference only when the required motor adjustments are exactly opposite". However, the authors used an out-and-back reaching task, where under the viscous fields, the subjects experienced CCW forces on the outward movements and CW forces during the inward movements. Thus for their conclusions to hold, it should be assumed that the inward movements did not influence the learning of outward movements, which although possible (since the two movements had different starting positions), is not necessarily true.

In summary, early studies by Shadmehr and colleagues suggested a two-step model of motor learning, whereby any learning is first stored in a fragile state in short-term memory immediately after the acquisition. This short-term memory is then consolidated to a more stable long-term memory that is resistant to erasure. However, it is not clear what forms of learning give rise to interference and which ones, instead, cause facilitation. Furthermore, some of the more recent studies have failed to reproduce the earlier results and do not provide evidence for consolidation.

One important thing to note from all the above studies is that the consolidation of learning has almost never been found to be perfect, in that, although the performance on re-test is better than that of naive subjects, it is not as good as that at the end of adaptation during the previous session. This can be due to various reasons (I speculate here, without evidence): it may be a fundamental characteristic of motor memories– i.e., the nervous system may not attempt to store a perfect record of previous learning, but rather keep a "scaled-down version" that is good enough to reproduce desired performance. On the other hand it may just be a deficit peculiar to the experimental paradigms that have been used so far. Furthermore, it is also difficult to determine if this is a deficit in consolidation or recall (see Krakauer, Ghez, and Ghilardi, 2005).

1.6 Acquisition of multiple internal models

A computational model of motor learning and control proposed by Wolpert and Kawato (*MO*dular *S*election *A*nd *I*dentification for *C*ontrol (MOSAIC) model; Wolpert and Kawato, 1998; also see Haruno, Wolpert, and Kawato, 2001) suggested a modular architecture wherein motor learning by the nervous system is accomplished through the acquisition of multiple internal models which are then selected (*gated*) and weighted appropriately by using the contextual cues and sensory feedback available to the animal from his surroundings (see Fig 1.2). Briefly, the architecture consists of multiple sets (modules) of paired forward and inverse internal models, along with structures called the responsibility predictors. The forward model in each module generates predictions of sensory consequences based on the current motor commands while the corresponding responsibility predictor generates predictions based on the contextual cues and both are combined to generate

a responsibility signal in proportion to the applicability of their module to the present context. This responsibility signal is then used as a weight to guide the adaptation of both the forward and inverse models in each module, as well to gate the contribution of the respective inverse internal models to the final motor command. This ensures that only the "appropriate" models adapt and contribute to the control in a specific context. The proposed architecture can simultaneously learn the multiple inverse models necessary for control as well as select the inverse models appropriate for a given environment.

This model is very attractive in that it explains the ability to make a large number of movements via a large number of combinations of relatively few internal models that would need to be stored. However, a proof that this is actually the case requires showing that contextual cues can be effectively used by organisms for motor learning (*acquiring* internal models) and for motor performance (using the cues to *predictively choose and switch* between different internal models). Efforts have been directed into this and initial results have been mixed. Some studies have shown that human subjects can acquire two conflicting dynamic internal models if they are cued by different postures (Gandolfo, Mussa-Ivaldi, and Bizzi, 1996) or spatial location of a visual cue (Rao and Shadmehr, 2001) but not if cued by arbitrary colors (Gandolfo, Mussa-Ivaldi, and Bizzi, 1996; Shadmehr et al., 2005) or presented as an alternating sequence (Karniel and Mussa-Ivaldi, 2002; they used alternating force fields which subjects could not adapt to even after separately learning the individual fields). Wainscott, Donchin, and Shadmehr (2005) recently used the concept of a *generalization function* and re-examined adaptation to alternating force fields. They found that although behavioral measures did not show consistent improvements in performance, the brain continued to adapt to the errors. Moreover, if two-trial sequences of the two fields were delineated by sufficiently long time intervals between the end of one sequence and the start of the next, subjects did demonstrate adaptation to the alternating opposite-rotating force fields. The time gaps can thus be interpreted to have served as a temporal cue.

Krouchev and Kalaska (2003), showed that monkeys can predictively switch, based only on color cues, between opposite force fields that have been over-learned via extensive previous practice. This suggests that color cues can at least be used to recall multiple models. Other studies have shown that humans cannot adapt to force fields that depend exclusively on time, and in fact they model a time-dependent field as a state-dependent field (Conditt and Mussa-Ivaldi, 1999; Karniel and Mussa-Ivaldi, 2003). Thus, overall it seemed that ability of the contextual cues to enable selection of, and switching between, internal models may be limited. Specifically, only cues that were directly related to the performance of the movement (posture, state, spatial location), and not abstract, symbolic cues that had an arbitrary association (visual color cues), seemed to have any influence on the ability to switch predictively between multiple models.

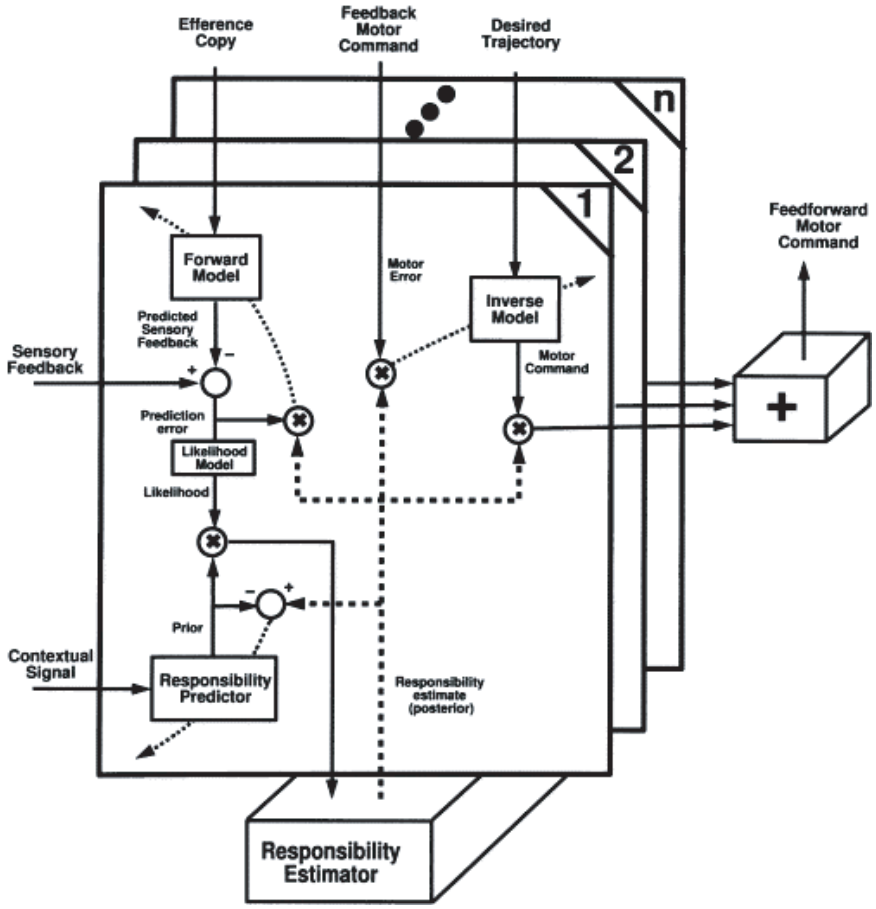

Figure 1.2: A single module within the multiple paired internal model architecture. The forward model component predicts the next state based on the motor command and current state. The prediction is delayed and compared with the actual next state (via the sensory feedback). The inverse model component produces a feedforward motor command and receives as error the feedback motor command weighted by the responsibility estimate of its paired forward model. The responsibility signals also weigh the contribution of each inverse model's output to the final feedforward motor command. The responsibility predictor produces an estimate of the module's responsibility based on contextual cues. The predicted responsibility is combined with the transformed prediction error from the forward model for each module and the resulting signal from all the modules is combined by the responsibility estimator to assign responsibility to each module. The thick dashed line shows the central roles of the assigned responsibilities. Dotted lines passing through models are training signals for learning. Figure reproduced from Wolpert and Kawato (1998).

Two recent studies (Osu et al., 2004; Wada et al., 2003), in contrast, provided results that apparently contradicted previous observations. The authors in these studies showed that human subjects could successfully adapt to, and predictively switch between, opposite viscous force fields applied at the elbow (single-joint movement; Wada et al., 2003) or the hand (multi-joint movement; Osu et al., 2004), cued only by color. The key point was that adaptation to conflicting fields was possible only if they were presented randomly. Intrigued by these studies, we conducted an experiment with human subjects to study the generality of the effects observed there. Specifically, instead of using two consistent force fields, one in each direction, as the above two studies used, we exposed subjects to two Gaussian-distributed viscous curl force fields as they made reaching movements in only one direction (straight ahead in a para-sagittal plane). One of these force fields perturbed the subjects' hand toward the right, while the other pushed it to the left. At the beginning of each trial the magnitude of the viscosity coefficient was selected randomly from either of the two distributions, and the direction of the upcoming force was indicated via a color cue. This environment is more naturalistic, closer to what one might expect in real-life. Earlier studies have used such an unpredictable force-field structure, but perturbations were applied only in one direction and thus there was no conflict (Scheidt, Dingwell, and Mussa-Ivaldi, 2001; Takahashi, Scheidt, and Reinkensmeyer, 2001). It was shown by these authors that subjects tended to learn and compensate for the approximate mean of the distribution, both for a unimodal distribution and a bimodal distribution. We found that the subjects were unable to form internal models of the applied force fields, either individually or as one complex field, indicating that the effects of random presentation and context-based switching documented in Osu et al. (2004) and Wada et al. (2003) may not apply to more general settings (Gupta and Ashe, 2007). The results of our experiment are discussed in Chapter 3.

1.7 Neurophysiological studies of force-field learning

To put the last few sections together, although the fact that the motor system is capable of adapting to altered dynamics is well established, the results of behavioral investigations of motor interference have been quite conflicting. There is a need for studies that investigate neural mechanisms that underlie this complex and intriguing behavior. These would help us gain insight into what is happening inside the brain at a cellular level and bring us, hopefully, a step closer to an understanding of the mechanisms of motor learning and interference. Neural studies of motor learning of force fields have been very limited in number. Furthermore, as far as I know, there is no published study yet that has described an experiment to directly study neural responses during tasks involving interference in motor dynamics (Gribble and Scott (2002) conducted related experiments, however). I

present below a brief overview of the current literature.

Recent studies from the Bizzi group studied neural responses from a number of different areas while monkeys adapted to a viscous force field (Gandolfo et al., 2000; Li, Padoa-Schioppa, and Bizzi, 2001; Padoa-Schioppa, Li, and Bizzi, 2002; Padoa-Schioppa, Li, and Bizzi, 2004; Xiao, Padoa-Schioppa, and Bizzi, 2006; Richardson et al., 2008). Recording from the primary motor cortex (M1), Gandolfo et al. (2000) found a significant number of cells that changed their tuning properties during adaptation to the force field (Force epoch). A significant number of these cells also retained their modified tuning throughout the Washout epoch after the adaptation, when the forces were removed. The authors labeled these cells as *dynnamic cells* and *memory cells*, respectively. Cells that did not change their activity across Baseline, Force and Washout epochs were labelled *kinematic cells*. Furthermore, some of their cells were recruited when the forces came on ("tune-in") while some others lost their tuning activity in the presence of forces ("tune-out"). Li, Padoa-Schioppa, and Bizzi (2001) extended this study by quantifying the neural reponses during a movement-time window in terms of the cells' preferred direction (direction of the vector average of the tuning curve; PD), average firing rate (average of the tuning curve; Avf), and tuning width (angle over which the activity was higher than half of the maximum activity, defined only for unimodally tuned cells; Tw). They found cell categories similar to those found by Gandolfo et al. (2000); in addition they found a second class of memory cells that did not change their activity during the Force epoch but exhibited a change opposite to the direction of the force applied in the Washout epoch. At a population level, the authors found that the neurons showed a shift in PD that matched with the direction of the applied force in the Force epoch and that the PD returned back to baseline during the Washout epoch. The latter implied that the two classes of memory cells balanced each other, so that the net deviation observed between Baseline and Washout epochs was zero. Moreover, the shift in the PD of the neuronal population was also consistent with the shift of the PDs of the muscles recorded. Finally, although the authors used two force fields, CW and CCW (over periods of a few months, with both fields presented uninterrupted, one after the other), they do not discuss possible interference. On the other hand, the behavioral measure of performance used by them showed a steeper learning curve (implying faster learning) for the second field, as compared to the first.

Interestingly, the classification of cells based on the three different parameters (PD, Avf, Tw) was found to be unrelated and thus seemed (to me) to raise doubts on the suitability of the parameters as good measures of the neural responses. The authors did not carry out any further detailed analyses. In addition, a recent report showed that "non-human primates are capable of generating reaching movements to spatial targets even though population vectors based on M1 activity do not point in the direction of hand motion" (Scott et al., 2001), thus raising questions on the ability of the population

vector to adequately represent the direction of reaching movements.

The same group followed up the investigation of M1 by two studies of the supplementary motor area (SMA) under the same task. First, Padoa-Schioppa, Li, and Bizzi (2002) showed that the activity of neurons in SMA comes to reflect the movement dynamics increasingly over the course of an instructed-delay period, starting from a kinematics-related signal. This indicated that the SMA may be involved in a "kinematic to dynamic transformation". Padoa-Schioppa, Li, and Bizzi (2004) then examined the dynamics related activity of the SMA neurons and their plastic behavior as the animals adapted to force fields. They found that, as a population the SMA neurons shifted their PD in the direction of the external force, both during the instructed-delay (DT) and the movement-time (MT) periods, indicating that the cells reflect the movement dynamics during movement planning as well as execution. As for the case of M1, the authors again classified the cells into various types according to the three parameters discussed above. Aditionally, the classification was done separately for DT, MT and target-hold (TH) time windows. The classification of SMA cells based on PD during DT activity was found to be similar to that of M1 cells based on PD during MT activity. However, the interpretation of the role of the observed plasticity of SMA cells in the acquisition of the internal model of the new dynamics was complicated by the finding of similar plastic behavior of some cells recorded during a control task with no forces (Rokni et al., 2007). Similar analyses were performed in the dorsal and ventral pre-motor areas (Xiao, Padoa-Schioppa, and Bizzi, 2006) and in the cingulate motor areas (Richardson et al., 2008).

Rokni et al. (2007) further analyzed the finding of plastic behavior of some cells in the control task as reported in Padoa-Schioppa, Li, and Bizzi (2004). Furthermore, they presented new data showing such plastic behavior unrelated to learning in the M1 also. To explain these findings, Rokni et al. (2007) showed that the non-learning-related plastic changes were random across the cells and time, and intrepreted them as "background changes" that occur independent of the task being performed. They then showed that the process of learning a new force field biases the plasticity so that the changes in PDs are now correlated across cells. Nevertheless, these findings create doubts regarding the suitability of using PDs of single cells to measure the dynamic changes in the motor cortex related to the acquisition of new motor skills. Our results (discussed in Chapter 4) lend further support to these doubts.

1.8 Comments on our experiments

In this dissertation I describe the two experiments we conducted to investigate acquisition of, and switching between, multiple internal models. The first was a behavioral study with humans while the second was a neurophysiological experiment with non-human primates.

Here, I briefly summarize the thoughts behind our studies.

In Sections 1.5 and 1.6, I described the results from the behavioral studies of motor interference. Specifically, researchers are interested in finding out whether the motor system can acquire and store conflicting internal models, simultaneously or sequentially, and, if so, under what conditions can the motor system successfully switch between the stored models based on the changing task requirements. In the latter section, I expanded on the role the environmental context can play in enabling successful switching (and, quite often, even acquisition). Specifically, while postural or spatial cues seemed to help subjects to learn conflicting models, temporal and arbitrary color-association cues did not. Osu et al. (2004) and Wada et al. (2003), on the other hand, showed that color-cue based acquisition and switching was possible if the two conflicting fields were presented randomly. This interesting development led us to our first experiment– a behavioral study in human subjects, where we tested if the efficacy of random presentation and color cues in enabling learning could be extended to more complicated force fields. It had been shown (Scheidt, Dingwell, and Mussa-Ivaldi, 2001) that subjects adapted to the mean of force-fields of random, Gaussian-distributed, magnitudes that were consistently applied in one direction. We wondered if random presentation might help subjects to simultaneously learn two such force fields applied in opposite directions.

I wish to emphasize the vast gap that exists between the behavioral investigations of motor learning and interference and their neurophysiological counterparts. While the behavioral studies of force-field learning started to come out in the early 1990's, even the most basic investigations of its neural mechanisms did not surface until a decade later (Section 1.7). The focus in those studies was on the direction-tuning and average firing rates of single cells, and the roles of oscillations and synchrony (of local field potentials as well as single cells) or the global representation of the movement parameters was not touched upon at all. Furthermore, although researchers have explored a number of nuances of motor interference in behavioral studies, we still lack a systematic neural investigation of even the most basic paradigms.

With an intention to fill this gap, we decided to take a step (or two) back. Instead of exploring the sophisticated paradigms that have been used for the behavioral studies, we went back to the most basic set-up that has been used to explore interference– the A-B-A paradigm introduced in Section 1.5– and designed an experiment where we could examine the neural activity during the processes of motor learning and interference. As in the case of human studies, we started out with monkeys who were naïve with respect to the force fields. This represented a significant departure from traditional neurophysiological studies that use trained monkeys (save the Bizzi studies discussed in the previous section). This feature of our design allowed us to record the neural signals throughout the initial learning process, in addition to the period in which we interfered with the monkeys' learning. To

stretch out the time over which we could record the learning-related signals, we exposed the monkeys to force fields that were strong enough to require them to learn over a period of a few days. This is another major difference between our experiments and the current literature, where learning has been confined within a single day. Next, when the monkeys started to show signs of having learnt the field (field A) to a large extent, as evidenced by approaching a plateau in the behavioral performance, we exposed them to interfering fields (field B). We then went back to the familiar field (field A) the next day, thus completing the A-B-A exposure.

To summarize, both our experiments were designed to examine more closely the processes of adaptation and interference in the context of force fields, albeit at different levels of sophistication as dictated by the different levels of current understanding in the two different experimental domains. While our neurophysiological experiment was designed to study both learning and interference, in this dissertation I present neural results related only to the learning of, and switching between, multiple force environments.

1.9 Summary

In this introductory chapter I provided a general introduction to the notions of kinematic and dynamic motor learning and talked about the Internal Model theory of motor control and learning, which fits in with our experimental paradigms. I reviewed evidence that, generally speaking, humans and animals are able to adapt to altered kinematics and dynamics. However, not all forms of perturbations have been found to be learnable, especially if they are "complex". I introduced the concept of interference in motor learning and proceeded to give a detailed account of the behavioral investigations into interference in the context of learning force fields. I hope to have convinced the reader that the behavioral results have not yet been able to elucidate the mechanisms involved. I then touched upon some of the neural studies of force-field learning. I concluded this chapter with an introduction to our experiments.

The rest of the dissertation is organized as follows. In the next chapter, I provide details about the experimental design and methods of both our experiments. In the subsequent chapter, I present results from our behavioral experiment. The next two chapters describe results from our neurophysiological experiment, where I talk about the behavior, the EMG recordings, the single cells and the local field potentials. In the penultimate chapter, I describe some of the work we did towards decoding the instantaneous force applied by the monkey from the firing rates of simultaneously recorded neurons, with an aim to eventually apply the ideas towards the design of a brain-machine interface that could actively compensate for the required forces while simultaneously performing the desired movement. I conclude this thesis with a general discussion.

Chapter 2

Experimental Methods

In this chapter, I present the details on the design of the two experiments we conducted. I start with the behavioral study performed with human subjects and then describe the neural recordings performed in Rhesus monkeys.

2.1 Behavioral experiment with human subjects

Twelve right-handed human subjects (6 males, 6 females; 20-36 years old) participated in the study after providing informed consent.

2.1.1 Robotic manipulandum

We used a two-joint robotic manipulandum (Interactive Motion Technologies, Inc., Cambridge, Mass.) that is frequently used in force field perturbation experiments in humans and non-human primates. The manipulandum has two torque motors that produce forces in a two-dimensional x-y plane. The resultant of the forces is applied at the handle of the arm which the subjects grip while moving the arm. The forces are servo-controlled via a personal computer using the RTLinux operating system. To track the robotic arm, encoders sample the joint angles which are then converted into position and velocity in Cartesian coordinates. The software allows the user to specify the desired temporal and spatial characteristics of the applied force. A force transducer at the base of the grip-handle measures the force that the subject applies at the handle.

2.1.2 Experimental set-up

Subjects sat in a chair holding the handle of the manipulandum and executed timed reaching movements in the horizontal plane. An LCD monitor displayed 'start' and 'end' target circles of 3 cm diameter and a cursor of diameter 1.5 cm representing the hand position(equivalent to the robot endpoint); the hand and arm was visible throughout the

experiment. The reach was a 15 cm movement and corresponded to an upward motion of the cursor on the screen and a movement of the subjects' hand away from the body in a para-sagittal plane. Subjects were instructed to position themselves so as to keep the forward movement aligned with the axis of the shoulder joint. However, their posture and position were not constrained in any way.

On most trials, the robot produced forces on the subjects' hand (see section 2.1.4 for details). The forces were applied only during the outward movement from the start to the end target and subjects were allowed to return to the start circle however they chose (the start circle was visible at all times). A trial began when the subject positioned the cursor completely within the start circle. In force trials, a colored rectangular frame was displayed at the beginning of the trial, around the workspace, as a contextual cue. For group 1, the frame was blue for rightward forces and red for leftward forces (*vice versa* for group 2). For trials in which no force was produced (null trials), a cue was irrelevant and was therefore not provided. After the cue was displayed for 300 ms, the end target came on following a random delay of 200-500 ms. Subjects were instructed to wait for the target to come on and then make point-to-point reaching movements that were "as straight and smooth as possible", and to "stop and hold at the target". During force trials, forces were applied once the subject crossed a circular window that was 1.5 times the radius of the start circle and concentric with it. The movement was required to be completed within 400-700 ms; this relatively large time window was used because of the wide variation in the magnitudes of the field strengths we used. A trial was complete after a target hold time (700 ms) and the forces were turned off. At the end of each trial, feedback was provided regarding the movement duration: the target turned red if the movement was too slow, turned green if it was too fast, and turned black if subjects did not stop and hold at the target for a sufficient length of time. After that, the trajectory of the movement was displayed to the subject for 300 ms.

Incorrect movements were classified into four types: limit errors, when the subjects' hand strayed outside a virtual boundary in the workspace; slow and fast errors, when the movement was less than 400 ms and greater than 700 ms respectively; and target hold errors, when the subject did not stop and hold at the target for the required time.

2.1.3 Task design

The twelve subjects were divided into two groups of six subjects each. The first group (1 male, 5 females) performed the task only on one day, while the second group (5 males, 1 female) returned on the following day (a separation of approximately 24 hrs) to repeat the task. The first day was exactly the same for both the groups. Trials were grouped into blocks of 20 and a break of 15 seconds was provided after each block. The blocks were as described below.

On day 1 (groups 1 and 2), subjects first performed one block of reaching movements under full on-line visual feedback, in the absence of forces (the NULL field). This was followed by another block in the NULL field, but without online visual feedback of the motion of the hand. This was accomplished by blanking out the cursor when a window, of radius 1.5 times the radius of the start circle, was crossed. After these two blocks in the NULL field, subjects were asked to perform 25 blocks in the presence of forces, without visual feedback (similar to the second block). The exact structure of the force fields is described below.

On day 2 (group 2 only), the subjects started with 25 blocks in the presence of forces that were structured exactly as for day 1. This was followed by two blocks in which the forces were not applied on certain trials (catch trials), randomly chosen with a probability of 0.25. It should be noted that the catch trials were never allowed to occur consecutively, irrespective of whether a trial was completed correctly or not. Furthermore, for the catch trials, the cues were presented as for the force trials, so that the subjects could not predict their occurrence.

2.1.4 Generation of the force field

The forces were generated by two torque motors acting on the handle of the robotic arm, which the subjects held with the right hand. The forces were proportional to the tangential hand velocity and directed perpendicular to the desired direction of motion either to the left or to the right; i.e., the forces tended to perturb the subject's hand perpendicular to the direction of motion. The force fields can be expressed as

$$F_x = b \times v_y, \qquad F_y = 0 \qquad \text{[Group 1]} \tag{2.1}$$

$$F_x = -b \times v_y, \qquad F_y = 0 \qquad \text{[Group 2]} \tag{2.2}$$

where v_y represents the y-component of the hand velocity, F_x and F_y are the x- and y-components of the force, and b is the viscosity coefficient. This viscosity coefficient was picked at the beginning of each trial, randomly from either of two Gaussian distributions of identical variance (22 N^2s^2/m^2) and respective means +15 Ns/m and 15 Ns/m. To ensure complete randomness, the viscosity coefficients were selected right before each trial without any sort of constraint (on number or order). As a consequence, the sequence of coefficients was independent for individual subjects (in contrast, for example, with Scheidt et al., 2001). Note that the different signs for F_x for the two groups in Eqs. 2.1 and 2.2 above does not result in any fundamental difference in the force fields produced. Rather, it merely causes a positive viscosity coefficient to generate rightward forces for group 1, and leftward forces for group 2 (vice versa for negative viscosities). When describing the results (Chapter 3), we refer to 'right' (RF) and 'left' (LF) forces instead of 'positive' and

'negative' viscosities as the direction of the force is what is relevant and not the sign of the viscosity.

2.1.5 Data analysis

To assess the performance of subjects, we calculated an average signed hand-path error for each trial by first computing a sample-by-sample difference between the hand trajectory of the subject and the straight line connecting the start to the end target, and then averaging it over the trial (Eq. 2.3). This approach was motivated by several studies that have shown the straight-line path to be the "desired" trajectory of such reaching movements, and that the hand-paths of subjects deviate in the direction of the force (Gandolfo, Mussa-Ivaldi, and Bizzi, 1996; Shadmehr and Mussa-Ivaldi, 1994; Morasso, 1981).

$$\text{Signed Error} = \frac{1}{N_{samples}} \sum_i (x_{i,actual} - x_{i,straightline}) \tag{2.3}$$

The coordinate system was such that 'up' on the screen and 'forward' in the movement plane corresponded to the positive-y axis, while 'right' on the screen as well as in the movement plane was the positive-x axis. x in the above equation denotes the x-component of the manipulandum's instantaneous position.

To analyze the trend of the errors over the course of the experiment, we first separated trials performed in RF from those in LF. Trials were then binned into blocks of 20 for each subject, the bins of the six subjects in a particular group were pooled, and an average signed hand-path error was calculated for the group. To analyze the catch trials, we first assigned them to LF or RF according to the color of the cue that was displayed before the trial. Then, for each subject, the mean of the last 20 trials in a particular force field was subtracted from the mean of the errors on the catch trials in the same force field. Finally, this difference was assigned the same sign as the direction of the force field if the mean catch error was in the same direction as the mean error on the last 20 trials (indicating no aftereffects). However, if the mean catch error was opposite to the mean error on the last 20 trials, then the catch error was assigned a sign opposite to the force fields (indicating aftereffects). These six differences were then averaged over the subjects.

2.2 Neural recordings in monkeys

We trained two male rhesus monkey subjects (*Macaca mulatta*, ∼4.5 kg and ∼6.1 kg; both left-handed) to operate the same robotic manipulandum as described above (section 2.1.1), initially performing point-to-point movements to visually displayed targets. Subjects were seated in the same position for all sessions, with the non-performing arm restrained. Further, during the recording sessions, subjects' heads were also restrained.

During the training phase, the subjects were not exposed to any of the force fields studied during the course of the experiment. However, before electrode implantation, each subject was exposed to 1-2 sessions of 'unlearnable' forces to gauge the strength of the forces at which the subject can perform reasonably (see below). Once the subjects were adept at performing the basic task, surgery was performed to sub-durally implant chronic microelectrode arrays (see Fig. 2.3). The relevant protocol for animal experimentation was approved by the Institutional Animal Care and Use Committee of the Veterans Affairs Medical Center (Minneapolis). The guidelines of "Public Health Service Policy on Humane Care: Use of Laboratory Animals by Awardee Institutions" and the "NIH Principles for Use of Animals" were followed.

2.2.1 Basic task design

Under all task conditions, the subjects executed two-dimensional horizontal reaching movements with the manipulandum from a central location to one of eight targets equally spaced around a circle of radius ∼9 cm. The center location and the targets were displayed on a monitor placed in front of the subject (at a distance of ∼55 cm). The monitor also provided the subject with real-time feedback of the position of the manipulandum via a cursor. To begin a trial the subject placed the feedback cursor inside a circular window (radius ∼1 cm) at the center of the display and held it for a control period (also referred to as the center-hold period; 800 ms in duration). After this, a peripheral circular target was displayed pseudo-randomly at one of the eight locations and remained visible for 500-700 ms serving as a cue for the subject. The target locations were randomized within sets of eight, and the subject had to complete correct movements in all eight directions before moving onto the next set. Following the disappearance of the cue there was a memory delay of 800-1000 ms after which the target reappeared, thus serving as a 'GO' signal. Successful movements were to be completed within 1000 ms and the subject finally had to stop and hold for 800 ms within the target circle (radius ∼1 cm) to obtain a juice reward. Fig. 2.1 shows the timecourse for each trial.

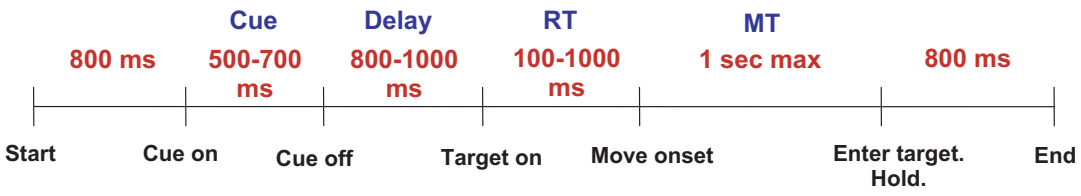

Figure 2.1: Time course of a trial depicting the order and duration of various epochs.

2.2.2 Design of the force fields

The force fields were designed to depend on the velocity (*viscous fields*) or position (*stiffness fields*) of the handle of the manipulandum. The forces were applied in a clockwise or counter-clockwise orientation, perpendicular to the direction of motion, a field structure known as 'curl fields'. In terms of equations the forces (in the units of Newtons) can be expressed as:

$$F_x = -b \times v_y, \qquad F_y = b \times v_x \qquad \text{(Velocity-based field)} \tag{2.4}$$

$$F_x = -k \times y, \qquad F_y = k \times x \qquad \text{(Position-based field)} \tag{2.5}$$

where F_x and F_y are the x- and y- components of the forces, v_x and v_y are the x- and y- components of the linear velocity of the manipulandum, x and y are the Cartesian coordinates of the location of the manipulandum, b is the viscosity coefficient and k is the stifness coefficient. For the first monkey, based on our preliminary sessions with the unlearnable force fields (see below), a value of 30 N/m/s was used for the viscosity coefficient while a value of 30 N/m was found to be appropriate for the stiffness coefficient. For the second monkey, we used a viscosity coefficient of 35 N/m/s and a stiffness coefficient of 40 N/m. A small note here: We started with a viscosity coefficient of 40 N/m/s for the first session for the first monkey (Session 4 of the recordings). However, considering the extremely poor performance of the monkey in that session, we decided to bring down the coefficient to 30 N/m/s for the rest of the experiment. The peak forces experienced by the subjects were higher in the viscous field as compared to the stiffness field, and, as will be discussed later, both subjects were faster at learning the stiffness field as compared to the viscous field. To allow the subjects to learn the fields (without getting frustrated), we relaxed some constraints on the movements, allowing a wider angle for the movement and, for the stiffness field for the first monkey, a 17% bigger target and center window.

The "unlearnable forces" were designed to depend sinusoidally on time. Further, they were applied at angles (120 or 300 degrees) different from the one at which the studied forces were applied (90 degrees). It has been shown that subjects are unable to adapt to time-dependent forces (Conditt and Mussa-Ivaldi, 1999; Karniel and Mussa-Ivaldi, 2003) and we made similar observations for the few sessions with our monkeys. We can reasonably say that these 1-2 sessions in the time-dependent force are unlikely to have any effect on the monkey's performance in the viscous and stiffness force-fields introduced more than a month later. The structure of these time dependent forces was as follows:

$$F(t) = A \times [1 - \cos(2\pi t/600)]$$

$$F_x(t) = F(t) \times \cos(\theta), \qquad F_y(t) = F(t) \times \sin(\theta) \tag{2.6}$$

where A was chosen as 1.5 and 2.0 for the two sessions for the first monkey and 2.0 for the brief solitary session for the second monkey, and θ alternated between 120 and 300 degrees for each trial.

2.2.3 Sequence of the force fields during neural recordings

We studied three different force fields for our experiment, in addition to the condition without any forces. The basic idea was to first allow the subject to adapt to one particular field (referred to as the 'main field') until his behavioral performance seemed to be approaching a plateau. We then repeatedly introduced the other (interfering) fields while allowing the subject a few sessions in the main field in between to allow him to get close to the pre-interference levels of behavioral performance. Subjects performed 1-2 sessions each day, with a session comprising of a variable number of trials, in general. On the day a new force-field was introduced, the subjects always performed two sessions. The first session consisted of 10-12 movements in each direction in the presence of the familiar force condition. The new condition was introduced in the second session and the subject was allowed to work as long as he wanted. On the day the forces were introduced for the first time, the subjects performed without any forces in the first session.

Tables 2.1 and 2.2 list the force field applied during each of the sessions for the first and the second subject, respectively, during the neural data collection and also the number of total trials as well as the number of trials correctly completed. For both monkeys, the viscous counter-clockwise field, VCCW, was chosen at the main field. For the second subject, we recorded for a few more sessions after the last one listed in the table. In these sessions we re-introduced the three intereferences for a second and a third time, in the same fashion as the first time. However, since we do not have the corresponding repetitions with the first monkey, I do not present their analysis in this thesis. The sequence of the force fields used for the two subjects is also shown in a pictorial form in Fig. 2.2.

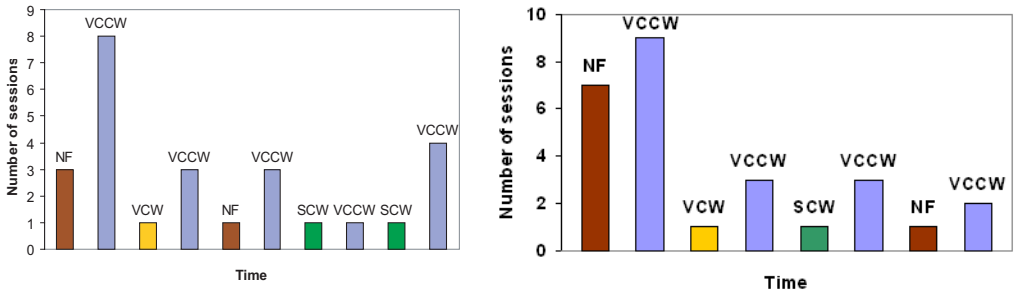

Figure 2.2: The temporal sequence of the introduction of the force fields during the recording sessions for the first monkey (left) and the second monkey (right).

Table 2.1: The force condition and the number of trials in each session during neural data collection for the first subject. NF: Null Field; VCCW: Viscous Counter-Clockwise Field; VCW: Viscous Clockwise Field; SCW: Stiffness Clockwise Field.

Day	Session number	Force field	Correct/Total trials
1	1	NF	199/211
2	2	NF	206/249
3	3	NF	103/112
3	4	VCCW	1/129
4	5	VCCW	22/415
5	6	VCCW	160/262
5	7	VCCW	110/156
6	8	VCCW	128/180
7	9	VCCW	160/204
7	10	VCCW	116/148
8	11	VCCW	80/99
8	12	VCW	5/304
9	13	VCCW	80/93
9	14	VCCW	417/447
10	15	VCCW	80/93
10	16	NF	94/102
11	17	VCCW	80/92
11	18	VCCW	286/316
12	19	VCCW	80/90
12	20	SCW	168/419
13	21	VCCW	80/95
13	22	SCW	326/442
14	23	VCCW	80/102
14	24	VCCW	517/533

2.2.4 Implantation of chronic electrode arrays

Once the subject was familiar with the control task, a surgery was performed under aseptic conditions using inhalation anesthesia. The implantation of the chronic electrode arrays was done by first removing a rectangular bone flap that allowed access to the primary motor and the dorsal premotor areas. The dura mater underneath the flap was then dissected and reflected (Fig. 2.3) enabling direct vision of the cortical surface. Each 96-electrode 'Utah' array (I2S Micro Implantable Systems [formerly Cyberkinetics, Inc.], Salt Lake City, Utah) was inserted using a hydraulic piston gun. The length of the individual electrodes in the arrays was 1.5 mm with an inter-electrode spacing of 400 μm. After that a layer of artificial dura was placed over the arrays, the dura mater was sutured back and another layer of artificial dura was tucked under the bone. The two reference wires for each array were slid under the top layer of the articial dura, thus lying on top of the dura

Table 2.2: The force condition and the number of trials in each session during neural data collection for the second subject. NF: Null Field; VCCW: Viscous Counter-Clockwise Field; VCW: Viscous Clockwise Field; SCW: Stiffness Clockwise Field.

Day	Session number	Force field	Correct/Total trials
1	1	NF	256/290
1	2	NF	264/290
2	3	NF	263/282
3	4	NF	165/171
3	5	NF	161/170
4	6	NF	348/368
5	7	NF	88/90
5	8	VCCW	1/100
5	9	VCCW	1/235
6	10	VCCW	24/266
6	11	VCCW	88/261
7	12	VCCW	125/183
7	13	VCCW	125/259
8	14	VCCW	84/135
9	15	VCCW	360/418
10	16	VCCW	80/98
10	17	VCW	12/449
11	18	VCCW	160/245
11	19	VCCW	272/314
12	20	VCCW	95/102
12	21	SCW	240/468
13	22	VCCW	132/195
13	23	VCCW	175/198
14	24	VCCW	96/107
14	25	NF	231/260
15	26	VCCW	449/480
16	27	VCCW	79/85

mater. Finally, the bone flap was replaced over the craniotomy and secured in place using a titanium strap screwed into the skull, and the area was covered with silastomer to seal the openings. The connector pedestals were secured on the skull using titanium screws and four titanium posts were implanted on the skull to allow a head-holding device to be attached.

2.2.5 Data collection

Behavioral data (position, velocity, forces, torques and event markers) were sampled and stored at 200 Hz via a Windows-based personal computer that was also used to control the behavioral task (using Visual Basic). Extracellular neural spike signals from the

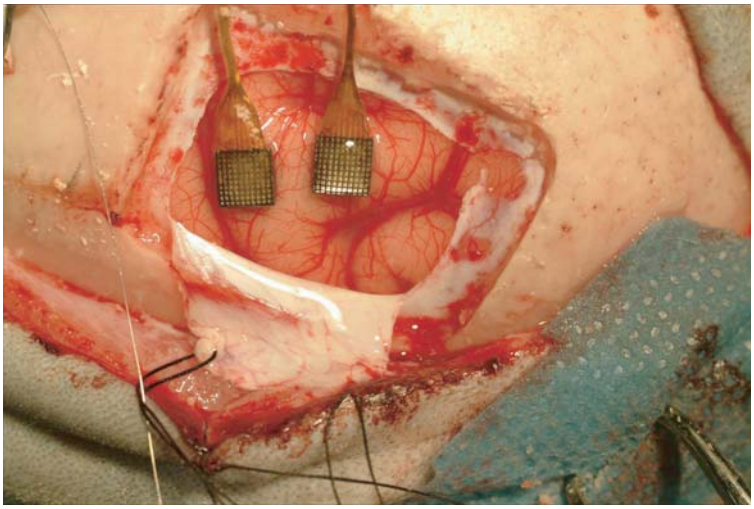

Figure 2.3: The implanatation site of the two electrode arrays for the first monkey. Right in the figure corresponds to anterior on the brain and up in the figure is approximately medial. The left array in implanted in the primary motor cortex just anterior to the central sulcus. The right array is in the dorsal premotor cortex, slightly dorsomedial to the spur of the arcuate sulcus.

chronically implanted arrays were band-pass filtered (500 Hz - 7.5 KHz) and sampled at 30 KHz. Only the waveforms that crossed a certain threshold, determined online at the time of recording, were stored for further analysis. LFP data was filtered between 0.3 Hz and 500 Hz and sampled at 2 KHz.

The electromyographic (EMG) recordings were made separately from the neural recording sessions. The EMG activity was sampled during performance of the task using intramuscular, teflon coated, 7-stranded stainless steel wires. The EMG signals were recorded differentially, amplified and band-pass filtered through a Grass amplifier system (the gain and bandwidth were adjusted each day depending on the signal quality), rectified and sampled at a rate of 200 Hz. The EMG activity of the following muscles was recorded: biceps, triceps, anterior and posterior deltoid, trapezius major, teres major, supraspinatus, infraspinatus, and pectoralis major. Four EMG channels were used at a time allowing us to record the activities of upto four muscles in any given session. The recorded data was inspected visually and only those recordings with stable and clean signals for the entire session were considered for further analysis.

2.2.6 Data pre-processing

For the purpose of analysis, some incorrect trials were also considered in addition to the correctly executed movements. This was necessitated due to the nature of the experiment: since the monkeys were performing under the forces for the first time, they made very few correct movements in the first couple of sessions in the forces. However, those first couple

of sessions are very important for analyses as they quite likely contain the earliest neural signatures of adaptation. Similarly, for the sessions where we introduced the interferences for the first time, there were a lot of error trials in the beginning as the monkey was trying to learn the new field; again these trials are important for the analysis. Therefore, to include them in the analysis we employed the following strategy. In addition to the correct movements, we also included trials in which the subject reached the target in time but was not able to hold there long enough (i.e., target hold errors). Further, for movements in which the monkey did not reach the target in time, either due to being too slow (move errors) or due to being too wide off the allowed range of paths (angle errors), we included those movements for analysis in which the monkey completed at least 4cm ($\sim$44%) of the movement toward the target before the trial was terminated due to an error.

Neural data

For the analysis of the neural data, different task epochs were defined as follows (in general). The baseline or the center-hold epoch, 'CHT', started at 100 ms after the subject entered the center and lasted for 400ms. The cue epoch, 'CUE', started 50 ms after the onset of cue display and lasted 350 ms. The memory delay epoch, 'DEL', started 50ms after the offset of the cue (marking the onset of the delay, with the screen blank) and lasted for 350 ms. The movement epoch, 'MOVE', started 250 ms before the onset of the movement (as detected by the subject leaving the center circle) and lasted 650 ms, thus ending 400 ms after the movement onset. Note that the 250 ms before the movement onset will contain part or all of the reaction time (which is between 100ms and 1s in duration). For some specific analyses, some of the epoch durations were varied or different epochs considered. These will be mentioned when I describe the analysis methods and the results.

Single-unit isolation

During neural recordings, the data collected from each channel is typically multi-unit, with noise present. The neural spike signals from each channel was checked for stability and classified into different units after removing the "noise waveforms". This was done using the Offline Spike Sorter from Plexon, Inc. Briefly, various features were calculated for each of the waveforms, including the first 8 principal components, peak-to-peak amplitude, peak, valley, width at half the peak height, energy, etc. The waveforms were then projected into two dimensional feature spaces selected from the above mentioned features. I then determined a set of features for which the spikes could be visualized as clusters that were as distinct as possible. These clusters were then separated, chiefly using manual techniques (drawing contours around clusters to delineate them). Finally, the waveforms in each cluster were visually inspected and re-assigned if desired. For the purpose of analysis we

considered only those units that fired at a rate greater than 0.75Hz on average during that session. The numbers of units that passed this test are shown in Chapter 4, Fig. 4.9.

Stability of single cells across recording days: For the purposes of this thesis, we did not attempt to verify whether the single cells recorded from a particular electrode were stable across days or not. As a consequence, all of the analysis using single cell data has been performed over the cells recorded during the same day, and cells from different recording days are treated as different.

Local field potentials

The LFP data was downsampled to 1KHz and usually filtered between 0 and 250Hz for most analyses. Channels were inspected visually (in the time-domain as well as the frequency domain) and the ones with significant line noise or 'bad signal' were not considered further. The numbers of such channels were small for the first subject (mean $\pm$ std: 9.35 ± 2.19 out of a total of 128) while the numbers were much higher for the second subject (30.75 ± 1.78 for the PMd and 17.63 ± 3.54 for the M1, out of a total of 64 for each area). In addition, some channels contained artifacts for one or more trials (very large amplitude, atypical of other trials and channels). To remove these, channels with a root-mean-square (RMS) value, calculated over the entire trial, greater than 5 times the standard deviation for more than 15% of the trials in that session were marked and removed from analyses. Finally, trials during which more than 15% of the channels had RMS values greater than 5 times the standard deviation were also removed from analyses. The numbers of such "outlier" channels and trials were usually small for all sessions (less than 4 channels for both subjects; less than 10 trials for the first subject 5 ± 6 trials for the second subject).

Chapter 3

Lack of Adaptation to Random Conflicting Gaussian-Distributed Force Fields

I will now present the results from our behavioral experiment where we studied the adaptation of reaching movements to randomly applied force-fields in human subjects. As explained in previous chapters, subjects readily learn to operate in new mechanical environments (Shadmehr and Mussa-Ivaldi, 1994). However, simultaneous exposure to opposite or conflicting force-fields (e.g. clockwise and counter clockwise) (Brashers-Krug, Shadmehr, and Bizzi, 1996; Caithness et al., 2004) often interferes with the learning process. The interference has been observed both when the fields were alternated trial-by-trial, or presented in alternating blocks. It is generally believed that the interference observed following exposure to opposite force fields in close temporal proximity is due to disruption in the consolidation of the short-term memory (but see Caithness et al., 2004).

This view has been recently challenged by demonstrating that simultaneous learning of conflicting viscous force fields is possible provided these fields are presented randomly and appropriate contextual cues are provided (Osu et al., 2004; Wada et al., 2003). To explain their intriguing result, the authors in these studies proposed that the subjects formed two internal models simultaneously and were able to switch between them using the available contextual cues, in accordance with the MOSAIC model (Wolpert and Kawato, 1998; Haruno, Wolpert, and Kawato, 2001). The latter finding raised the question of whether such simultaneous context-based learning of conflicting environments could be applied to other situations as well. One important generalization would be to uncertain environments in which the forces varied randomly in magnitude (Scheidt, Dingwell, and Mussa-Ivaldi, 2001; Takahashi, Scheidt, and Reinkensmeyer, 2001) as well as direction. Based on these earlier results, we reasoned that given sufficient practice and appropriate contextual cues,

subjects should be able to adapt to a combined field comprising two randomly switching identical distributions of viscosity coefficients, one generating clockwise (CW) and the other generating counter-clockwise (CCW) forces. Specifically, they would be expected to compensate for a perturbation close to the mean value of the applied force fields. Our results, discussed below, demonstrate that human subjects were not able to form internal models of such an unpredictable and conflicting environment.

3.1 Results

3.1.1 Time course of adaptation

We initially asked a group of six subjects (Group 1) to perform a single session of reaching movements during which their arm was perturbed by two randomly presented conflicting viscous force fields (see Section 2.1 for detailed methods). The viscosity coefficient was selected randomly at the beginning of each trial from either of two Gaussian distributions. As expected, the initial trajectories of the subjects deviated in the direction of the forces in both fields; Fig 3.1a depicts the hand-paths of a typical subject from the group during both early (left panel) and late force blocks (right panel). However, the pattern of deviation persisted throughout the experiment so that the hand-paths were still curved at the end of the experiment; in fact, at times the extent of the curvature of the trajectory appeared to increase over time. This indicates that the subjects were unable to adapt to the applied forces.

The time course of the average performance across the subjects is plotted in Fig 3.2a, separately for the left-directed (LF; red) and the right-directed (RF; blue) force fields. It can be seen that, on average, the hand-path errors did not decrease with practice, confirming that the subjects were not able to adapt to the force-fields. The errors at the end of the experiment (last 20 trials in a particular force field) were significantly different from zero ($p < 0.005$; two-tailed t-test) for all six subjects in RF and four subjects in LF ($p > 0.2$ for the other two subjects, S3 and S5). Further, they were not significantly smaller in magnitude ($p > 0.7$; one-tailed paired t-test) than the errors at the start (first 20 trials in a particular force field) for all subjects in RF and three subjects in LF ($p < 0.01$ for the other three subjects, S3, S4 and S5). Subjects seem to have performed, both quantitatively and qualitatively (Fig 3.2a), slightly better in LF than RF, which may have been due to possibly greater stability in the posture when the forces pushed their arms inward in LF as against outward in RF (all subjects were right-handed and the desired movement was approximately aligned with the right-shoulder joint).

To test for the possibility that the subjects may not have received sufficient practice on the task, we repeated the experiment with a second group of six subjects (Group 2) who performed two sessions over consecutive days. Fig 3.1b shows the trajectories

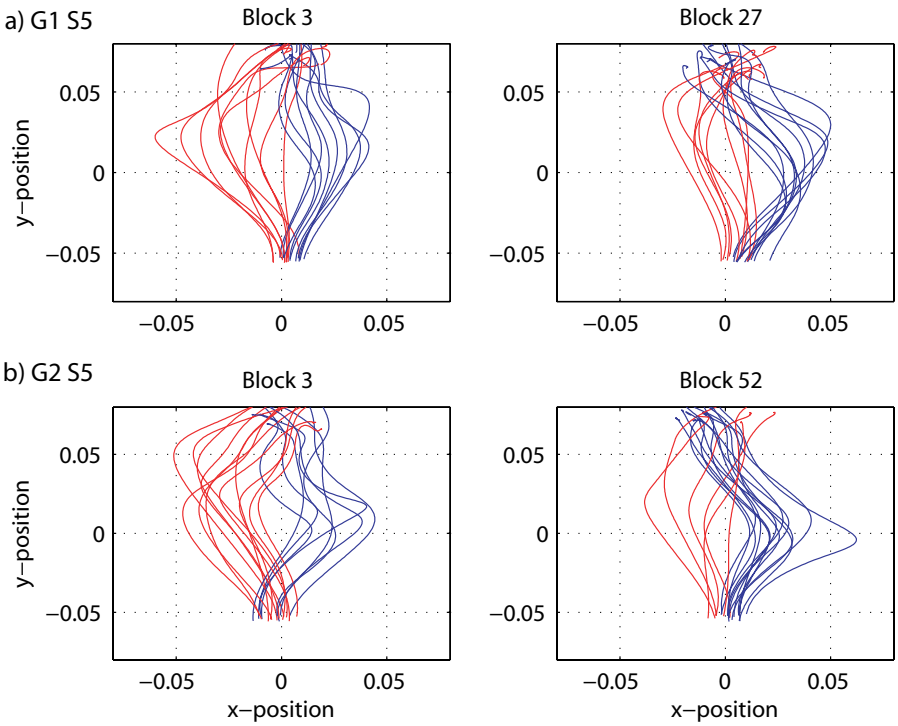

Figure 3.1: Hand-paths of a typical subject. Plots of hand trajectories of a typical subject in Group 1 (a) and Group 2 (b) for the first block (20 trials) in the force-field (left) and the last block in the force-field (right), not considering the catch blocks for Group 2. Trials in LF are shown in red, while those in RF are in blue. It is seen that, for both subjects, the hand paths deviate in the direction of the forces when the fields are introduced and remain perturbed even after extensive practice.

from a representative subject at the start (left) and the end (right) of the experiment. Trajectories remained curved even after extended practice, as was the case for Group 1. The average performance of the subjects is plotted in Fig 3.2b for both days. Again, there is no evidence of adaptation; in fact the errors seem to have increased in magnitude over the course of the experiment, indicating that the extra day of practice did not help. The error at the end of the experiment was again significantly different from zero ($p < 0.001$) for all subjects in RF and three subject in LF (for the other three subjects, $p = 0.02$ for S5, $p > 0.1$ for S4 and S6), and not significantly smaller in magnitude than the error at the start ($p > 0.7$) for all subjects in RF and three subjects in LF (for the other three, $p = 0.014$ for S5,

The two points on the far right in Fig 3.2b show the average error on the catch trials. The calculation of the average over the subjects was complicated by a subject (S2) that consistently showed rightward paths under LF conditions on Day 2. The error of this subject on catch trials was also on the right side, which, although is opposite to the

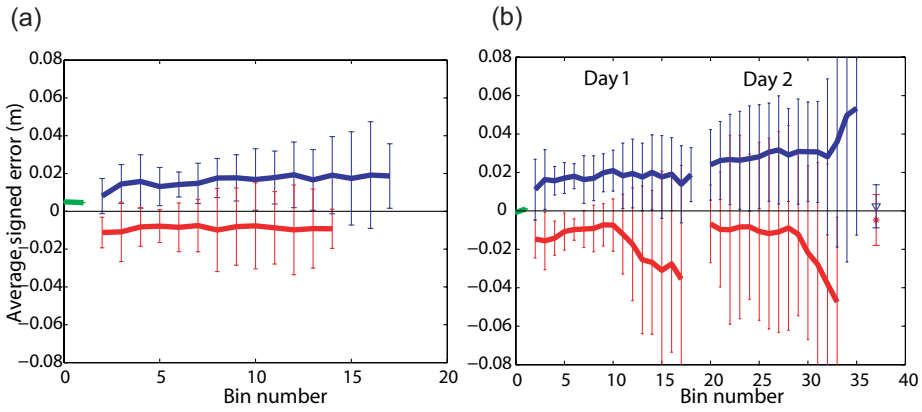

Figure 3.2: Average performance of the subjects. Average signed hand-path error ± SEM is plotted against bin number for subjects in Group 1 **(a)** and Group 2 **(b)** in the NULL trials (green), rightward deflecting force field (RF; blue) and leftward deflecting force field (LF; red). For Group 2, the left curves represent performance on Day 1 while the right curves are for Day 2. Trials in the last two blocks that contained random catch trials ("catch blocks") have been excluded from the plot for Day 2. It can be seen that the error does not decrease with time. The two points on the far right of the plot for Group 2 show the average ± SEM of the catch trials (see Section 2.1 for methods); there is no evidence of aftereffects. High standard errors are seen in force trials for both groups because of variations between performances of subjects and the fact that each subject performed different number of trials in either field so that the number of trials per bin is smaller for higher bin numbers. Note that the error bars overlap to some extent.

direction of the applied force, is still in the same direction as his errors on force trials. As such, it is inappropriate to consider this as evidence of aftereffects. With S2 included, the average of errors on all the catch trials (over all the subjects) in LF was +0.0123 (significantly different from zero and in the opposite direction, $p = 0.0141$, suggesting significant aftereffects), while if S2 was excluded the average was +0.0072 (not significantly different from 0, $p = 0.1142$, indicating no aftereffects). To work around this problem and include S2 in our analysis without misrepresenting the aftereffects, we used a different method to calculate the average (see Section 2.1 for methods). These are plotted in the figure and provide no evidence of aftereffects on average in both LF and RF.

3.1.2 Variation of hand-path errors with the applied forces

Having not found any signs of adaptation to the force-fields, we wondered if there was any pattern in the variation of the errors with the force magnitude (which was proportional to the viscosity). As expected, the hand-path error varied almost linearly with the applied force, both in LF and RF, with higher forces producing proportionally higher errors (Figs 3.3a,b). To estimate the value of the field strength that was "best compensated for", we calculated the viscosity at which the error was zero via linear interpolation of the curves

shown. This was found to be inconsistent among the subjects, and in particular, was not always close to the mean. For Group 2, the zero-error viscosity was 10.7 ± 7.6 Ns/m in LF (mean ± SD, $n = 4$; not defined for other two subjects– it would have required extrapolation) and −4.4 Ns/m in RF ($n = 1$). If the subjects would have "learned" the forces for a particular viscosity coefficient, one would expect the error at that viscosity to be close to zero. Figs 3.3a,b thus suggest that the subjects did not learn the mean value of either of the distributions, as against what might have been expected if the results of previous studies that used such force-fields for one direction only could be generalized to our set-up (see Discussion). The lack of consistency among the subjects does not permit us to attach any meaning to the value of the viscosity at which the error was indeed found to be zero. We also plotted similar graphs for the left and right forces together to see if the subjects, not being able to separate the left and the right forces, instead learned the mean of the combined distribution (theoretically zero). Again, no consistent pattern was found (Fig 3.3c; zero-crossing viscosity 7.3 ± 7.9 Ns/m, $n = 6$). Finally, we checked the viscosity values at which the error was equal to the baseline (the average error in the NULL blocks), rather than zero, for each subject and found similar results.

3.1.3 Another independent measure of performance

One might argue that the force distribution may have been a little too complex, making the task too difficult for the subjects. This may, then, explain the lack of improvement we observe in the performance of the subjects. To test this, for the second group of subjects we used an additional independent measure of performance– the number of incorrect movements that a subject makes during the course of the task. Fig 3.4 plots the number of four different types of incorrect movements (see Section 2.1 for methods) averaged over the six subjects. It can be seen that the numbers progressively decline during the course of a single day, as well as for the overall experiment. A peak is observed at the start of the second day, but the magnitude of this peak is substantially lower than that at the start of Day 1. Indeed, for all the subjects pooled together, the proportion of incorrect movements in the first two blocks of day 1 was significantly greater than that in the first two blocks on day 2 (difference of proportion test, $z = 7.0824$, $p < 0.0001$), indicating that there was a consolidation of whatever the subjects learned on Day 1.

This figure thus indicates that although the hand path error of the subjects did not decrease with time, the number of incorrect movements certainly did. Therefore, we can safely conclude that subjects could perform the task satisfactorily under the conditions, and in fact improved some aspects of their performance, suggesting that lack of practice was not a concern.

We have thus shown that the subjects were unable to form internal models of either the individual force distributions or of the combined distribution. However, they did

demonstrate an improvement in performance in terms of a reduction in the number of incorrect movements as the task progressed.

3.2 Discussion

In this experiment we investigated the role of random presentation and context-based switching in the learning of conflicting dynamic force-fields. Our results show that subjects were not able to adapt to the force fields via the formation of internal models of the fields themselves, or of the overall distribution of force magnitudes. However, they did exhibit a significant improvement in performance in terms of a reduction in the number of incorrect movements, showing that they did learn some of the task properties.

It has been shown repeatedly in previous studies that exposure to conflicting dynamic force fields in close proximity results in interference, such that no net performance improvement is observed (Brashers-Krug, Shadmehr, and Bizzi, 1996; Shadmehr and Brashers-Krug, 1997; Karniel and Mussa-Ivaldi, 2002; Caithness et al., 2004). The exact mechanism of this effect is not clear, but it is generally believed that exposure to a second conflicting field results in retrograde interference leading to disruption of the short-term motor memory associated with the first (Brashers-Krug, Shadmehr, and Bizzi, 1996; Shadmehr and Brashers-Krug, 1997), unless sufficient time has elapsed for consolidation of the first field to occur (for another view, see Caithness et al., 2004). Recent work (Osu et al., 2004; Wada et al., 2003), however, has challenged the belief that simultaneous learning of internal models of conflicting force-fields is not possible by showing that if the force-fields are presented in a random order (vs. a predicable sequence) using appropriate contextual cues in each trial, then learning does appear to occur. The authors explained this as a context-based switching of multiple internal models, though it was not clear what exactly the role of random presentation was and why such a context-based switching was not possible under predictable exposure conditions (in alternating trials, for example). Our experiment was designed to test whether their observation could be generalized to more naturalistic dynamic environments in which the conflicting fields could have a variety of different magnitudes, as one might expect in everyday life. It has been shown that subjects tend to learn approximately the mean value of force distributions, if only in one direction, both for unimodal and bimodal distributions (Scheidt, Dingwell, and Mussa-Ivaldi, 2001; Takahashi, Scheidt, and Reinkensmeyer, 2001). Our experimental set-up was, in principle, very similar to that of Osu and colleagues (2004) except for the important difference that we sampled from a distribution of viscosity coefficients for each field, while in the task of Osu and colleagues, two fixed coefficients were used to generate the CW and CCW force fields.

The subjects in the present experiment failed to show any learning of the conflicting

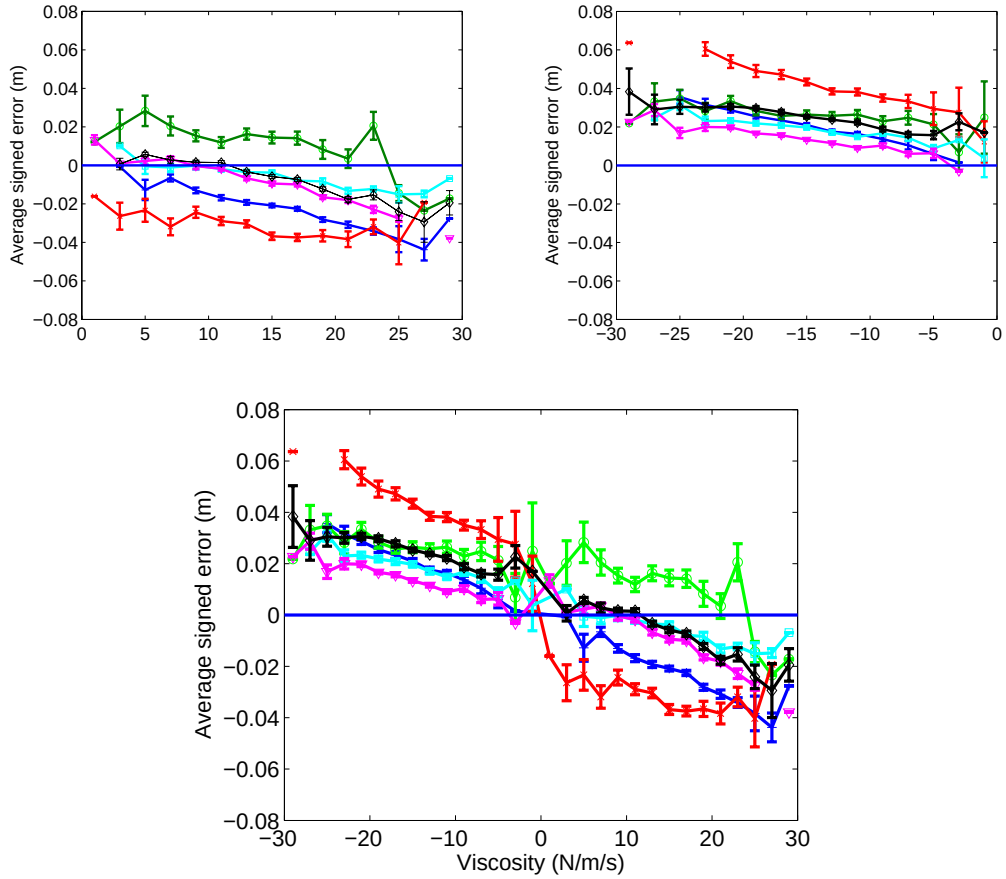

Figure 3.3: Hand-path error varies linearly with viscosity. Plot of average signed hand-path errors ± SEM vs. viscosity coefficients for LF (top left) and RF (top right) seprarately, and LF and RF together (bottom) for Group 2 subjects. Each subject is plotted individually (S1: blue, +; S2: green, o; S3: red, x; S4: cyan, square; S5: magenta, triangle; S6: black, diamond). Viscosity values were binned in 2 Ns/m bins and the mean error in each bin was calculated. Trials in the catch blocks have been excluded from the plots. The wide variation in standard error results partly due to different numbers of trials in each bin– due to the Gaussian distribution, viscosities were concentrated around the center (mean). It can be seen that for all the subjects, the errors are linearly correlated with viscosity. Also note that the curves are almost parallel in both (a) and (b). Plots for Group 1 showed a similar trend (not shown).

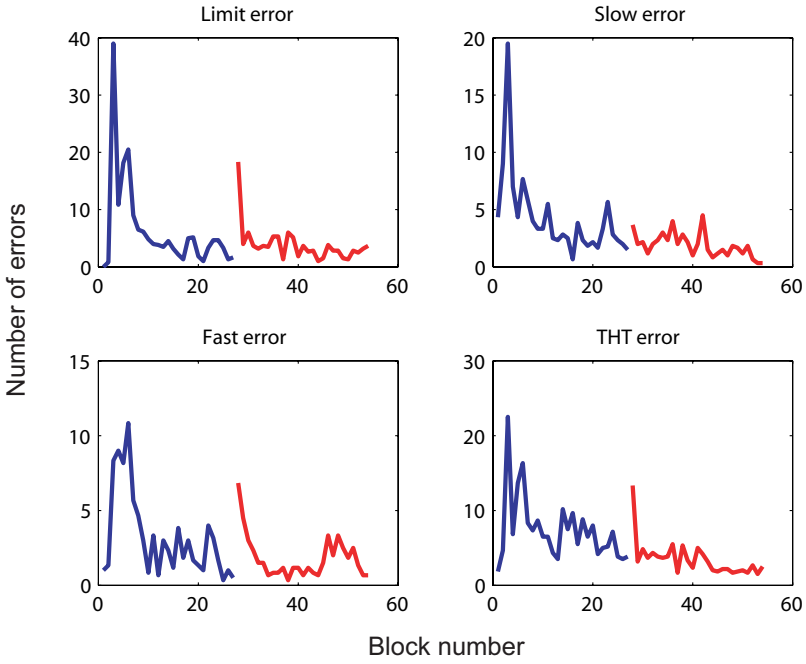

Figure 3.4: Subject performance improved with time. The number of the four different types of incorrect movements in each block (see Section 2.1 for methods), averaged over the six subjects in Group 2, is plotted against the block number. The blue curve is for day 1 (27 blocks, including NULL blocks), while the red curve is for day 2 (27 blocks; including catch blocks). The frequency of all the four types of incorrect movements decreased with time, overall as well as for each day separately, indicating that the subjects improved their performance with increased practice. The smaller peak at the start of day 2 as compared to start of day 1 suggests a consolidation of whatever the subjects learned on day 1.

force-fields. We also investigated whether the subjects learned the distribution of forces even though they did not acquire an internal model of the fields. Learning the magnitude could be done in one of two different ways. Subjects might learn the approximate mean of both the "left-centered" and the "right-centered" distribution of viscosity coefficients. However, if subjects were not able to separate the conflicting force fields they might treat the distribution of magnitudes to the right and left as being part of one continuous field in which case they will tend to learn the approximate mean of the combined (bimodal) distribution (theoretically zero). The calculated zero-error viscosity values (Fig 3.3) are inconsistent with either form of learning on the part of the subjects.

The efficacy of contextual cues in enabling subjects to simultaneously adapt to, and predictively switch between, multiple environments is a matter of debate. Some studies have shown that simultaneous learning of opposite environments, with appropriate switching (presumably of the two internal models), is possible if appropriate postural (Gandolfo, Mussa-Ivaldi, and Bizzi, 1996) or spatial (Rao and Shadmehr, 2001) cues are provided, but not with arbitrary color cues (Gandolfo, Mussa-Ivaldi, and Bizzi, 1996), even after extensive training (Shadmehr et al., 2005). Krouchev and Kalaska (2003), however, demonstrated that switching between opposite viscous fields based only on color cues is possible if monkeys are recalling a previously learned task (after extensive practice). One common thing about the training schedule in these studies is that they used predictable sequences of fields– either trial-by-trial switching or alternating blocked presentation. In contrast, other studies (Osu et al., 2004; Wada et al., 2003) showed that switching based entirely on color cues only is possible if the fields are presented randomly. Our results show that, for two opposite distributions of field strengths, switching based only on color cues is not possible, even with random presentation. Some possible reasons for the discrepancy in our results and those of Osu et al. (2004) and Wada et al. (2003) could be the difference in the amount of training days and saliency of the cues. Although we had over 1000 trials, the training was done only over two days. It is possible that it takes more time for the learning to consolidate. Further, our color cues were displayed only for a short amount of time (300 ms) as against 1.5- 3.5 s in Wada et al. (2003). We chose a short interval to decrease the total amount of experimental time for the subjects and thus avoid tediousness. Some of our subjects did report that they in fact found the cues helpful, some others expressed "boredom" while others did not find them explicitly useful. We believe, however, that the short cue interval cannot account for our results.

It might be argued that our task was not learnable in the allotted time since it involved two distributions and was thus much more complex than what is generally used by investigators. However, we used only one direction of movement and subjects performed more than 1000 movements in the force field. Scheidt, Dingwell, and Mussa-Ivaldi (2001) had a very similar set-up in their experiment except that the perturbation was applied

only in one direction (no conflict). Moreover, they used lot fewer trials (400 trials for the bimodal distribution, 200 for the unimodal distribution), but still demonstrated significant learning. In addition, the second group of subjects in our experiment had an overnight break that might have been expected to consolidate their learning. Therefore, it would not be unreasonable to say that subjects were allowed ample practice. This is supported by Fig 3.2, which shows that subjects provided with two days of practice did not fare better than subjects who practiced on only one day. Even more striking are the plots in Fig 3.4, which clearly show an improvement in performance in terms of a reduction in the number of incorrect movements as the task progressed. This was observed on both the days. We also observed an increase in the number of errors at the beginning of the second day, and, interestingly, this number was significantly smaller than that at the start of the first day. We interpret the incorrect-movement-number-reduction data as indicating that subjects really did learn aspects of the behavior although in a different 'dimension' from the one of interest.

These observations are somewhat paradoxical. The fact that the number of incorrect movements made by the subjects decreased with time, showed that subjects were able to figure out how to complete the movements correctly under the constraints imposed. On the other hand, despite prolonged exposure to the force condition, they did not regain the "expected" straight-line hand paths produced in the absence of forces. We speculate that this could be because they found an "easier" way to make the movements, viz., to follow a curved hand-path in accordance with the force applied, rather than trying to counter the forces. This idea is supported by the fact that the hand-path errors were linearly related to the viscosity magnitudes for all the subjects (Fig 3.3), with higher and lower viscosities giving rise to higher and lower errors, respectively. Furthermore, we believe this could also account for the increasing trends in Fig 3.2, which indicates that the error magnitudes actually increased with time. A final piece of supporting evidence is provided by plots of hand trajectories for subjects, which showed an increase in the curvature as the task progressed. In summary then, it seems that, being unable to form internal models that would adequately compensate for the applied external forces, subjects decided to forego the "desired" straight-line trajectories, and simply resorted to move with the force.

In conclusion, human subjects were unable to form internal models of simultaneously applied, randomly switched conflicting stochastic dynamic perturbations in the presence of contextual cues, even after practice on more than thousand trials. While it is possible that the time given may be not sufficient to allow learning, our results suggest that this is quite unlikely. Rather, our results indicate that the effects of random presentation and context-based switching documented in Osu et al. (2004) and Wada et al. (2003) may not apply to more general settings.

Chapter 4

Neural correlates of force-field learning in single cells

As I discussed in the introductory chapter (Chapter 1), there exists a wealth of behavioral data from studies dating as far back as (at least) the early 1990's that humans can adapt to a variety of force-field perturbations and retain their skill for extended periods of time. However, the neural basis of this adaptation has only recently begun to be explored (mainly by the Bizzi group; see Gandolfo et al., 2000; Li, Padoa-Schioppa, and Bizzi, 2001). In these studies, naïve monkeys were exposed to a session in the same viscous force field each day, before and after performing the same number of trials without any forces. The researchers then compared the direction-tuning properties and average firing rates of single cells across trials showing similar kinematics in the three sessions. As such, the learning phase of the monkey's performance, where the kinematics of the behavior changed, was ignored. Furthermore, the perturbation applied was very weak such that the subjects could perform pre-force kinematics after as few as 4-5 learning trials per direction.

We took a very different approach for our experiments. We exposed naïve monkeys to a much stronger perturbation, such that the learning of the force field took place over a few days, rather than within a few trials. This allowed us to examine in detail the neural activity over an extended period of time when the monkey was acquiring skill related to the force field, as evidenced by a gradual improvement in the behavioral performance. This experimental paradigm was complemented with a high-yield, chronic neural recording set-up (cf. the acute recordings in the previous studies). It is also important to note that our paradigm allowed the subjects to learn a particular force field without any interruptions for a few days (cf. the washout of learning each day in the studies by the Bizzi group). Furthermore, after a certain level of (uninterrupted) skill acquisition in the main field, we periodiclaly interfered with the subjects' learning using multiple conflicting fields that have been shown to disrupt motor learning in human behavioral studies. The interferences

were introduced in a controlled manner and followed the A-B-A paradigm used in human studies (see Chapter 1, Section 1.5). In this thesis, I present neural results related only to the adaptation to, and the switching of, force fields, and not the interference aspect of the task.

We found behavioral evidence for adaptation as well as interference in the hand trajectories of both of our subjects (Section 4.1). However, unlike the studies from the Bizzi group, we did not observe systematic changes in the preferred directions of single cells as the force conditions changed (Section 4.3). The muscles, however, did rotate their preferred directions in the direction of applied force (Section 4.2), as would be expected and has been previously shown (e.g. Li, Padoa-Schioppa, and Bizzi, 2001). Using a multiple regression analysis (Section 4.4), we found that the single cells adaptively change the relative weighting in their firing rates of important kinetic and kinematic variables depending on the force conditions of the task. Furthermore, we found that the number of cells actively engaged in 'coding' for a particular variable is modulated as a function of the novelty of the force fields to the subject, with an increase observed when the subjects are learning new fields. Our results suggest that single cells participate in internal models of multiple force-fields and can adaptively regulate their involvement towards performance in different force conditions. The results from the analysis of local field potentials are presented in the next chapter. Chapter 7 discusses our results in greater detail.

4.1 Evidence of adaptation from the behavior

Recordings for both monkeys began with a few sessions in the null field (i.e., no forces were imposed). After this, we introduced a viscous counter-clockwise force field (VCCW) as the main field for both subjects and allowed them uninterrupted practice in this field for a few sessions (see Chapter 2, Tables 2.1 and 2.2 and Fig. 4.1; Fig. 4.1 is same as Fig. 2.2, and has been reproduced here for reader's convenience). The hand-paths of the first subject on a few of the trials are shown in Fig. 4.2 for the last session before the introduction of the forces and for the first three sessions in the presence of the forces. The paths can be seen to be perturbed in the first force session and in the initial part of the second session, but they recover by the end of the third session. A similar pattern of results was found for the second subject (results not shown). To check if the subjects were compensating for the forces in a predictive manner, rather than co-contracting their muscles, we randomly turned off forces for a small fraction of trials– one trial for every 16 correctly completed movements (i.e., 2 movements per direction). These trials are called 'catch trials' and the subject is not given any clue to predict their occurence. Fig. 4.3 plots the trajectories in the presence of the forces and for the catch trials for two sessions for the first subject. While the trajectories in the presence of the fores are quite straight, the trajectories for

the catch trials show a marked deviation opposite to the direction of the applied forces, indicating the formation of an "internal model" of the force fields. Similar results were found for the second subject (figures not shown).

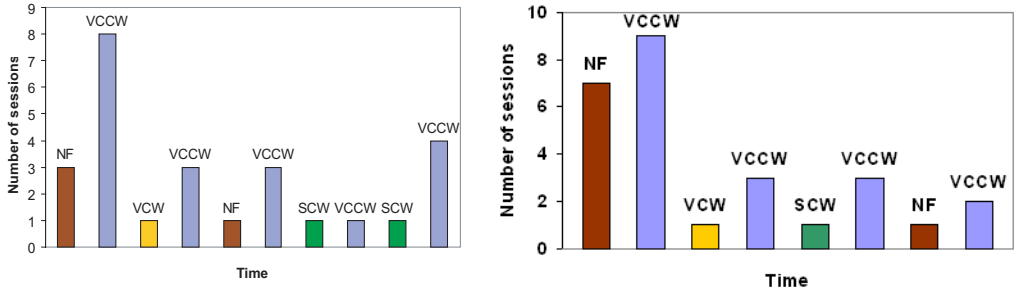

Figure 4.1: The temporal sequence of the introduction of the force fields during the recording sessions for the first monkey (left) and the second monkey (right). Same as Fig. 2.2; reproduced here for reader's convenience.

To quantify the perturbation of the hand trajectory from the ideal straight-line path from the center to the target, a number of different measures were tried out. These include the mean of the absolute difference between the actual and the ideal paths (mean area under the curve), the mean of the signed difference (similar in principle to Eq. 2.3) and the maximum difference. The pattern of results were found to be similar in general and I show here only the results using the mean signed difference. Fig. 4.4 plots the results for both the subjects. Different colors represent different force fields as described in the figure legend. For each session, the deviation measure was calculated for each trial that was analyzed (see Chapter 2, Section 2.2.6) and then smoothed using a moving-average method with a rectangular window of 17 trials. The sessions were then concatenated and plotted as in the figure. As would have been expected, when the forces were first introduced (the main field– VCCW; the first set of blue curves), both subjects' hand paths were pertubed strongly relative to the null field (the initial green traces). As the subjects performed more and more in the same field, their performance improved, as evidenced by the gradual decrease in the hand-path deviation toward the baseline levels. This indicates that the subjects were learning the force-fields during those sessions. I must remark here on the apparently anomalous pattern seen for the second monkey (the panel on the right). It is seen that as the subject's hand-path deviation in the VCCW field aproaches the baseline levels, it tends to transiently shoot past zero and then recover back. A negative value of the hand-path deviation indicates that the subject's trajectories deviated in the clockwise direction, inspite of the counter-clockwise field. This came about because in one particular direction (straight towards the monkey), the monkey tended to overcompensate initially, later allowing the forces to push him towards the target. However, with more practice the subject was able to learn the field, and thus compensate for it more efficiently

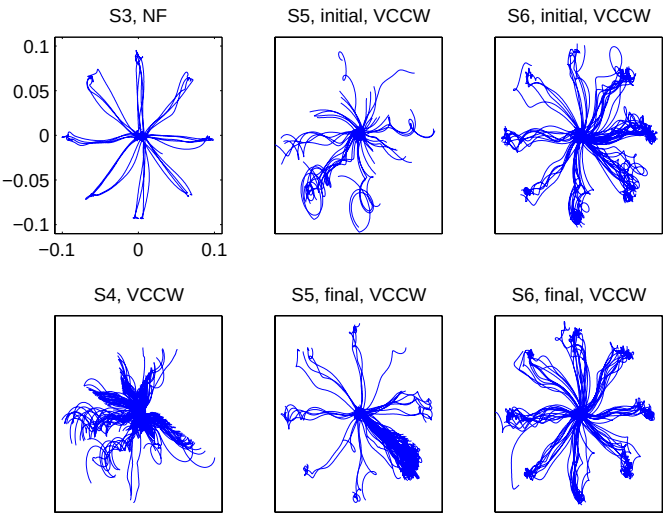

Figure 4.2: Trajectories for the first subject in the last session before the introduction of the forces (S3) and for the first three sessions in the presence of the forces (S4, S5 and S6). In the titles on each panel, 'initial' refers to the initial few trials in the session, while 'final' denotes the final few trials in the session. The first session of performance in the force fields shows a considerable perturbation from the straight-line trajectories of S3, but the trajectories can be seen to have recovered by the end of the S6. The x and y axes in the plots depict the x- and y-components, respectively, of the subject's hand position (in the units of meters).

(thus the recovery to the positive side). It must also be remarked that the second subject showed a smaller initial perturbation than the first.

Evidence for the acquisition of an internal model is provided by an analysis of catch trials. As Fig. 4.5 shows, the decrease of the subjects' hand-path deviation on the force trials is paralleled by a simultaneous increase of the deviation in the opposite direction on the catch trials.

Next, the introduction of the first interference, the viscous clockwise field (VCW), again caused a jump in the hand-path deviations, but this time in the opposite direction (the red traces in Fig. 4.4). Rapid learning was observed in this session for both subjects, although at the end of the session the first subject remains further away from the baseline as compared to the second. We can reasonably conclude that although the subjects haven't mastered the VCW field, they have demonstrated some level of learning and skill acquisition in the field. Importantly, in the session(s) immediately following the interference (the sessions on the next day), the subjects' performance can be seen to be poorer than in the session immediately preceeding the interference, more so for the second subject than for the first (the second set of blue curves in the figure). This is evidence that the subjects' "memory" of the main field (VCCW) was (at least partially) disrupted

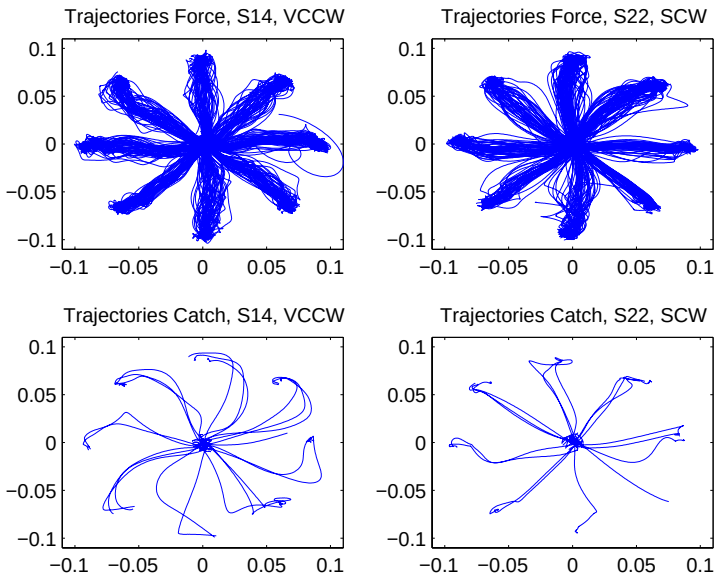

Figure 4.3: The trajectories of the first subject are shown for the force trials (top) and for the catch trials (bottom). The x and y axes plot the x- and y-components, respectively, of the subject's hand position (in the units of meters). The trajectories in the presence of forces are quite straight indicating that the subject can perform well. On the other hand, the catch trajectories show a marked deviation in a direction opposite to that of the applied forces, indicating the formation of an internal model of the force fields.

by the single session in the opposite field (VCW) and that the subjects had to re-learn the VCCW field to some extent. This is exactly what has been observed in the behavioral human studies using the same paradigm.

A similar pattern of the hand-path deviation was observed for the subsequent interferences (one NF and two SCWs for the first subject and one of NF and SCW each for the second; green and black curves in Fig. 4.4). However, it can be noted that the effect of the subsequent interferences is much smaller than that of the first, even for the same kind of interfering field (see the two instances of SCW for the first subject, left panel). At first glance, this might seem to suggest a gradual consolidation of the subjects' learning of the main VCCW field, thus making it more resistant to disruption. However, it is also possible that this results simply from a general improvement in the subjects' ability to perform in force-fields (a phenomenon that has been called "learning-to-learn"). We do not attempt to distinguish between these two possibilities for the purposes of this thesis.

To check for possible long-term learning in the main force field in spite of the transient disruptions due to the interferences, I performed the following analysis for the first subject. From all the sessions in the main field, I removed the sessions immediately after an interfering field (due to the fact that they showed high hand-path deviations because

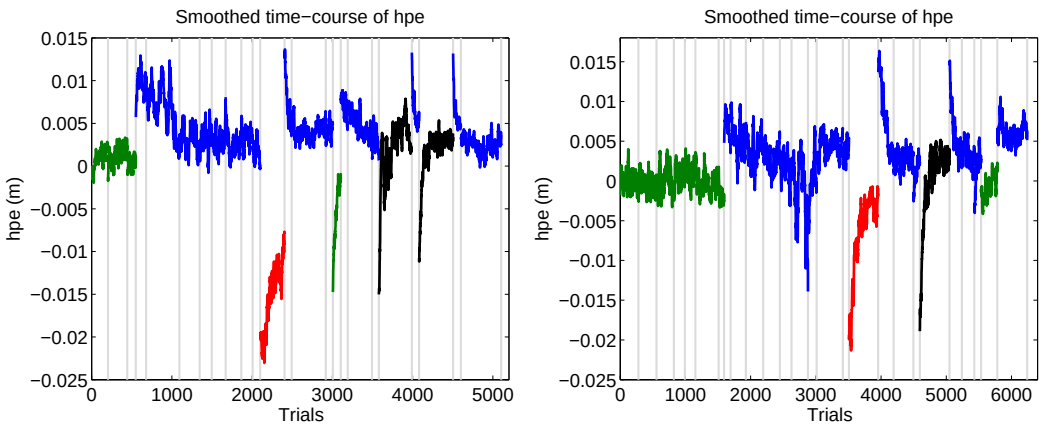

Figure 4.4: Summary of the behavioral performance of both subjects. The data plotted are the smoothed measures of the mean signed difference between the actual trajectiory of the subject and the ideal straight-line path between the center and the target. The data are plotted for the 24 sessions for the first monkey on the left, and the 27 sessions for the second monkey on the right. The vertical gray lines mark the boundaries between consecutive sessions. Each color depicts a different force field- green is for the null field (NF), blue is for VCCW, red is for VCW while black is for SCW.

of the interference of the previous field), and concatenated the other sessions into a continuous stream of trials. For each trial, I compute the average absolute deviation between the actual and ideal path (cf. the average signed deviation shown in Fig. 4.4) and, after smoothing, fit these data with an exponential function (Fig. 4.6). I found this exponential function to be still decreasing (slowly) at the end of the data, suggesting that despite the interferences, the monkey kept on improving his skill in the main field throughout the experiment.

In summary, the subjects' behavior provides evidence for the gradual learning of the VCCW field (concomitant with the acquisition of an internal model) and also for the interference caused by the VCW, SCW and NF fields.

4.2 Rotation of the preferred directions of muscles

Previous studies have shown that muscles rotate their preferred direction in the direction of the applied forces (e.g. Li, Padoa-Schioppa, and Bizzi, 2001). To verify this in our experiments, we recorded EMG activity from a total of nine muscles (Section 2.2.5 and Table 4.1). The EMGs were mainly recorded in sessions after the neural recordings were completed, and I do not present any data or analysis from simultaneous recording of neural and EMG data. Importantly, by the time of the EMG recordings, both subjects had had a lot of exposure to working with the forces, and we do not expect to see a lot of learning in these sessions. As such, all trials in all sessions with stable EMG signals from a particular

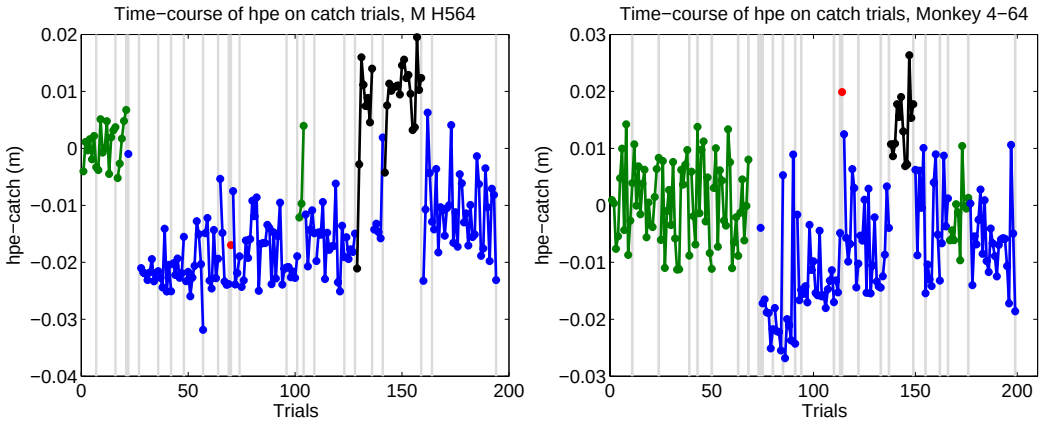

Figure 4.5: The time course of the hand-path deviation on the catch trials are plotted on the left for the first subject and on the right for the second subject. No smoothing has been performed due to small sample size. Same format as Fig. 4.4.

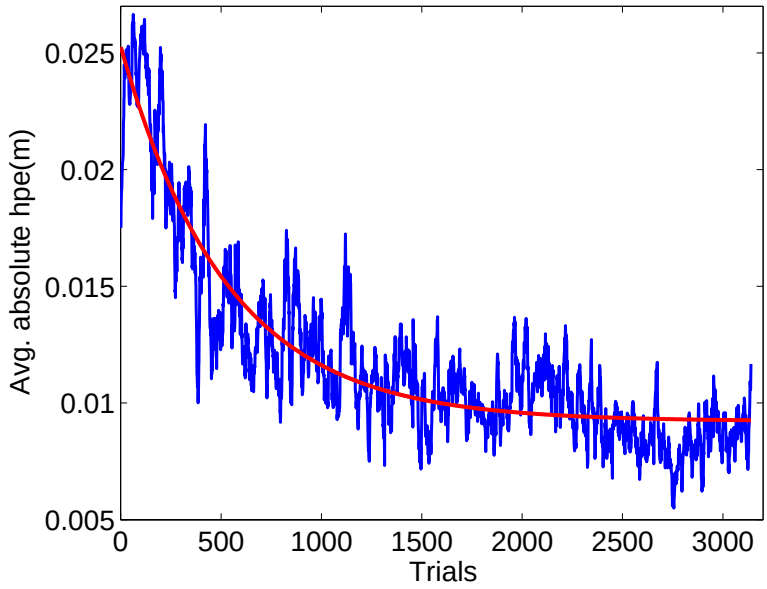

Figure 4.6: Plot of the average absolute hand-path deviations (blue curve) of the first subject during the sessions in the main field throughout the experiment, showing long-term learning. Sessions immediately after an interfering session were removed and the other sessions were concatenated. The data have been smoothed using a moving average method with a 17-trial window as in previous figures. The red curves denotes an exponential fit to the data.

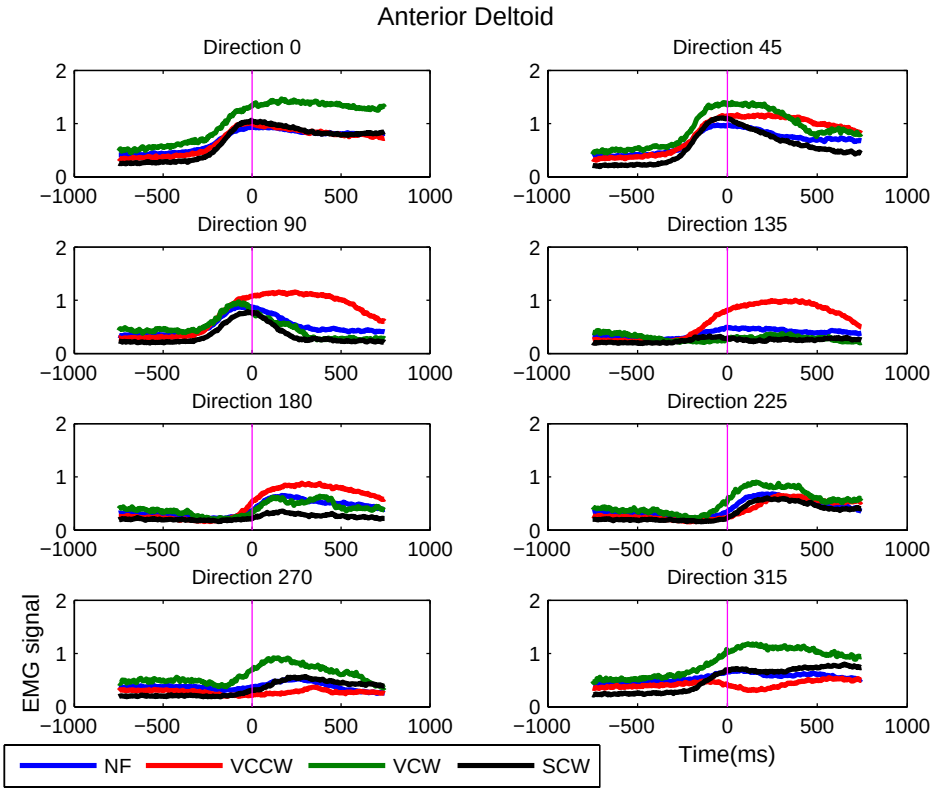

Figure 4.7: Plots of the trial-averaged EMG signal recorded from anterior deltoids in the first subject under all four force conditions (different colors). EMG was aligned to the onset of the movement before averaging (indicated by the vertical line).

muscle under a particular force condition were pooled together, irrespective of the day of performance. For each trial, I took the average of the rectified EMG signal in a window of -750 ms to 750 ms around the movement onset. This value was then averaged over all trials separately for each direction, thus giving a direction-tuning curve for each muscle under each force condition. Fig. 4.7 plots the trial-averaged EMG signal recorded from the anterior deltoids in the first monkey, aligned at the movement onset. All the four force conditions have been overlaid in the plots using different colors. The differential modulation of the EMG signal with respect to the direction of movement in different force fields can be clearly observed.

To show this more explicitly, Fig. 4.8 plots the tuning curves (blue) of the same muscle under the four force conditions. The red line gives the preferred direction of the muscle, computed simply as the vector average of the tuning curve. The star next to it denotes that the muscle was significantly tuned, as determined by bootstrapping over the length of the resultant vector. As would be expected the muscle rotates its preferred direction faithfully according to the direction of the applied force. This was found to be the case for all significantly tuned muscles for both monkeys. Table 4.1 lists the preferred directions of each muscle in each of the force conditions for both the monkeys.

4.3 Direction tuning of single cells

The ideas of direction-tuning and preferred direction were first introduced to characterize the single cells in the motor cortex by Georgopoulos and colleagues (Georgopoulos et al., 1982). Ever since, these concepts have played an important part in all studies of cellular firing properties in relation to the production of movements. As discussed in the introductory chapter, the neural studies of motor learning by the Bizzi group essentially categorized single cells into different classes on the basis of the direction of rotation of their respective preferred directions. One of the claims made in those studies was that the average shift in the preferred directions of the cells in the population tends to be in the direction of the applied forces. We performed similar, and some additional, analyses on our data. We did not find correlates of learning and switching force fields in the preferred directions of single cells or in the number of tuned cells. However, we did find changes in the quality of fit of a cosine function to the tuning curves on the days when the monkey showed a big improvement in behavioral performance. I describe our results in this section.

4.3.1 Task-related cells

The number of cells that were considered for analysis (see methods in Chapter 2, Section 2.2.6) for both subjects are shown in Fig. 4.9 for M1 and PMd separately, as well as for both areas combined. As the first step in the analysis of single-cell activity, we determined

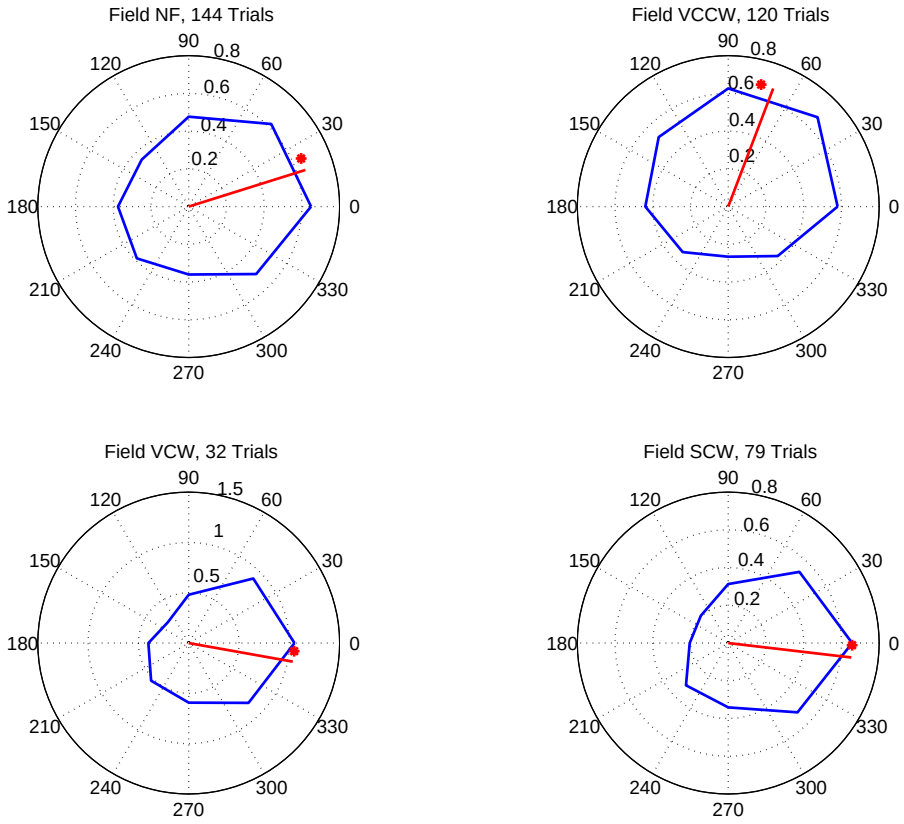

Figure 4.8: Tuning curves (blue) and the preferred directions (red) of the EMG activity recorded from anterior deltoids in the first subject under all four force conditions: from top left clockwise, NF, VCCW, VCW, SCW. A star next to the preferred direction vector denotes statistical significance ($p < 0.05$)

.

the number of cells that modulated their firing rates in any of the task epochs (CUE, DEL, MOVE) with respect to their rates in the center-hold period (CHT) over the entire session. The epochs were as defined in Section 2.2.6, except that the DEL epoch was 550 ms long, instead of the 350 ms mentioned there. I also analyzed the combination of the entire movement time and the reaction time (RT+MT) and found the results to be similar to the MOVE epoch; in what follows, I report only the results from the MOVE period. I performed a two-way analysis of variance (ANOVA), separately for each epoch, of the firing rates in the task epoch with 'epoch' (task vs. CHT) and 'direction' (eight levels) as factors. Cells with a significant main effect ($p < 0.05$, not corrected for multiple comparisons) of the epoch or a significant interaction between epoch and direction were considered as task-related. Fig. 4.10 plots the fraction of task-related cells for each epoch over all sessions for both monkeys (the fraction is taken the ratio of task-related cells to the total number of cells analyzed [see Fig. 4.9]). As expected the fraction was highest

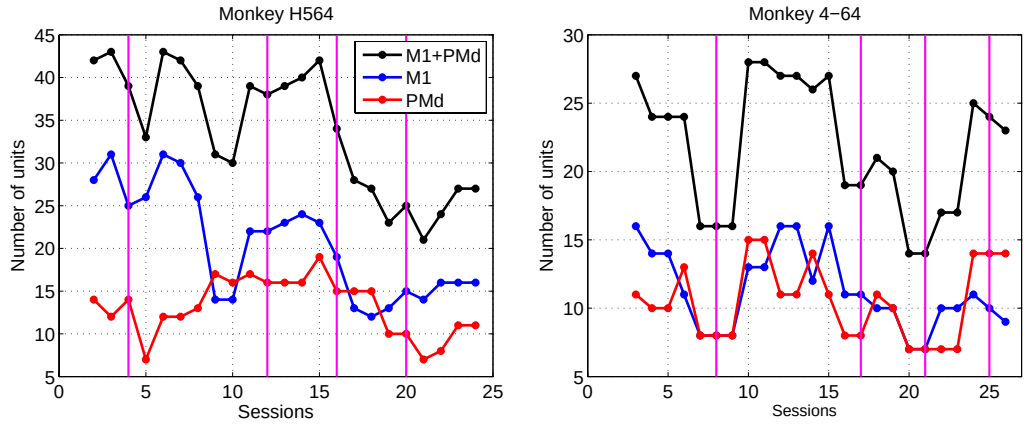

Figure 4.9: Number of cells that were considered for analysis for monkey 1 (left) and monkey 2 (right). These are the cells that fired at a rate greater than 0.75 Hz on average over the entire session. The vertical magenta lines mark the sessions in which a new force was inroduced (the second session of the corresponding day). For the first monkey, the lines represent (in order): the introduction of the main field, VCCW; the introduction of the first interference, VCW; the introduction of the second interference, NF; and, the introduction of the third interference, SCW. For the second monkey, the lines represent (in order): the introduction of the main field, VCCW; the introduction of the first interference, VCW; the introduction of the second interference, SCW; and, the introduction of the third interference, NF. Note the reverse order between the two monkeys, of the introduction of the last two interfering fields. Wherever these line appear in subsequent plots, they represent the forces in the order described here, unless otherwise mentioned.

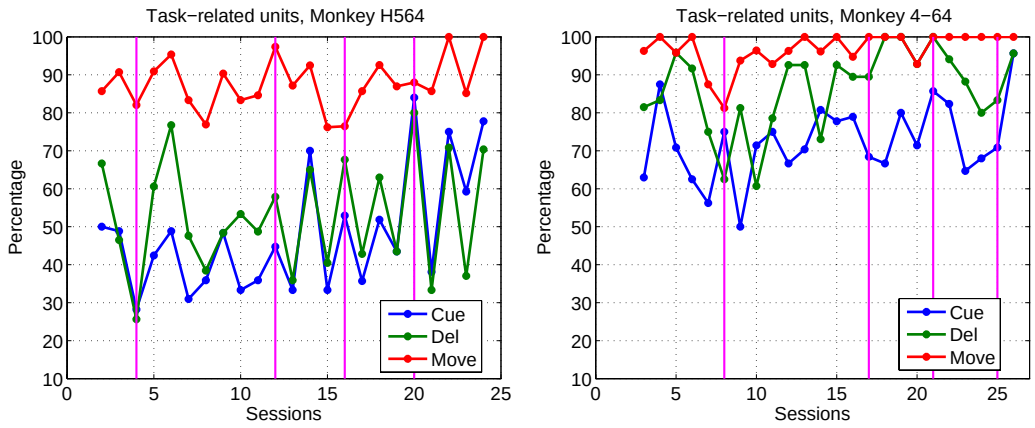

Figure 4.10: The fraction of cells found to be task-related (as defined in the main text), shown for each recording session and for the three task epochs considered. The plot on the left shows the numbers for the first monkey, while the one on the right is for the second monkey. The vertical magenta lines mark sessions where a new force was introduced (see the legend of Fig. 4.9).

Table 4.1: Results of the direction tuning analysis for each muscle under each force condition for both monkeys. Each entry has the following format: "preferred direction in degrees (number of trials per direction considered for analysis)". All the muscles were significantly tuned under all recorded force conditions ($p < 0.001$ for all except where mentioned otherwise; '*' denotes that the muscle was not significantly tuned, $p > 0.05$). NF: Null Field; VCCW: Viscous Counter-Clockwise Field; VCW: Viscous Clockwise Field; SCW: Stiffness Clockwise Field; NR: Not Recorded.

Muscle/Force	NF	VCCW	VCW	SCW
Monkey 1				
Anterior deltoids	17.42 (144)	69.16 (120)	349.88 (32)	353.31 (79)
Posterior deltoids	172.16 (88)	246.50 (120)	155.01 (32)	138.70 (79)
Infraspinatus	160.05 (40)	216.37 (72)	NR	115.97 (63)
Supraspinatus	119.16 (90)	165.58 (69)	NR	46.23 (72)
Pectoralis major	8.61 (33)	60.82 (41)	335.47 (35)	311.97 (72)
Teres major	244.46 (60)	272.30 (25)	169.42 (35)	209.06 (56)
Biceps	NR	238.34[a] (10)	133.69 (35)	NR
Triceps	NR	182.82 (49)	67.17 (35)	NR
Trapezius major	NR	172.57 (15)	NR	63.28 (63)
Monkey 2				
Anterior deltoids	24.85 (24)	123.28 (11)	17.00 (12)	44.81 (12)
Posterior deltoids	226.92 (24)	273.08 (11)	108.00 (12)	110.23 (12)
Infraspinatus	5.72 (14)	69.64 (12)	296.37 (12)	300.43 (12)
Supraspinatus	290.90 (12)	214.11 (10)	10.24 (7)	NR
Pectoralis major	171.98* (26)	305.74* (22)	90.44 (19)	91.95 (12)
Teres major	NR	NR	NR	NR
Biceps	8.79* (25)	41.38[b] (12)	233.77 (9)	340.23[c] (14)
Triceps	184.42 (25)	237.29 (12)	81.57 (9)	87.89 (14)
Trapezius major	191.38 (12)	237.13 (8)	NR	102.36 (14)

[a] $p = 0.014$
[b] $p = 0.015$
[c] $p = 0.036$

for the MOVE epoch, followed by DEL and CUE.

4.3.2 Direction tuning: Variation in the number of tuned cells across sessions

For the task-related cells found thus, a direction tuning curve was obtained using the standard methods for each of the CUE, DEL and MOVE epochs. The data points were fitted with a von Mises function to determine the preferred direction (at a resolution of 1 degree). The significance of the tuning was determined by using a bootstrap method on the length of the resultant vector (vector average of the tuning curve) using a False Discovery Rate (FDR) less than 10%. We also fitted a cosine function to the data points using a linear model in the sine and cosine of the movement direction; the significance of this fit was determined using the F-test on the linear regression (again using a FDR$<$ 10%).

Fig. 4.11 plots the number of significantly tuned cells as a fraction (i.e, divided by the total number of cells analyzed) across the different sessions for the vector average method (top row) and for the cosine fit (bottom row) for both subjects. As expected, a large fraction of cells were tuned in the MOVE epoch, while the numbers were much less in the other two epochs. Furthermore, the numbers with the vector average method tended to be higher than with a cosine fit. However, the numbers do not show any consistent pattern across the different task conditions.

Now it is clear that the behavior in all sessions is not stationary, particularly for the sessions where the subject shows marked improvement in performance. Thus, one might expect the neural responses to not be stationary either. In particular, calculating tuning curves based on all the trials in a session can give misleading results since it may not be appropriate to average over trials across the entire session. Under these circumstances, ideally one would like to obtain a tuning curve using as few trials as possible; but that may result in only a noisy, non-robust estimate. I calculated single-cell tuning curves for the first 50 trials and the last 50 trials of each session and looked for any changes in the tuning characteristics. As expected, vey few cells were found to be significant (using either method) for either the first 50 or the last 50 trials. Furthermore, similar to the data shown in Fig. 4.11, no clear pattern was observed in the number of tuned cells as a function of the sessions (data not shown). I repeated the analyses using the first and the last third, and the first and the second halves, of the sessions, but again nothing could be concluded from the variation in the number of tuned cells across the sessions.

4.3.3 Direction tuning: Changes in the quality of fit

However, for the case of fitting a cosine function to the tuning curve, the 'quality of fit' did seem to show a big change in some sessions (the R^2 value from the linear regression was

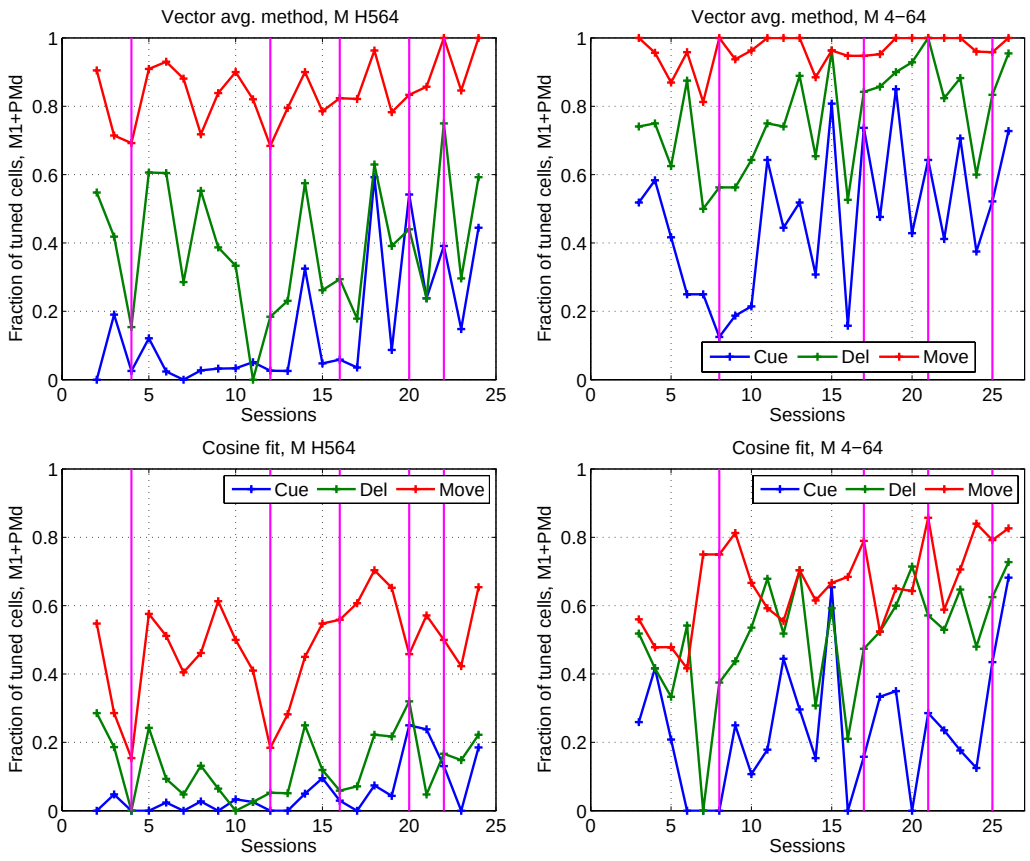

Figure 4.11: Fraction of tuned cells for the different task epochs using a vector average method (top row) and for the cosine fit (bottom row), for the first monkey (left column) and the second monkey (right column). The vertical magenta lines mark sessions where a new force was introduced (see the legend of Fig. 4.9).

taken as a proxy for the quality of fit). Fig. 4.12 plots the median over all cells in the area M1 (including the ones that were not significantly tuned) of the change in the R^2 value between the fit for the last 50 trials and the fit for the first 50 trials for each day. When the day had two sessions, the difference was taken between the last 50 trials of the last session and the first 50 trials of the first session. This is important to note for the days on which a new field was introduced, because on those days the initial and the final sets of trials were performed under different force fields. For the first monkey (left plot), the median R^2 can be seen to increase from the start to the end of the day after the introduction of the forces (the difference, between final and initial R^2, is positive in the figure) and also on the day of the first interference, both days when monkeys showed a large improvement in the behavioral performance (Fig. 4.4). A similar pattern is observed for some of the epochs for the second monkey as well (right plot)− in addition to the peaks for the day of the first introduction of the force (VCCW) and the first interference (VCW), a peak is also observed on the day of the third interference (NF), albeit only for the CUE epoch. There

also seems to be a much less prominent decrease on the day of the second interefernce (SCW) for the second monkey; this decrease is more clearly observed in Fig. 4.13, which plots the median change in R^2 between the start and the end of a single session (instead of the entire day as was the case for Fig. 4.12). However, such a clear pattern was not observed for the first monkey. It should be noted from this figure that the increase in R^2 for the second monkey occurs in the session after the introduction of the forces, as was observed for the first subject– it is just that this session falls on the same day for the second subject, but on a different day for the first subject (see Tables 2.1 and 2.2), hence the apparent difference in Fig. 4.12. Similar results were observed for the cells recorded from the PMd, except that for the first subject changes on the days with interfering fields were not prominent. These results suggest that a change in the quality of fit could be related to the learning process.

4.3.4 Comparison of tuning between different force fields

We next attempted to replicate the analysis from the neural studies of force-field adaptation from the Bizzi group (Li, Padoa-Schioppa, and Bizzi, 2001; Padoa-Schioppa, Li, and Bizzi, 2004). Specifically, we compared the tuning properties of cells between different force conditions. However, due to the particular design of our experiment, we encountered two main difficulties (see Chapter 7 for more discussion). The first arose because we could not assume that any of the cells recorded over consecutive days were the same. This meant that although we had data from some cells that were recorded under two force conditions, we lacked another session in the familiar force field, after performance in the novel field, that would have served as a crucial control (cf. the no-force–force–no-force set-up in the Bizzi studies). This made it difficult for us to ascertain whether any changes that we may observe between the tuning under the two fields were actually task-related or were simply a consequence of the changes in the cells' properties over the course of the day. The way we got around this issue, though not exactly ideal, was to use days with only a single force field as a kind of control/baseline. Thus if the changes in the tuning between two different force were of a much greater magnitude than between two arbitrary divisions of the data from a single force field, we could attach some level of confidence (and importance to it).

The second issue was that, since the behavior in our experiments was one long continuous process, we could not pool cells across days even though the force conditions permitted it. This greatly reduced the number of cells that we could analyze. The pool of cells was further reduced by the constraint that we could only compare cells that were significantly tuned under both conditions. To get the highest numbers, we divided data from each session into halves (increasing the number of trials over which the tuning is computed should increase the stability of tuning). For the days with only one session, we compared the first half of the session with the second. For the days, with two sessions, we compared

the first half of the first session with the second half of the second session (which would be in different force fields for certain days).

The first thing we extracted from this analysis was the number of cells that significantly changed their tuning properties each day, whether between two different forces or between two sets of data in the same force field. To compute the significance of difference between the tuning curves we chose the non-paramteric method proposed in Stark and Abeles (2005) over the parametric method employed in the Bizzi studies (Li, Padoa-Schioppa, and Bizzi, 2001). The non-parametric method is essentially a permutation test that checks separately for significant differences in the resultant vector of the tuning curve, in the magnitude of this vector, and in the direction of this vector (which is the preferred direction of the cell). Fig. 4.14 plots the results for the first monkey, as the ratio of the number of cells with a significant difference in each of the three parameters, to the total number of cells analyzed. This latter number was the number of cells significantly tuned in both the halves of the data, as determined using the vector average method mentioned above. Small increases were seen on all the four days when we introduced a new field (not couting the second introduction of NF in S16 as new), but there were some peaks elsewhere too and we did not find the resuls terribly convincing. While these results from the first monkey at least looked encouraging, the second monkey disappointed us. Almost all the cells from the second monkey tended to show significant differences between the two halves even on days when the forces did not change. In fact, on some of the days with new forces, some of the numbers tended to drop. It is possible that these anomalous results are a consequence of a much smaller sample of cells for the second monkey as compared to the first. However, I would like to point out that such plastic changes in tuning properties of single cells that are not related to adaptation have also been reported in previous studies (Rokni et al., 2007; (Padoa-Schioppa, Li, and Bizzi, 2004)). Given that our confidence in this analysis was already tempered by the two caveats discussed above, we did not pursue it further.

In summary, we did not find consistent patterns in the variations of the number of significantly tuned cells across different force conditions. Nor did we find any consistent patterns in the changes in the tuning curves of single cells under different force fields. Our inability to show stable recordings over days and the small numbers of cells we recorded in any one day created some problems for us in interpreting the results from this latter analysis. However, we did find greater changes in the quality of fit of a cosine function to the tuning curve on the days marked by a greater behavioral performance by the subjects.

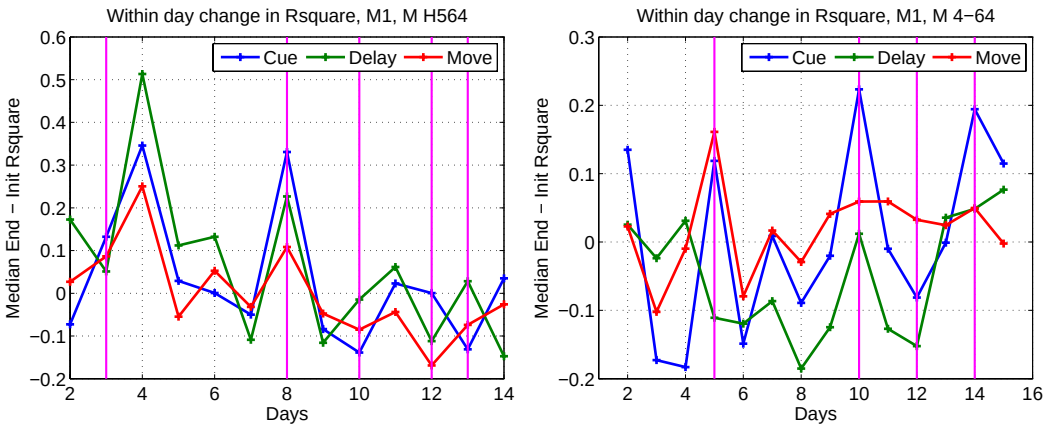

Figure 4.12: Median change for the cells in M1 in the quality of fit (R^2) between the cosine fit to the tuning curves calculated for the final and initial 50 trials for each day. The left panel shows data from the first subject, while the data in the right panel is from the second subject. The vertical magenta lines in this figure mark the days when a new force field was introduced. They represent (in order) the days of introduction of: VCCW, VCW, NF, SCW and SCW for the first subject; VCCW, VCW, SCW and NF for the second subject. Again, note the different order of the last two interferences for the two subjects.

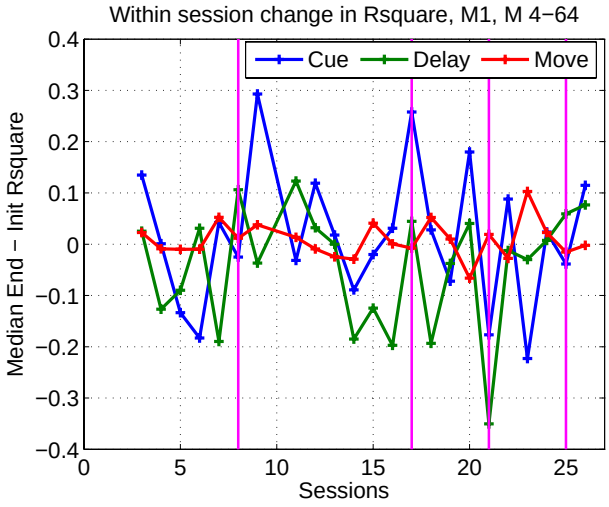

Figure 4.13: Median change for M1 cells from second subject, in the quality of fit (R^2) between the cosine fit to the tuning curves calculated for the final and initial 50 trials for each *session* (not *day* as was the case in 4.12. The vertical magenta lines mark sessions where a new force was introduced (see the legend of Fig. 4.9).

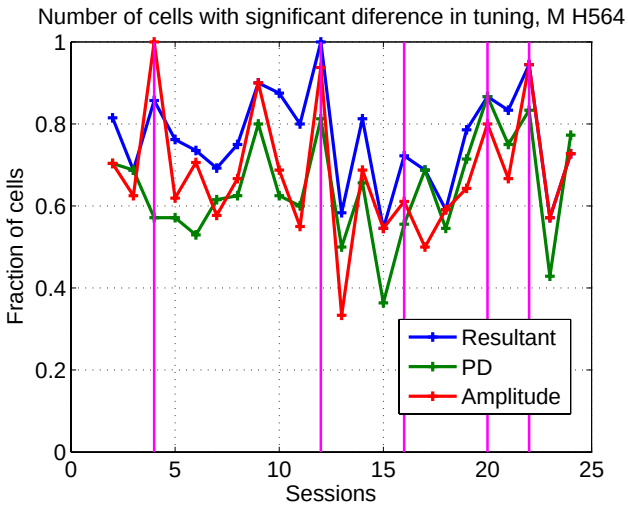

Figure 4.14: Plots of the fraction of cells that showed a significant difference in one of the three aspects of their direction-tuning properties, between the first and the second half of each day. Results are shown for the first subject.

4.4 Changes in the relative weightings of kinematic and kinetic variables related to changes in force fields

Ashe and Georgopoulos (1994) proposed a multiple regression method that can be used to analyze the relationship between the time-course of the firing rate and the time course of kinematic and kinetic varibles at a fine time resolution. Among other things, this method allows us to find how much can each behavioral variable explain the variation in the firing rates of single cells. The relative contribution of each variable can be estimated from the regression coefficients if the independent variables have been z-scored prior to being used in the regression (the so-called 'standardized regression'). From a different perspective, these (standardized) regression coefficients also tell us the relative weight assigned to a particular task variable by the cell, from among all the variable that it encodes (actually, from among only those variables that are included as independents in the regression).

We carried out this analysis for the firing rate and the behavior binned into 5ms bins. Note that although no explicit smoothing was performed for the binned rates, the fact that they were calculated using the fractional inter-spike intervals conferred some degree of smoothness on them. The binned rates were square-root transformed to stabilize the variance. The multiple regression was carried out at different time lags between the neural activity and the behavioral data. The time lag was varied between -250 ms to 0 ms in steps of 5 ms. A negative time lag here indicates that the neural activity leads the behavior. For the first monkey, out of a total of 24 sessions, the first two NF sessions (S1 ans S2), a session in the VVCW field (S18) and the second SCW session (S22) were not considered for this analysis due to incomplete or partially corrupted data sets. For the second monkey, the first two (NF) sessions and the last session (S27, VCCW) were ignored. Only the cells that were found to be task-related for the movement period were considered for this analysis (see Section 4.3). The behavior was analyzed starting from the onset of the movement (when the monkey leaves the center circle) and going upto the end of the movement (when the monkey enters the target circle). A non-zero time lag in the regression implied that the neural data window (of the same length) had been shifted to the left of the behavioral data window by that time (i.e., neural activity occuring before the behavior). We could not study positive time lags, such that the neural activity would have lagged the behavior, because some of our trials were incorrect movements (see Section 2.2.6). As such, the data collection on these trials was terminated at the end of the movement. So, we could not extend the neural data window beyond that time, as would have been required if the time lags were positive.

The firing rates were regressed on the following independent variables: time, t; cosine of the movement direction, $\cos(\theta)$; sine of the movement direction, $\sin(\theta)$; x- and y-components of position, velocity and forces (x, y, v_x, v_y, F_x, F_y) and the firing rate of the

cell in the center-hold epoch, f_{CHT} (Eq. 4.1). The time lag is denoted by the variable τ. All terms entered the model as a linear factor, and as all pair-wise interactions; a constant term was also included (for a total of 56 terms). Note that the term 'force' here refers to the forces applied by the monkey on the manipulandum and not *vice versa*. For all the following analyses, I considered only the regression coefficients of the terms linear in the x- or the y-components of direction, position, velocity and force.

$$\begin{aligned} f(t+\tau) = \quad & b_0 + b_1\, t + b_2\, \cos(\theta) + b_3\, \sin(\theta) + b_4\, x(t) + b_5\, y(t) + b_6\, v_x(t) + b_7\, v_y(t) \\ & + b_8\, F_x(t) + b_9\, F_y(t) + b_{10}\, f_{CHT}(t) + b_{11}\, t\times \sim (\theta) \\ & + \ldots \text{other pairwise interactions} \end{aligned} \tag{4.1}$$

4.4.1 Learning modulates the number of cells actively engaged in the task

Fig. 4.15 plots for all sessions the fraction of cells for which a particular variable (direction, position, velocity or force) made a significant contribution towards explaining the variation in the firing rates (as evidenced by a regression coefficient significantly different from zero, t-test, FDR$<$ 10%). A variable was taken to be significant if either of the x-or y-components were significant. The numbers were then averaged over all the time lags studied (-250 ms to 0 ms) and have been plotted in the figure as mean $\pm$ SEM.

More than 90% of all cells had a significant contribution from the direction and position variables for both the monkeys; these numbers, however, do not show a consistent variation corresponding to the changing force conditions across the sessions. However, the velocity and force variables showed very interesting dynamics. For the first monkey, the fraction of cells with a significant contribution from the force variable showed large increases in the first session after the introduction of the forces (VCCW, S5) and during the first interfering field (VCW, S12), along with a smaller rise for the stiffness interference (SCW, S20). The fraction of cells with a significant velocity contribution correspondingly increased for all the session in which a new field was introduced. Another interesting observation was the gradual decrease in the fraction of cells with significant velocity and force contributions for sessions 5-11, paralleling a decrease in the behavioral error measure as the subject adapts to the main field (VCCW). Similar patterns can be observed for the velocity variable for the second monkey, and to a lesser extent for the force variable as well. We interpret this as an increased participation/recruitment of single cells when the subject is required to learn something new, and a gradual decrease in the numbers as the subject becomes better at the behavior. In terms of internal models, our results suggest that the number of cells particpating in the current internal model(s) varies depending on the learning demands of the task. This implies one or both of two possible alternatives: learning could cause a variation in the number of cells in the same internal models, or, it could cause a pruning of

internal models themselves– i.e., it is possible that when the subject is learning something new, the brain "tries out" a number of internal models, and as the subject learns the task, the brain is able to pick out the models relevant to the current task, and discard the others, thereby improving the efficiency of the system.

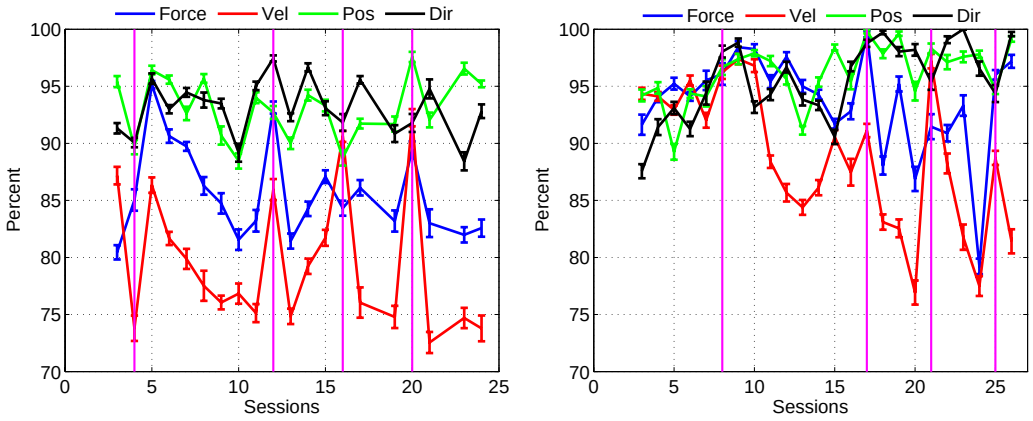

Figure 4.15: Average percent of cells that had a significant regresssion coefficient for one of the four independent variables (shown in different colors): direction, position, velocity and force. The numbers were averaged over all the time lags studied and have been plotted as mean $\pm$ SEM. The left plot is for the first monkey, while the right one is for the second monkey. The vertical magenta lines mark sessions where a new force was introduced (see the legend of Fig. 4.9). Note that session 22 (the second session in SCW) was not analyzed and is missing from the figure (cf. the figures for the direction-tuning analyses).

We also plotted this fraction of cells as a function of the time lag between the neural and behavioral data, after averaging over all the sessions (Fig. 4.16). The numbers do not seem to change much with the time lag (observed also for the second monkey; results not shown).

4.4.2 Adaptive changes in the relative weights of different task variables in different force conditions

We also sought to determine the fraction of cells for which a particular variable makes the most contribution. This was determined using the regression coefficient of that variable. The coefficients of the x- and the y-components were squared, added, and then the square root was taken, in the manner of calculating the amplitude of a vector quantity. Then, each variable was ranked according to the magnitude of the corresponding 'amplitude' coefficient. For example, the force variable received a rank one for a particular cell if the regression coefficient of the force term for that cell (calculated as described above) was highest among the four variables considered. Fig. 4.17 plots the fraction of cells for which a particular variable was ranked one, across the recorded sessions. In general, the fraction of cells with direction as the most important variable was the largest followed

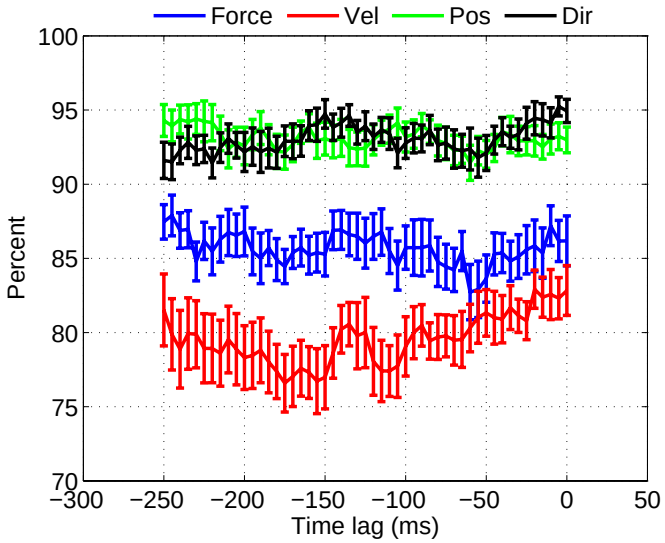

Figure 4.16: Average percent of cells that had a significant regresssion coefficient for one of the four independent variables plotted as a function of the time lag between the neural and behavioral data. The numbers were averaged over all the sessions and have been plotted as mean ± SEM. Results have been shown for the first monkey. Similar patterns were observed for the second monkey, except that the percentages were a little higher in general.

by force, position and velocity. Notable observations from this analysis were that: a) the fraction of cells with force as the most important variable (subsequently referred to as 'force-cells' [similar terminology for other variables also]) increased when the forces were introduced and were high in all sessions in the velocity-dependent force; b) the fraction of position-cells increased when the subject performed in a position-dependent force field; and, c) the fraction of velocity-cells was higher in the sessions without the forces. The fraction of direction-cells appears to drop in first force session and in the first interference session for the first monkey, but the change is less consistent for the second monkey. It should be noted that all the four percentages for each session sum up to a constant (100%) for each individual time lag (not exactly for the averages over time lags as shown in the figures, but it should be close); therefore, if one of the variables becomes most important for a larger fraction of cells, the other variables lose importance. In general, the results from the second monkey are less consistent after the first interference. Another anomaly is the brief increase in the fraction of velocity-cells in the second session in the main field (S9). I am not sure why that is so, but it could be because of the transient abnormality in the way the second subject's behavior improved in the main field (see Section 4.1 and Fig. 4.4, right panel).

The fraction of such cells was also plotted against the time lag (Fig. 4.18, for the second monkey). From this figure, we see that the fraction of force-cells peaks around a lag of 150ms. The fraction of position-cells seems to be decreasing with decreasing time

lags, while the fraction of direction-cells (and to a lesser extent, velocity-cells) shows the opposite trend. Similar results were observed for the first monkey (figures not shown).

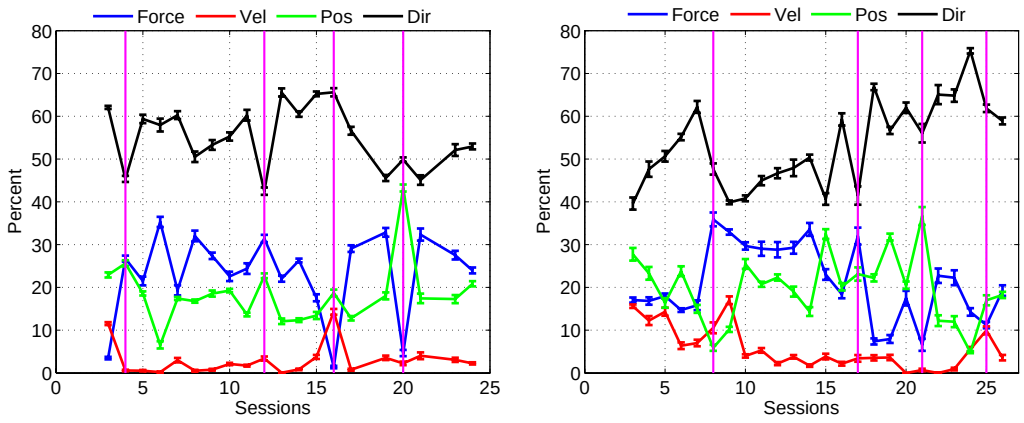

Figure 4.17: Average percent of cells for which a particular independent variable made the most contribution, i.e., had the highest regression coefficient. The numbers were averaged over all the time lags studied and have been plotted as mean ± SEM. Same format as in Fig. 4.15.

We also checked for differences between the two cortical areas (M1 and PMd); although we found quantitative differences between the percentages of cells representing a factor best, or just representing it significantly, there were no consistent patterns across the task conditions. Hence no meaningful conclusions could be derived. Fig. 4.19 plots the differences between the two areas for the first monkey; similar results were observed in the second monkey (data not shown). A square symbol in the plots signifies that the differences were statistically significant (paired t-test, $p < 0.05$).

4.4.3 Time lag with the best R^2 of the regression

Finally, we studied how the R^2 of the regression varied with the time lag. To this end, we fitted a simplified form of the regression described above. Only the x- and y- components of direction, position, velocity and force were used as independents, along with the constant term; no interaction terms were included in this regression. The idea was to capture the R^2 of the fit involving only a linear model of the relevant factors. Furthermore, to study the variation in R^2 for an extended range of lags, we performed the regressions for time lags varying from 0 ms to -1000ms at intervals of 25 ms. We then determined the time lag at which a particular cell showed the maximum R^2 (i.e., maximum over all lags). Fig. 4.20 plots for all sessions the number of cells that showed the maximum R^2 at a particular time lag. It can be seen that most of the cells lie between 0ms and 350ms, as is also shown in the small histograms on the right of each plot. Again, there does not seem to be much qualitative difference, however, between the two cortical areas, except that the histograms

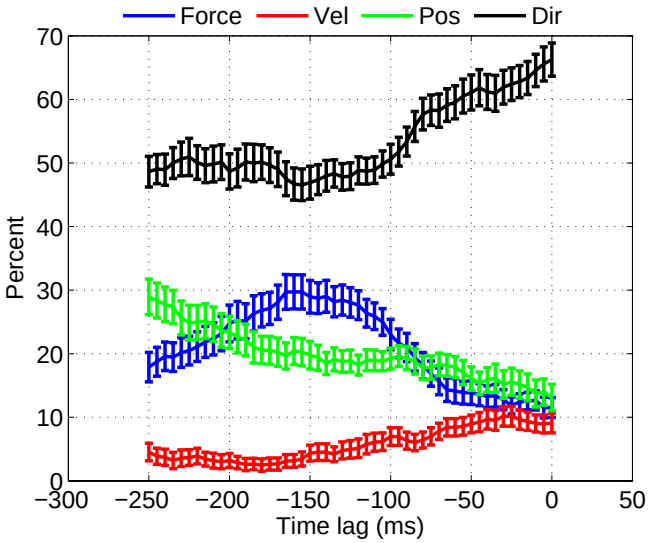

Figure 4.18: Average percent of cells for which a particular independent variable made the most contribution, plotted as a function of the time lag between the neural and behavioral data. The numbers were averaged over all the sessions and have been plotted as mean ± SEM. Same format as Fig. 4.16. Results have been shown for the first monkey. Similar pattern was observed for the first monkey.

for PMd are more concentrated towards the smaller lags, as compared to M1.

In summary, from this multiple regression analysis we found two posisble correlates of adaptation and switching in single cells. The first was in terms of enhanced recruitment of single cells whenever a new force was introduced. The second was reflected in the changing of the relative weights of the relevant task variables in the firing rates of single cells. Furthermore, we did not find consistent differences between the properties of cells in M1 and PMd. Finally, not surprisingly a majority of cells showed maximum R^2 values for the smaller time lags. Chapter 7 provides an extended discussion on our results.

4.5 Summary

In this chapter I provided evidence for learning and interference in the behavioral performance of both subjects. I showed that the preferred directions of muscles rotated faithfully in the direction of the applied forces. We did not find a lot of consistent results from the direction-tuning analysis, but admittedly that could be because we had small samples of cells each day and because we did not have cells recorded in more than two force conditions (this was not an issue for the EMG signals). We did find, however, a greater change in the quality of fit of a cosine function to the tuning-curves on days when the monkey showed major improvements in behavioral performance. Our main results came from the multiple regression analysis where we found two possible correlates of adaptation and switching–

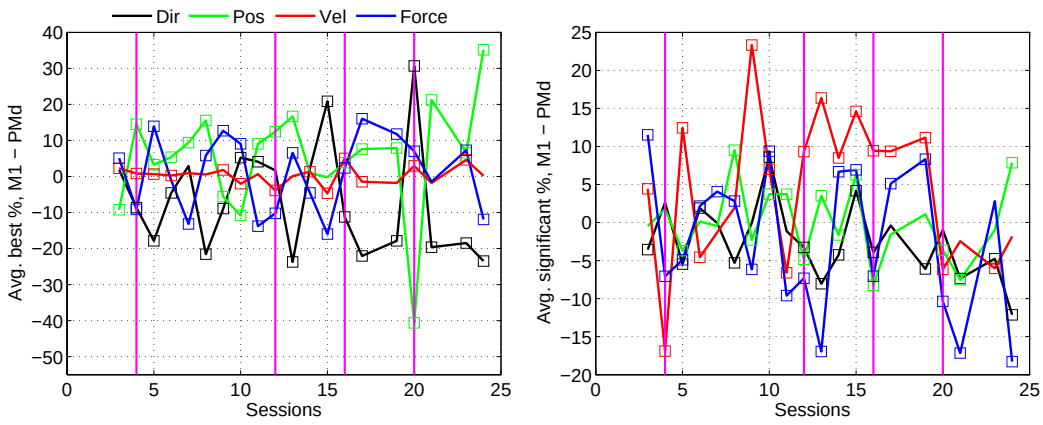

Figure 4.19: The difference between M1 and PMd of the percentage of cells representing a variable best (left column) and the percentage of cells that had a significant regression coefficient for a particular variable (right colum) for monkey 1. The square symbols indicate that the difference was statistically significant at 5% level (paired t-test). Similar results were observed for the second monkey (data not shown). Same format as in Fig. 4.15.

enhanced recruitment of cells and *changes in the relative weight of relevant task parameters*. Chapter 7 provides an extended discussion on our results presented in this chapter and also discusses some of the methodological issues.

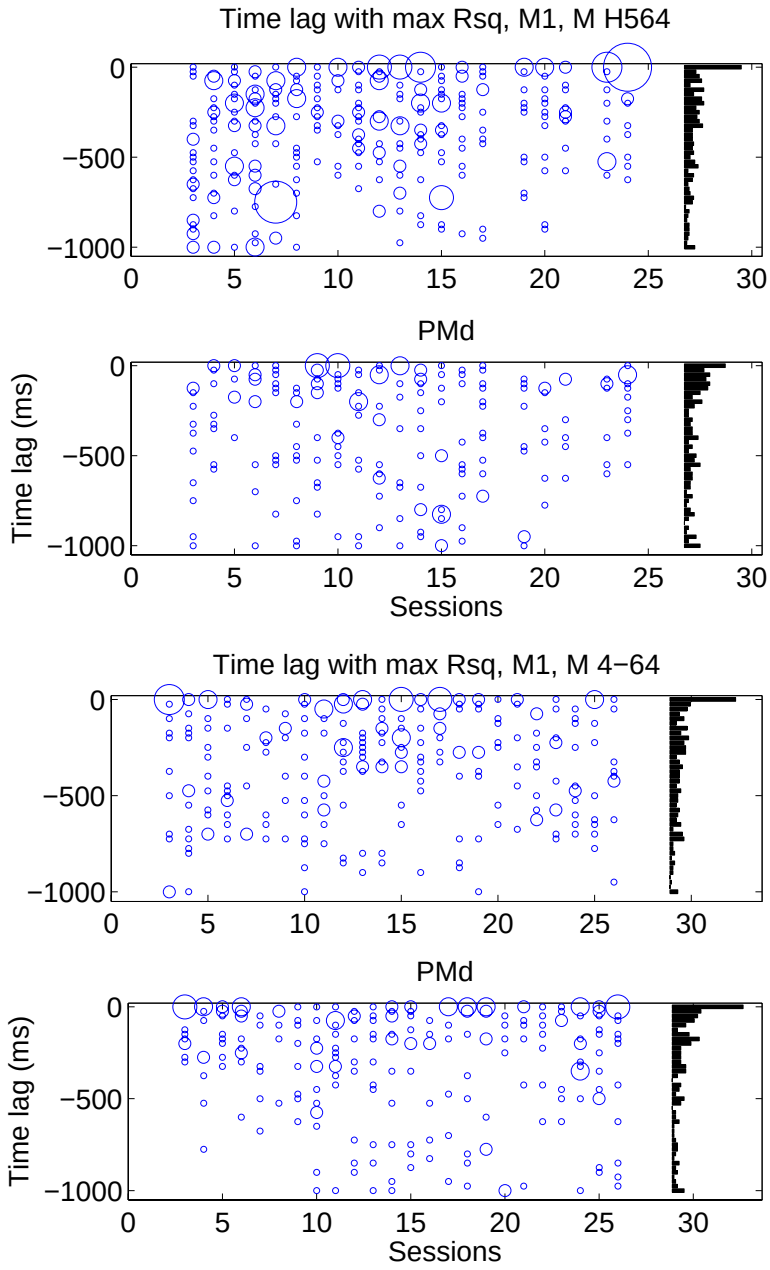

Figure 4.20: Plots of the number of cells that showed maximum R^2 at a particular time lag for area M1 (top row) and area PMd (bottom row), for the first monkey (left) and for the second monkey (right). The sizes of the blue circles are proportional to the number of cells at the lag. The black histograms on the right of each figure show the normalized count at each time lag, aggregated over all sessions.

Chapter 5

Neural Correlates of Force-field Learning in Local Field Potentials

Local field potentials (LFPs) are thought to represent the aggregate synaptic input to a cortical area. This signal is carried in the lower frequencies ($\leq \sim$ 200Hz) of the voltage measured during extracellular recordings. LFPs have been found to carry information independent from the single cells recorded from the same electrode and thus represent an important signal in the cortex for computation and transfer of information. Although LFPs provide lower spatial and temporal resolution than the action potentials recorded from single cells because they represent a continuous trace of the aggregate activity, for the same reason they offer an excellent opportunity to study oscillations and rhythmicity on a broader scale. Further, in the context of extracellular recordings using chronic multi-electrode arrays, a big advantage of the LFP signal is that it can be recorded in a much more stable fashion than the single cells over a period of months. The yield of LFP data is also much higher since even the electrodes that do not detect single cell activity, can carry useful LFP signals.

In this thesis, I assume that the LFP signals recorded from each electrode are stable across all the recording days. This allows me to analyze the same electrode throughout all the learning and interfering phases of the behavior– something which I could not do with the single cells. The focus of my analysis has been in the spectral domain of the LFP signals, by calculating the power spectrum and the coherence spectrum of the continuous-time signals. Most studies of LFPs (in motor cortex or elsewhere) tend to favor a frequency-domain approach over the time-domain because of the greater robustness of the signal characteristics that can be extracted using statistical and mathematical techniques. Furthermore, since most of the information in the LFPs appears to be carried in the oscillations of the signal, the frequency domain provides a much more compact representation of the signal. Nevertheless, there are specific analyses that are better suited

to the time-domain signals, for example an analysis of the instantaneous phase (as was done in Rubino, Robbins, and Hatsopoulos, 2006), and quite often a combination of both approaches proves useful.

In the following sections, I describe the characteristics of the LFP power and coherence spectra, with a special focus on the beta and the gamma bands. These two frequency bands are of particular interest in movement-related neural activity for at least three reasons. First, a number of studies have found modulation of cortico-muscular coherence in these two frequency bands during the performance of various motor tasks (Baker, 2007; Omlor et al., 2007; Schoffelen, Oostenveld, and Fries, 2005). Second, the LFP signal in the beta band has been found to show a decrease in the power and coherence during the performance of a movement relative to the condition when the subject is at rest– a phenomenon that has been called "event-related desynchronization", borrowing the usage from the EEG literature. On the other hand, the LFP in the gamma band show elevated power and coherence levels during the movement production relative to the rest phases (correspondingly called an "event-related synchronization"). Finally, pathological oscillations in both of these frequency bands are becoming increasingly implicated in the neural corrlates of various neurological movement disorders (like Pakinson's disease, essential tremor, Huntington's disease, and others; Hammond, Bergman, and Brown, 2007; Hutchison et al., 2004). After describing the general characteristics of these frequency bands, I outline one of our approaches to relate the power in these bands to the subjects' behavioral performance on our adaptation task. This work is not yet complete, and what I present in this chapter are best described as preliminary results.

5.1 Characteristics of the LFP power spectra

It has been shown earlier that the beta-band shows elevated power during periods of rest or when maintaining steady posture, while there is a drop in the power during movement (Rubino, Robbins, and Hatsopoulos, 2006; Baker, 2007). We observed the same general characteristics in our data from both cortical areas (M1 and PMd). Fig. 5.1 plots the average power spectrum of the LFP signal recorded during one session in the VCCW field for the first subject, computed using the multi-taper method (Thomson, 1982; Percival and Walden, 1993; Mitra and Pesaran, 1999; implemented in the Chronux toolbox for Matlab). The top panels plot the actual spectrum in the dB scale while the bottom panels show the spectra in the task epochs normalized by the spectrum in the center-hold period. The epoch durations were as described in Chapter 2, Section 2.2.6. The spectra have been averaged over all trials in the session and over all channels in M1 (left column) or PMd (right column). Fig. 5.2 plots the spectra for one session for the second subject. Several general features can be noticed in these plots. First, the spectra from M1 and

PMd are broadly similar except that the power in the LFP signal from PMd is, in general, lower than the power from the M1 LFP. The difference is more pronounced for the first subject than for the second. Next, the increase in beta-band power is clearly observed in the center-hold, CUE and DEL epochs, as is the relative drop in the power in the MOVE epoch. This can be more clearly seen in the center-hold normalized spectra in the bottom panels. A close examination also reveals that the beta-band peak in the CUE and DEL epochs happens at a slightly higher frequency than that in the center-hold epoch, more so for the second subject than for the first. However, it must be kept in mind that the spectra have been calculated with a frequency resolution of ∼2.8Hz; thus the differences in the frequency of peak power pretty much lie within the resolution. Finally, the MOVE epoch carries greater power in the higher frequencies (gamma band) as compared to the other epochs, and more so in M1 than in PMd (Figs. 5.1 and 5.2, bottom row). Similar general characteristics were observed in all sessions and we did not notice a significant change in the shape of the average spectra as the monkey adapted to the VCCW field or as the forces fields were changed.

It is likely that there is a lot of variation present between individual channels, which may get masked when computing the average. To take a closer look at the per-channel spectra, I plotted in Fig. 5.3 the spectrum of each channel (for frequencies less than 50Hz) in a pseudo-colorscale plot for the CUE epoch (left column) and MOVE epoch (right column) for the same session as shown in Fig. 5.1 for the first monkey. In addition to the general features of the spectrum discussed above, it can be seen that certain groups of channels carry greater power than certain others, indicating a lot of heterogeneity in the distribution of power across the recording arrays in both areas. A qualitatively similar pattern was observed for the other sessions (and in the other monkey) as well.

5.2 Characteristics of the LFP coherence spectra

Coherency is a complex quantity defined as the normalized cross-spectrum (Eq. 5.1). Its absolute value is termed the coherence and ranges from 0 to 1. A coherence of 1 indicates that the two signals have a constant phase relationship (and amplitude covariation), while a value of 0 indicates the absence of any phase relationship.

$$C_{yx}(f) = \frac{S_{yx}(f)}{\sqrt{S_x(f)\, S_y f}} \tag{5.1}$$

I computed the coherence between pairs of channels using the multi-taper method. Fig. 5.4 (top row) plots the average coherence between channels in the M1 (averaged over all M1 channel pairs for all trials in a particular session) for the first subject(left column,S14, VCCW) and for the second subject (right column, S13, VCCW). The beta-band can be

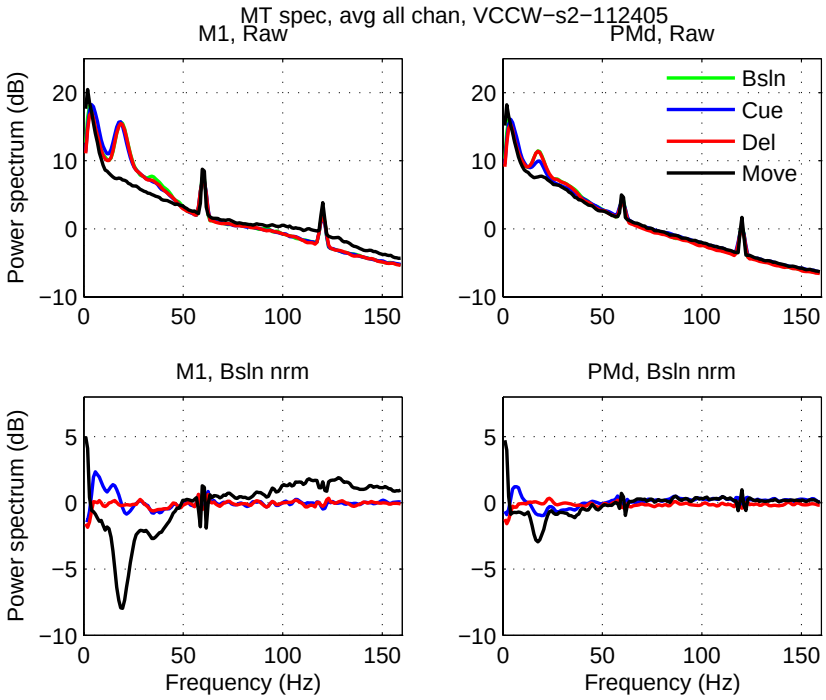

Figure 5.1: Plots of power spectra of the LFP signal for the first subject computed using all trials in a particular session (S14, VCCW) and averaged over all channels in M1 (*left column*) and PMd (*right column*). The top panels plot the actual spectrum in the dB scale while the bottom panels show the spectra in the task epochs normalized by the spectrum in the center-hold period (normalized by division, then converted to log scale). All four trial epochs are plotted in different colors as shown in the legend in the top row ('bsln': baseline or CHT; 'del': memory delay). The bottom row plots the there epochs except baseline (as that has been used to normalize the data).

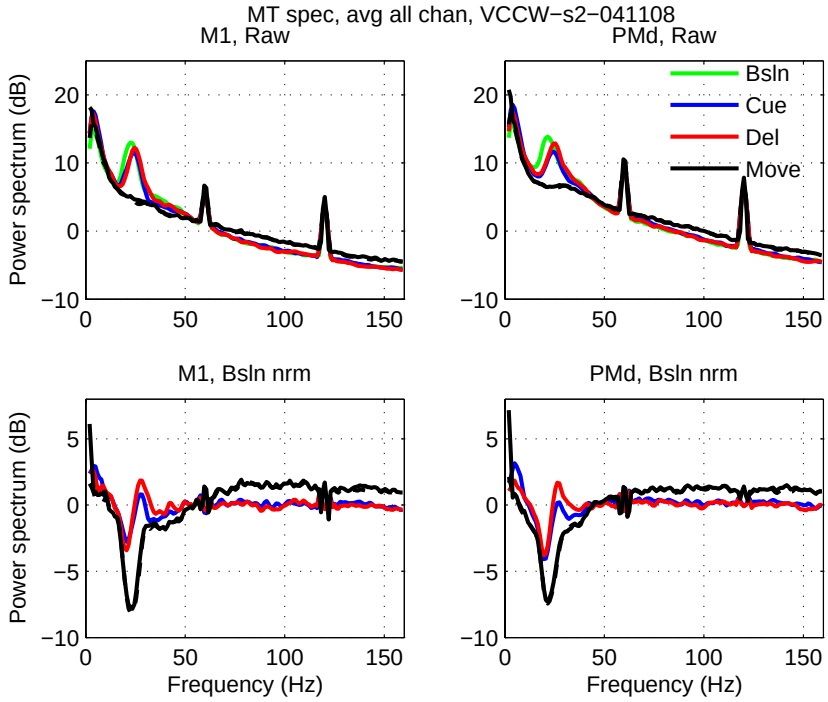

Figure 5.2: Plots of power spectra of the LFP signal for the second subject computed using all trials in a particular session (S13, VCCW). Format and notation same as is Fig. 5.1.

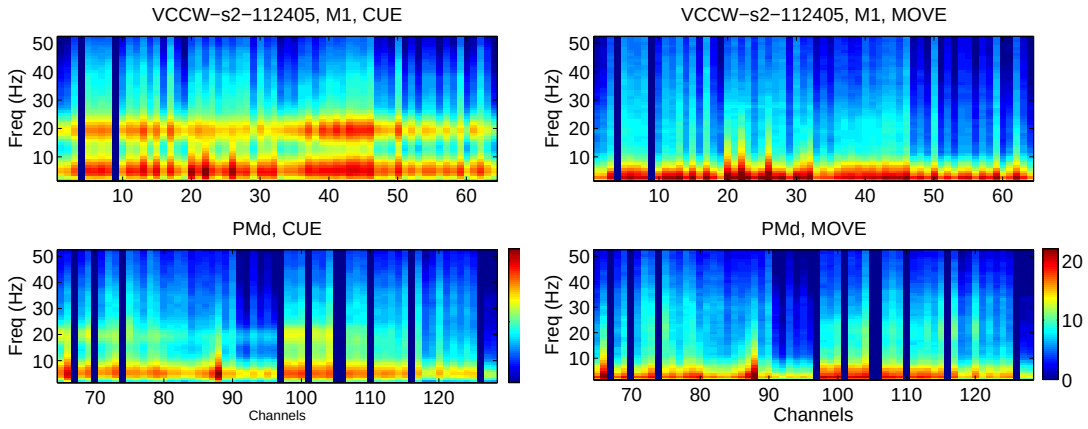

Figure 5.3: Depiction of the LFP power spectrum of each channel from the first subject in a pseudo-color plot. The spectrum has been shown for the CUE epoch (left) and the MOVE epoch (right). The frequencies vary on the y-axis (limited to lie between 0 and 50Hz) and the channels vary along the x-axis. The top sub-plot for each condition shows the channels from M1 while the bottom plot shows the channels from PMd. The session plotted is S14 (VCCW).

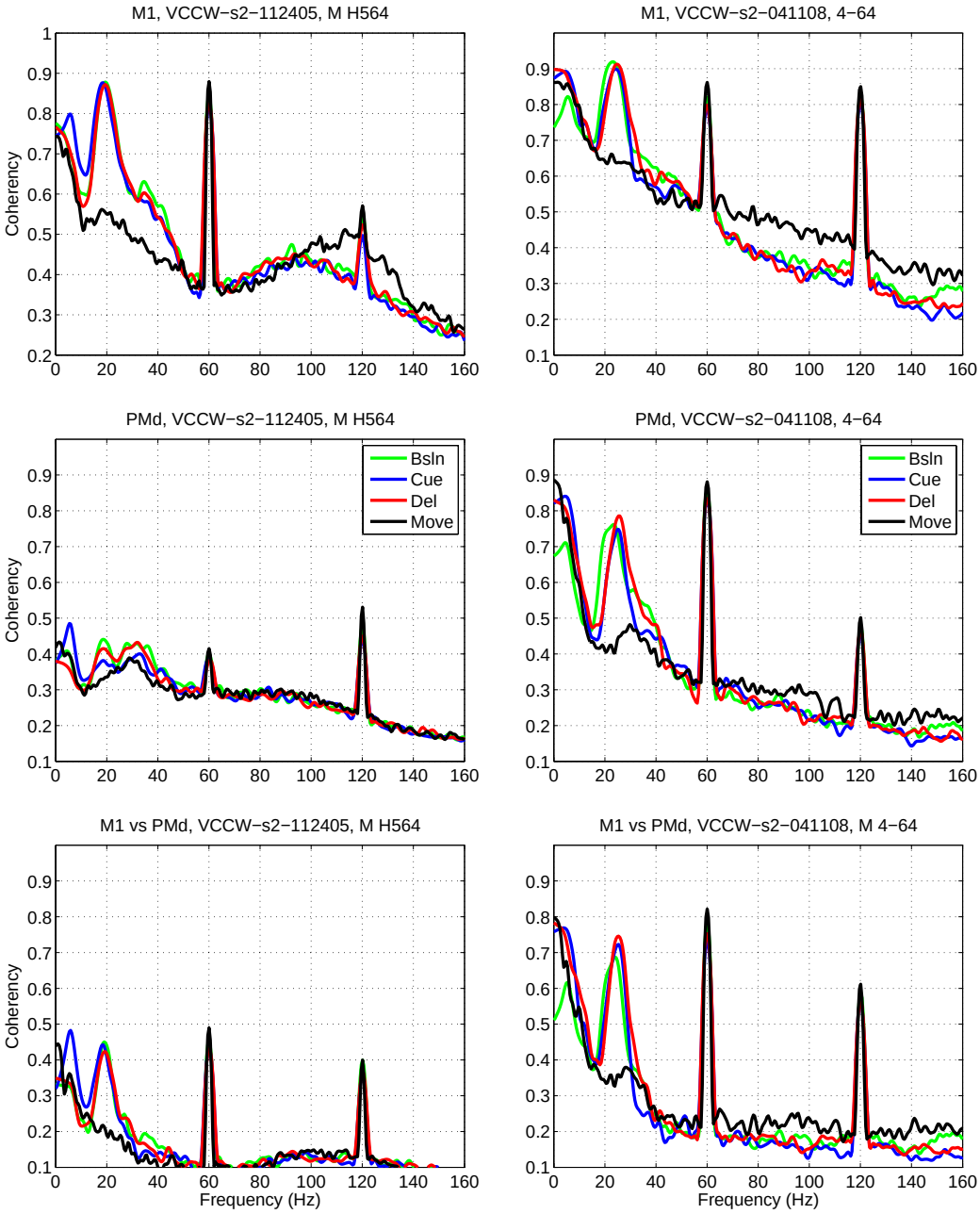

Figure 5.4: Plots of the coherence spectra of the LFP signal for the first subject (*left column*) and the second subject (*right column*) computed using all trials in a particular session (S14, VCCW for the first subject; S10, VCCW for the second subject) and averaged over all channel-pairs in M1 (top row), in PMd (middle row) and cross-channel-pairs between M1 and PMd (bottom row).

seen to exhibit elevated coherence levels, reaching as high as 0.9, during the baseline, CUE and DEL epochs while a sharp drop is observed in the MOVE epoch. Also clearly seen is the relatively high movement-period coherence in the gamma band in both monkeys. The middle row in Fig. 5.4 plots the results for channel pairs in the PMd. While for the second subject the beta-band coherence in PMd is quite similar to that in M1 (except a being little lower), the first subject shows a quite different pattern. Specifically, the elevated rest-period coherence that is seen in M1 is completely absent in the PMd. This appears to be consistent with the observation made in the previous section that the LFPs from PMd in the first monkey carry much less power in the beta-band than the corresponding signals from the M1. Note also that the increased gamma-band coherence seen in the movement period for M1 channel-pairs is almost completely absent for the PMd channel-pairs in both monkeys.

We also studied the "cross-coherence" between the channels in the two cortical areas, such that the two channels in each pair analyzed belonged to different areas. (Fig. 5.4, bottom row). An elevated beta-band average cross-coherence was again seen for the there non-movement epochs (albeit a little lower than seen in M1), but not for the movement epoch. Furthermore, not much increase was observed in the gama-band coherence in any of the epochs (similar to what was seen for the PMd channel-pairs).

To see the coherence spectrum for individual channel-pairs, I plotted the frequency vs. channel-pair data in a pseudo-colorscale plot in a manner similar to that for the power spectrum. As an example, Fig. 5.5 plots the data for the CUE epoch for session S14 for the first subject (same as in Fig. 5.4). The top panel shows all channel pairs from M1, the middle panel shows channel pairs from PMd, while the bottom panel depicts the cross-coherence between channels in M1 and PMd. Again, all of the general features described above can be observed in this plot, in addition to the variations between the channel pairs. The striated appearance of the plot probably results from the fact that one, or a few, of the channels show high coherence with all the other channels. Since the channel pairs have been arranged in increasing numbers for the first of the two in the pair, a high-magnitude band results in the plot whenever a high-coherence channel is part of the pair.

Finally, as was the case for the power spectra, the observed patterns in the average coherence were also found to be fairly consistent across various behavioral task conditions.

5.3 Correlates of learning and interference in the LFP power

As I mentioned at the start of this chapter, this analysis is still under progress. In this section, I present some of the interesting preliminary results. As a first step, I tried to visualize the LFP spectrum for each channel across all sessions. To do this, I computed

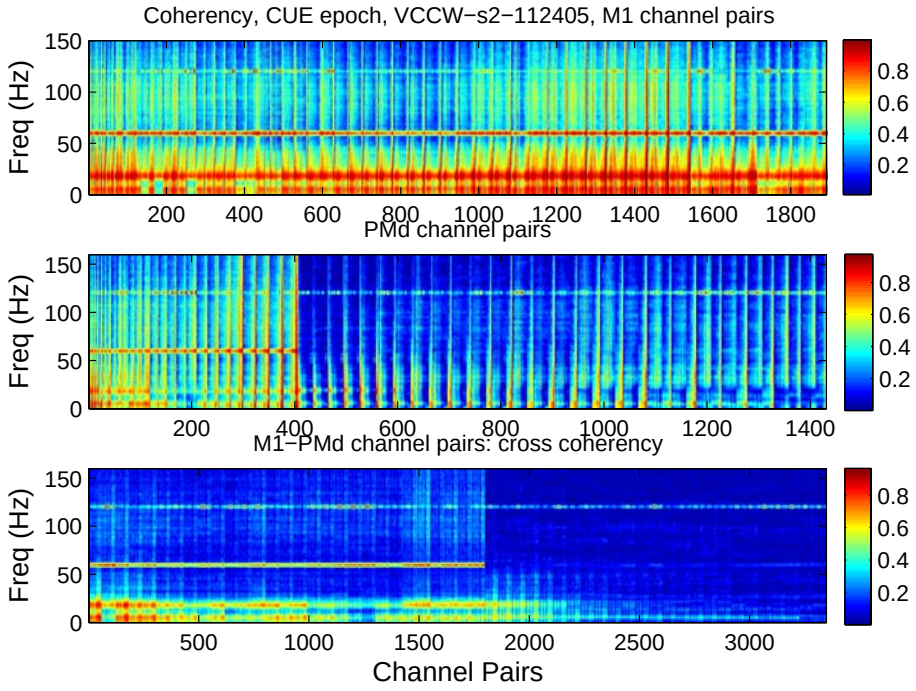

Figure 5.5: Depiction of the LFP coherence spectrum of each channel for session S14 for the first subject in a pseudo-color plot. The coherence has been calculated in the CUE epoch, and has been shown for all channel pairs in M1 (top), all channel pairs in PMd (middle) and all channel pairs between M1 and PMd (bottom).

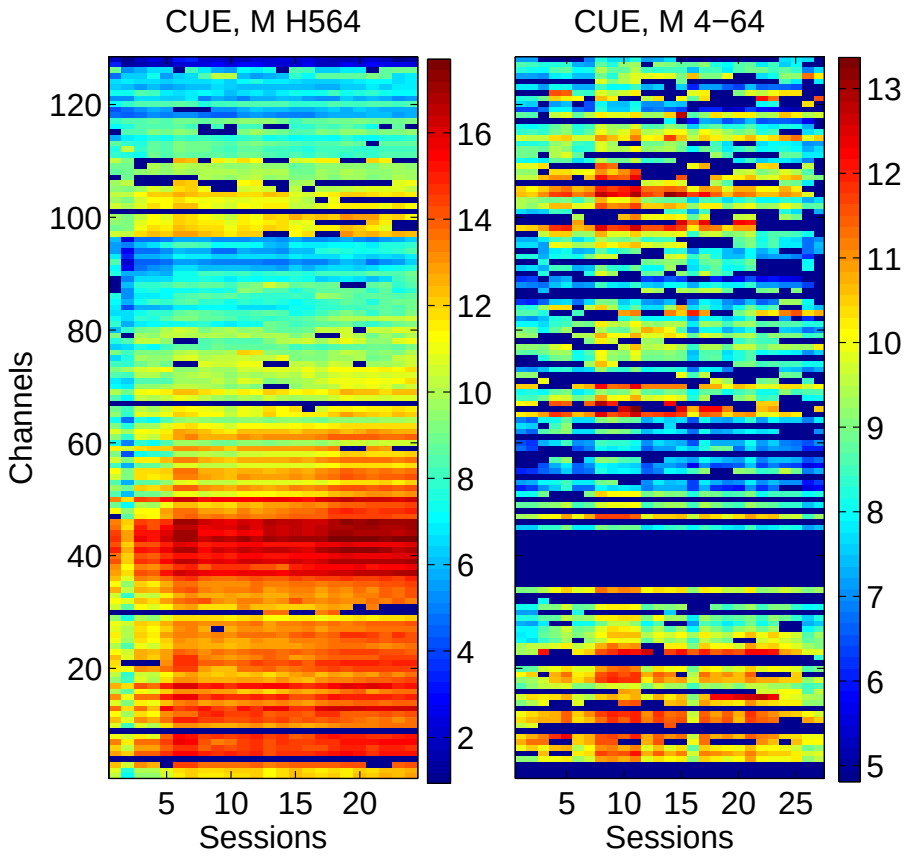

Figure 5.6: The average power in the 15-25 Hz band for the spectra calculated for the CUE period is plotted for all channels across all sessions as a pseudo-color plot. Data for the first subject is shown in the left panel, while the data for the second subject is shown in the right panel. The dark blue bands in the right panel that run through all sessions, denote channel that were not considered for analysis due to excessive noise or other artifacts. As mentioned in Chapter 2 (Section 2.2.6), this number was quite high for the second monkey.

average power in different frequency bands for each channel, averaged these over all the trials in a session and plotted the data as color maps. One example is shown in Fig. 5.6, where I plot the average power in the 15-25 Hz band for the spectra calculated for the CUE period for the first subject (left) and the second subject (right). It can be seen that some channels show an increase in the average LFP power time-locked to the introduction of the forces or soon after it (the forces were introduced in session 4 for the first monkey and session 8 for the second monkey). However, little else can be said from the figure.

In general, this analysis did not yield any strong results as the changes in the average power were not always consistently aligned with the changes in the force fields in the task. Furthermore, most often we simply observed a general increase in power after the introduction of forces (as in Fig. 5.6). This did not provide us with any insight on what was happening around the sessions in which we introduced the interferences. We thought one possible reason could be that averaging power over all trials in a session, was probably not allowing us to detect transient changes in power upon the introduction of the interferences, especially since the changes in behavior were also transient. Therefore, I computed the power spectra of the LFP signal for each trial for each channel. Then, as before, I averaged the power in different frequency bands. Fig. 5.7 shows one example from the first monkey; here I show the average power (the green curves) in the beta band (defined as 16-32 Hz), further averaged over all channels in M1, plotted against the trials around the first introduction of the forces (second session from left). The blue traces overlaid on the same axis denote the measure of the behavioral performance (avg. absolute deviation between actual and ideal paths) for the same set of trials. It can be seen for all four epochs, the average LFP power tends to increase gradually as the hand-path deviation decreases; the effect is a little stronger in the three non-movement epochs as compared to the movement period. Slightly different patterns were observed around the interference sessions. There the changes in the power were usually transient and stronger for the movement period relative to the non-movement period.

Fig. 5.8 shows another example from the same monkey. The data shown in this figure are from the gamma band (70-170 Hz, after taking out $\pm$10 Hz around the line noise harmonic at 120 Hz), averaged over all channels in the PMd, plotted against trials from sessions 19-23. The stiffness field was introduced in sessions 20 and 22, second and fourth from left, respectively. Transient increases in the hand-path deviation can be seen to correspond to transient increases in average gamma band power, most clearly for the movement period, and to some extent for the delay period. Overall, the changes in the power in the gamma band seemed to correlate with the changes in the hand-path deviation, although the results were not always consistent.

While these results seem very encouraging to begin with, our attempts to quantify the relationship between the power and the behavioral hand-path deviation have not been

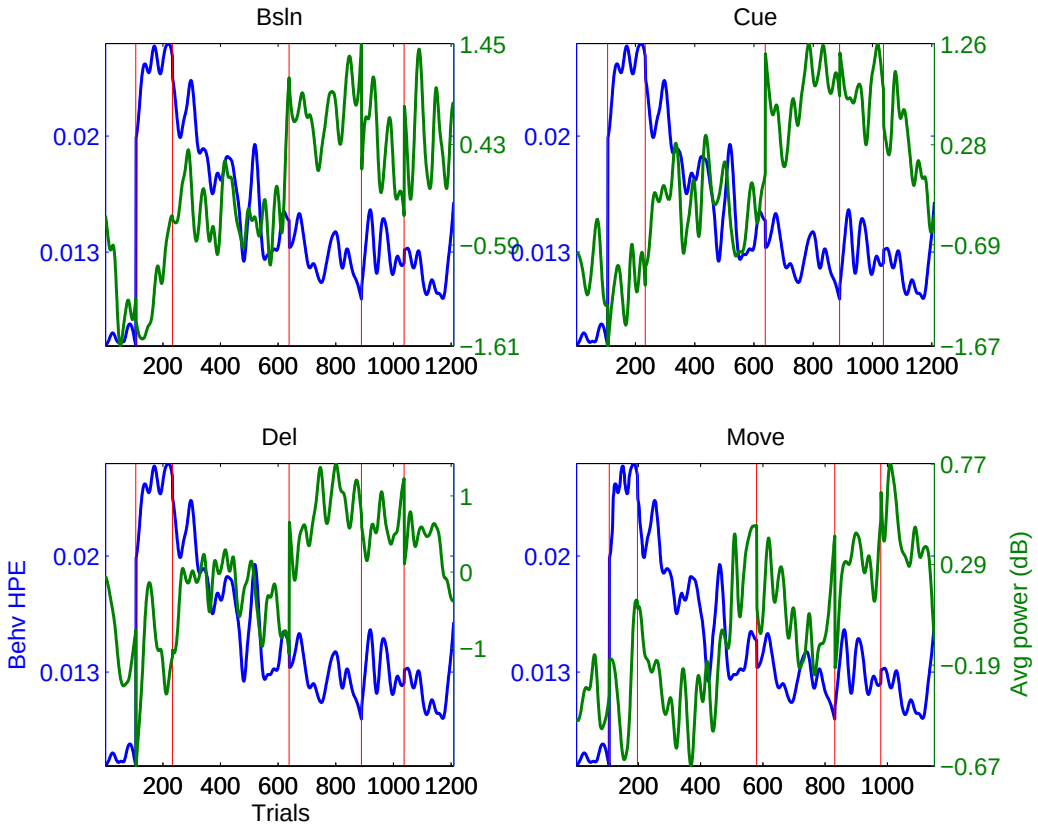

Figure 5.7: The average power (green traces) in the beta-band(defined as 16-32 Hz), further averaged over all channels in M1, is plotted against the trials for sessions 3-8 for each of the four epochs– baseline (or CHT), cue, delay and move. Data is shown for the first subject. The vertical lines denote the session boundaries. The forces were first introduced in session 4, the second from left. The blue traces overlaid on the same axis denote the measure of the behavioral performance (avg. absolute deviation between actual and ideal paths) for the same set of trials. All data have been smoothed using a 55-trial wide Gaussian filter with a standard deviation of 9 trials; note that the smoothing was carried out within individual sessions, so as not to blur the transition from one session to the next.

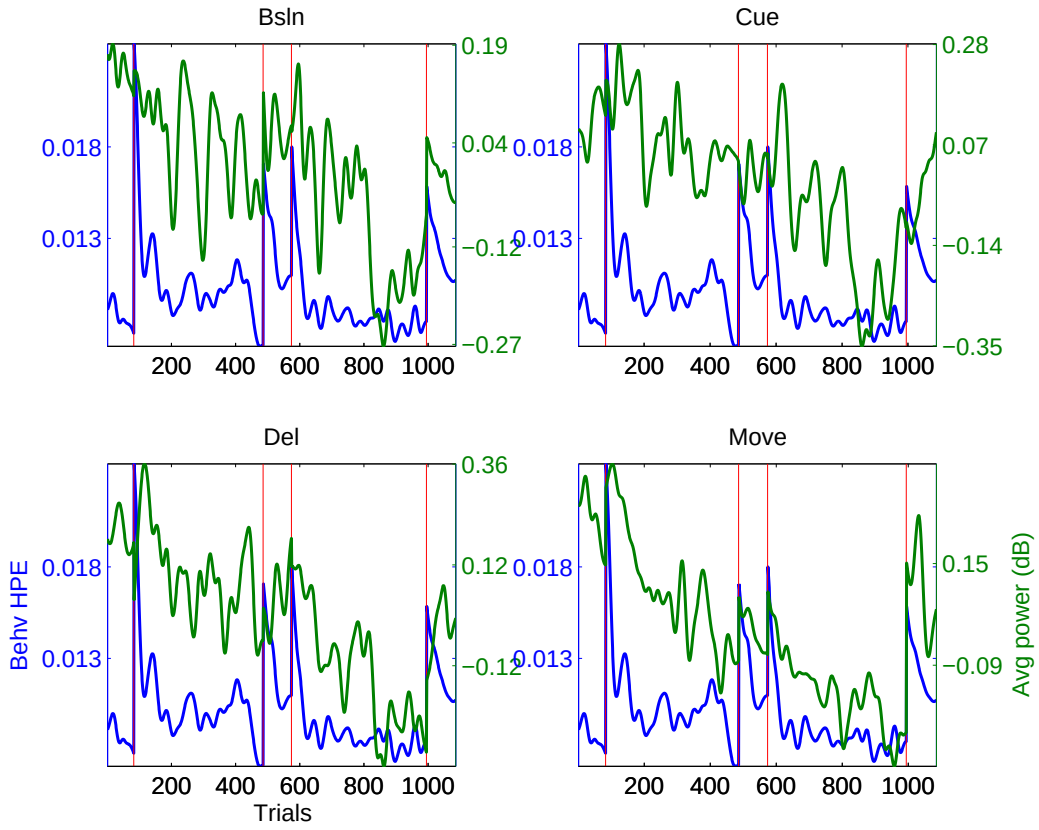

Figure 5.8: The average power (green traces) in the gamma band (70-170 Hz) further averaged over all channels in PMd, is plotted against the trials for sessions 19-23 for each of the four epochs. Stiffness interference was introduced in sessions 20 and 22. Data is shown for the first subject. The blue traces overlaid on the same axis denote the average absolute hand-path deviation of the subject's trajecypries. Same format as Fig. 5.7.

successful so far. The biggest problem was noise in the data, especially for the second monkey (data not shown). Another counfounding observation was the presence of very low frequency "oscillations" in the smoothed data (see the two figures). These oscillations are particularly perplexing because they occur in average power measures across trials (not in time within trials. It is quite possible that they are an artifact of smoothing, but it is not possible to compare these with the raw data as the latter is extremely noisy. We tried a rectangular filter instead of a Gaussian, but still observed the oscillations in a large majority of cases. My attempts at calculating correlation coefficients and modeling the data in some ways (e.g. calculating the covariance function of the pre-whitened data) led to results that were not consistent acros all conditions, partly because a large number of conditions. It is possible that it is not appropriate to average over the channels, especially considering the differences in the average power that I demonstrated earlier in the chapter, but considering each channel separately further increases the dimensionality of the problem, in addition to making the data noisier.

In summary, my preliminary conclusions from these analyses are that the power in the beta-band tends to increase gradually as the subject learns force fields for the first time, implicating this increase in power in the acquisition of novel motor skills. Furthermore, for the rest of the interferences, the power in the beta and gamma bands tends to show transient increases corresponding to the transient increases in the behavioral hand-path deviation.

Chapter 6

Off-line Decoding of End-Point Forces Using Neural Ensembles: Application to a Brain-Machine Interface

In this chapter, I deviate a little from the primary focus of this thesis to discuss some of our results concerning decoding of instantaneous end-point forces exerted by the monkey subjects from the activity of simultaneously recorded ensembles of single neurons. I present these results in the context of brain-machine interfaces (BMIs). BMI is an umbrella term for the technology in which the motor behavior decoded from the neural activity in real-time is used to control an external electro-mechanical device. This area of research aims to develop prosthetic devices for the rehabilitation of patients who suffer from limb paralysis or loss due to neurological disease or traumatic injury. The implementation of BMI technology (for reviews see Fetz, 2007; Schwartz et al., 2006; Schwartz, 2004) has been viewed as one of the more exciting recent developments in the application of neuroscience to rehabilitation medicine. Recent technological advances in neural recordings have provided a significant boost to BMI technology and several human clinical trials are currently under way (Hochberg et al., 2006; Patil et al., 2004; Ojakangas et al., 2006).

Current BMI technology has developed to the extent that rudimentary control of a prosthetic device (e.g. opening and closing a gripper attached to an artificial hand) is now possible in human subjects (Hochberg et al., 2006), and much more sophisticated trajectory and grip control has been achieved in the non-human primate (Taylor, Tillery, and Schwartz, 2002; Santhanam et al., 2006; Velliste et al., 2008). However, almost all of the research in BMIs to date has focused on kinematic (position, velocity) control of the external device (see Kim et al., 2007; Moritz, Perlmutter, and Fetz, 2008; for exceptions).

It is not difficult to appreciate the importance of being able to control the forces applied during the operation of a prosthetic arm. We know from everyday experience that making precise movements requires sophisticated control of movement dynamics, i.e. the various forces that need to be applied to guide the limb along a desired path. In addition, the force requirements of motor behavior change frequently, depending on the interaction of the limb with the environment and the particular behavior being performed. Using the data recorded in our neurophysiological experiment (Chapter 2), we demonstrate the feasibility of off-line extraction of force information from neural signals, with the ultimate goal of making real time ('on-line') control possible.

A recent study by Kim and colleagues (Kim et al., 2007) proposed a method to predict the hand forces off-line and showed that their model could adapt to externally applied force-fields. However, to use their method one would need to have a realistic model of the dynamics of the arm, which may be very cumbersome, if not impossible, to build. Furthermore, it is not always possible to know the various complex interactions among different segments of a real arm under previously unexperienced conditions. Our approach, on the other hand, requires no such model or any other assumptions and can be used to predict forces under very general conditions. Another advantage of our approach is that it is easily extendable and amenable to improvements (e.g. making the process adaptive). Furthermore, we use straightforward methodology which has already been implemented successfully for the decoding of position and velocity. This allows for the seamless integration of the prediction of kinematics and kinetics and facilitates the development of a more holistic BMI.

In the following sections I first describe the application of linear multiple regression and Kalman filter techniques to the prediction of two dimensional end-point forces [i.e., forces applied at the contact point between the effector (the hand, in our case) and the manipulated object]. I next discuss various important aspects of the performance of the algorithms. Finally, I apply the methods to simultaneously decode both kinematics and kinetics, thus demonstrating how the two can be integrated in a straightforward fashion. The data used in this study come from our first monkey subject see Chapter 2 and Table 2.1).

6.1 Analysis methods

The force and position data analyzed in this study were taken between the movement onset (defined as the time of leaving the center circle) and the end of the movement (defined as the time of entering the target circle). Median movement durations were about 600ms. The neural data were taken over a variable-duration window that was aligned at different lags with the start of the behavioral data. Details of the neural data window are given

where applicable in the Results section. For this study, we used data from 4 recording sessions, three when the monkey was performing under a viscous counter-clockwise field (VCCW; sessions S9, S14 and S24)) and one under a stiffness clockwise field (SCW; session S20) (see Table 6.1). We selected these sessions because they had a reasonably large number of correct trials and the monkey's behavioral performance was stable (such that there was not a big change in his hand-path deviations) during the session. The data sets were recorded at a time when the monkey had had only a limited prior exposure to the viscous field and no prior exposure to the stiffness field (see Chapter 2 and Table 2.1). It is quite likely that the monkey was not performing at his best under the force fields. We believe this is an appropriate level of performance in which to test BMI applications because, in general, patients are also likely to have sub-optimal performance. In each dataset we have the firing activity of neurons simultaneously recorded from the M1 and PMd. The number of neurons varied from session to session (see Table 6.1).

Table 6.1: Description of the data sets. VCCW viscous counter-clockwise field. SCW stiffness clockwise field.

Force field type	Number of cells M1/PMd	Number of trials
VCCW - 1 (S9)	12/16	159
VCCW - 2 (S14)	23/14	402
VCCW - 3 (S24)	16/11	493
SCW - 4 (S20)	14/7	163

6.1.1 Prediction algorithms

We implemented two different algorithms to predict applied forces from the neural firing rates.

Linear multiple regression

This method has been successfully applied in a number of different studies to reconstruct hand trajectories or velocity from neural firing rates (Averbeck et al., 2005; Paninski et al., 2004; Carmena et al., 2003) and is simply a form of a Wiener filter. In this method we estimate the optimal weighting function, h, which, when convolved with the binned firing rates, $z(k)$, minimizes the squared error of the estimate of the forces applied by the subject, $f(k)$. One such weighting function is obtained for each of the two dimensions, x and y. The convolution formula for one dimension can be written as

$$f_x(k) = \alpha + \sum_{i=1}^{N} \sum_{n=1}^{W} h_{ni}(n)\ z_i(k - n + \tau) \tag{6.1}$$

where α is a constant, W is the filter width in bins, N is the number of neurons, f_x is the x-component of the force and $z_i(k)$ is the firing rate of the cell i in the bin k (see Averbeck et al., 2005, for details). The models can be optimized over the filter widths, W, and lags, τ, with the only constraint that the lags should be negative for a causal system, capable of predicting the forces in real-time. Note that the time lag here is defined as the time difference between the start of the most recent neural activity bin and the time at which the force is predicted.

Kalman filter

One drawback of the above method is that it considers the dependent variable (the applied force, in our case) to be uncorrelated at each time step. Dynamic state models that exploit the correlations between nearby values of the dependent variable have great potential because they use features of the movement that are predictable in their own right, in addition to predictions based on the neural activity. Since the applied force is a continuous and fairly smooth variable, prior values carry information about future values, and incorporating them in the analysis can enhance the power of the prediction. This approach can be formulated using a Kalman filter. The Kalman filter method has been successfully applied for estimating the kinematics of the hand movement, both in an open loop (Wu et al., 2003; Wu et al., 2002) and in a closed loop brain machine interface set-up (Wu et al., 2004). Let $f(k)$ be the force applied by the subject at time step k and $z(k-\tau)$ be the vector of discharge rates of all the neurons ($[Nc \times 1]$, where Nc is the number of cells) at time $(k-\tau)$, where τ is the time lag between the prediction instant of the force and the firing rate, as for the linear regression method above. The state and observation equations, respectively, can then be written as

$$f(k+1) = A\, f(k) + w(k) \qquad \text{and} \qquad z(k-\tau) = H\, f(k) + \nu(k) \tag{6.2}$$

where $w(k)$ and $\nu(k)$ are noise terms. Decoding involves estimating the state of the system, $f(k)$, at the current instant in time. The Kalman filter works iteratively, beginning with an initial guess of the force $f(0)$ from an initial distribution specified by a mean and a covariance matrix. We assumed the noise terms to be normally distributed with zero means and covariance matrices $\mathbf{W}$ and $\mathbf{V}$. An initial estimate of $\mathbf{A}$, $\mathbf{H}$, $\mathbf{W}$ and $\mathbf{V}$ was obtained from the training set of the data and the filter was then recursively applied to the test data set. The details of the method can be found in (Wu et al., 2002). For our model, the force is a two-dimensional vector $[f_x(k), f_y(k)]$, the matrices $\mathbf{A}$ and $\mathbf{W}$ are [2x2], $\mathbf{H}$ is [Nc x 2] and $\mathbf{V}$ is [Nc x Nc], where Nc is the number of neurons. For the four test cases we discuss in this study, the matrix A was observed to be mainly diagonal, with the diagonal values ranging between 0.94 and 0.99, and the off-diagonal ones between (-0.12) and 0.05.

For example, for S14, **A** was [0.96 0.04; -0.10 0.94]. Note that while the linear regression method needs the storage of a window of data to allow decoding at each time step, the Kalman filter explicitly needs only the data in the immediately preceding bin.

6.1.2 Performance evaluation

To evaluate the performance of the prediction algorithms, each data set was divided into 10 disjoint subsets, 9 of which were used to build the model (training data) and the last one was used as the test (similar to 10-fold cross-validation). Each of the 10 subsets was used as the test set once so that we could generate the predicted data values for the entire session. We then calculated the Pearson-correlation coefficient and the mean-squared error (MSE) between the actual and predicted force values over the entire session. The MSE was defined as the sum of squared differences between the actual and the predicted values. To make the MSE values more meaningful and comparable across different sessions, we took its square root and then normalized by the range (maximum minimum) of the force magnitudes (vector magnitude) for each session. We call this measure normalized error (NrmE) and report this value in this chapter. As a reference, the range of force magnitudes was [4.18, 5.02, 4.66, 3.55] for sessions S9, S14, S24 and S20, respectively.

6.2 Results

We first performed a straightforward linear multiple regression to model the x- and y-forces applied by the subject as a function of the binned firing rates of simultaneously recorded cells from the M1 and the PMd. For this regression, we used a filter width of 420 ms (60ms bins and W= 7 bins) and a filter lag, τ, of $-$20ms. The behavioral data was also correspondingly binned into 60ms bins. Table 6.2 (top half) lists the values of the correlation coefficient and the NrmE for the four data sets. It can be seen that the model performed fairly well, with high correlation coefficients and low normalized errors. As an example, the predicted values are overlaid on the actual values in Fig. 6.1 for a particular case. We next used the Kalman filter to do the prediction. The performance of this method is listed along with the linear regression method in Table 6.2. It can be seen that the Kalman filter performs slightly better than the linear regression method. One probable reason for this could be that the Kalman filter is better able to exploit the temporal correlations in the force values; the force values can be seen to be quite smooth in Fig 6.1.

We also performed the prediction at 20ms intervals using data binned into 20ms bins to see if a finer binning would improve the performance. For the linear regression method, the number of bins, W, was increased to 20 for a data window of length 400ms. The results for this analysis are reported in Table 6.2 (bottom half). It can be seen that results with

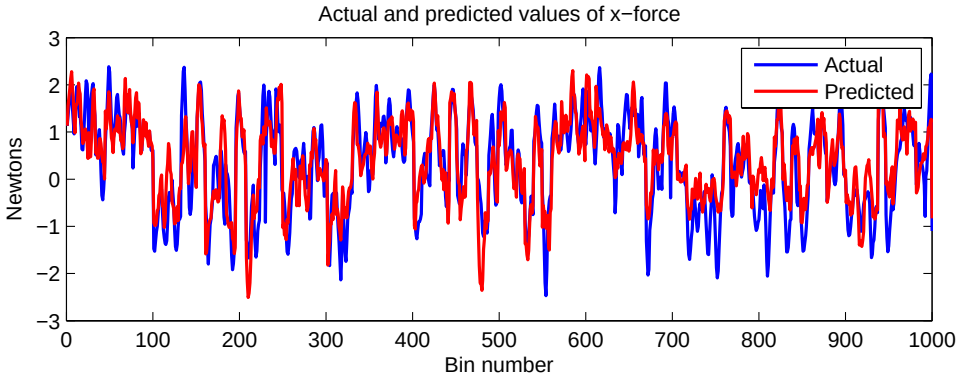

Figure 6.1: The values of the x-component of the force (in Newtons) decoded using the linear regression method (red) overlaid on the actual values (blue) for part of the second data set (S14). The numbers on the x-axis are the bin numbers of the data using 60ms bins (trials have been concatenated).

Table 6.2: The evaluation metrics for the two methods discussed in this chapter, applied to each of the four data sets S9, S14, S24 and S20, reported in that order. F_x- force in x-dimension, F_y- force in the y-dimension. Data for bin sizes 60ms and 20ms are shown.

		Linear Regression				Kalman Filter			
Bin Size 60ms									
Correlation Coeff	F_x	0.73	0.82	0.82	0.67	0.86	0.80	0.86	0.60
	F_y	0.80	0.81	0.73	0.75	0.86	0.82	0.81	0.74
NrmE		0.28	0.22	0.30	0.17	0.23	0.22	0.26	0.19
Bin Size 20ms									
Correlation Coeff	F_x	0.71	0.79	0.78	0.58	0.81	0.77	0.79	0.60
	F_y	0.71	0.79	0.69	0.70	0.82	0.79	0.77	0.70
NrmE		0.27	0.21	0.30	0.18	0.24	0.23	0.29	0.21

20ms bins are qualitatively similar to, if not slightly worse than, those with 60ms bins. As expected, the analysis time was greater with the smaller bin width due to an increase in the number of bins. The bin width becomes an important issue during online control and prediction, because a smaller bin width trades-off response time of the system with smoothness and the time consumed for the analysis. We would like to mention here that we observed that the increase in analysis time for the 20ms bins was much less for the Kalman filter than for the linear regression.

Overall, it can be seen that both methods are able to predict the end-point forces well and that the bin width makes only a small difference. The bin width will be kept fixed at 60ms for the rest of analyses in this chapter and the time lag will be set at -20ms (neural activity preceding the time of prediction, to allow the construction of a causal model),

unless otherwise mentioned (see the next section).

6.2.1 Optimum lag and filter width

We next studied how the performance of the algorithms varied with the lag, τ, between the time at which the force was to be predicted and the time when the neural window began. It would be expected that as the time difference between the neural activity and the current forces increases, the neural signals would carry less and less relevant information and thus the decoding performance would deteriorate. Fig. 6.2(a) plots the performance metrics over a range of positive and negative time lags (-200 to 220ms, in 60ms increments; note that the model becomes non-causal for positive τ, and so can not be used for real-time prediction we have included them in these plots to show the full 'tuning' curve). It can be seen that while the performance of the Kalman filter shows only a modest 'tuning', the linear regression generally tends to show its best performance around a lag of zero milliseconds. Still, the lack of a pronounced tuning is a little surprising and we discuss some possible reasons in the Discussion section. To construct a causal filter, we need a negative lag, and -20ms seems to be the best choice in general.

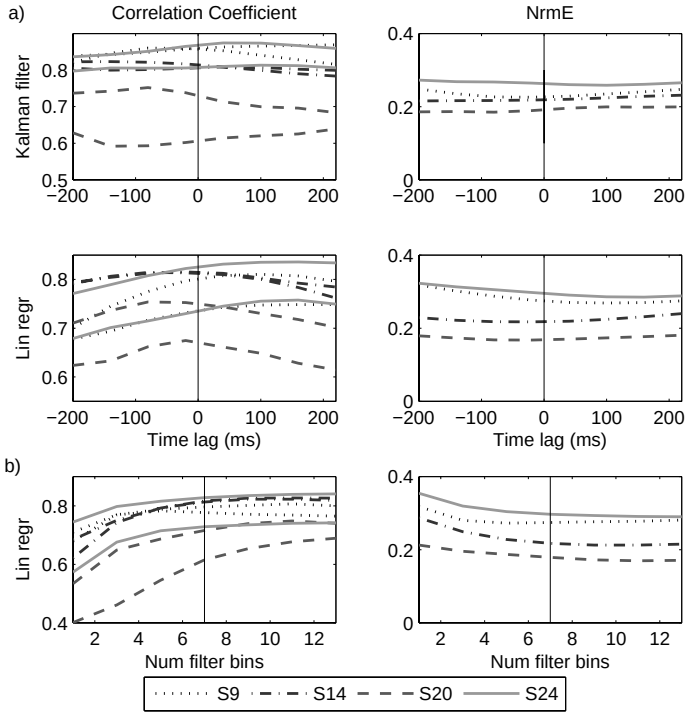

Figure 6.2: (a) Variation in performance with the time lag between the prediction and the start of the neural data window. *First row*, Kalman filter; *second row*, Linear regression. (b) Variation in performance with the length of the filter for the linear regression method. The additional improvement in performance becomes very small after ∼7 bins. All four sessions have been plotted in each sub-figure.

For the linear regression method, we also studied the performance as we varied the length of the filter window (by changing the number of bins, W), with the expectation that the performance would improve as the window becomes larger, eventually reaching a plateau when the new data added would not contain any useful information. As expected, the results in Fig. 6.2(b) indicate that the performance stopped improving after about $W = 7$ bin lengths, which gives a time window of 420ms.

6.2.2 Effect of the number of cells

Previous studies have shown that the prediction performance improves with the number of single cells used in the model (Averbeck et al., 2005; Wessberg et al., 2000). Since the number of single cells that one needs to record simultaneously to achieve a desired performance is an important consideration for the design of a BMI, we evaluated the performance of our model as a function of the number of cells. Given the similar performance of M1 and PMd (see Fig. 6.4 and the next sub-section), cells from both areas were pooled together. We ran the algorithm for 20 different randomly chosen subsets of cells ranging from 1 to 21 in number and then averaged the results over the 20 sets. Fig. 6.3 plots the average results for the Kalman filter (Fig. 6.3a) and the linear regression (Fig. 6.3b). It can be seen that while the linear regression algorithm shows a marked improvement in performance with an increasing number of cells, the Kalman filter showed a relatively flat response, except for session S20. In fact, for sessions S9, S14 and S24, there were statistically significant decreases in the correlation coefficient metric (ANOVA; $p < 0.05$) between sets with one cell and sets with five. However, given the magnitude of this difference (Fig. 6.3), we do not believe that it is of any import. We are not certain about the reasons behind the initial drop in correlation. However, one possibility is that the correlation coefficients are not very reliable when using only one cell to perform the decoding, due to that fact that we have only one predictor variable.

The session that seems to stand out among those that we examined was the one taken during performance in a stiffness force field (S20, field SCW) while the other three were in the viscous field (field VCCW). However, since we do not have more sessions in the stiffness field, it is not possible to ascribe the difference in correlations to the difference in the nature of the force fields alone. Another possibility is that the response to S20 was related to novelty; S20 was the animals first exposure to the stiffness field, while prior to the other three sessions the monkey had already had some practice in the viscous field. However, we tested this possibility on another session, with a viscous clockwise (VCW) force field, which would have also been novel in the context of the VCCW sessions, and found that the results (not shown) did not differ from those for VCCW shown in Fig. 6.3. The final possibility that we considered is that the temporal structure of the stiffness and viscous fields might account for out result. We did find that both the x- and y-components

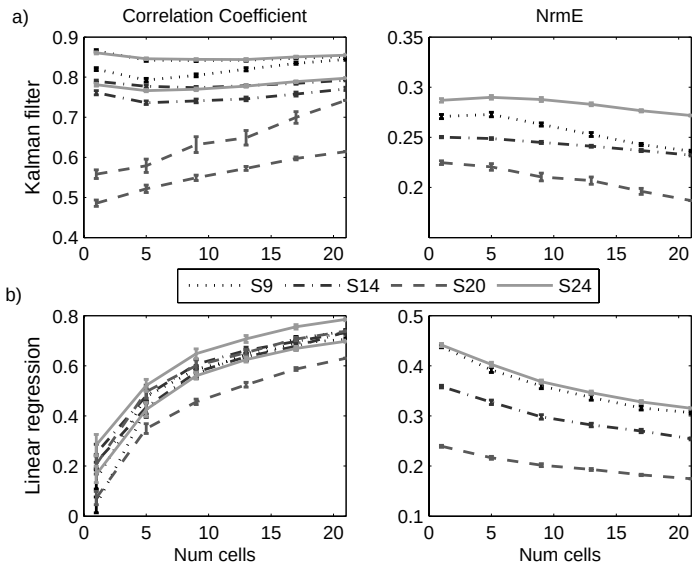

Figure 6.3: Variation in decoding performance for different number of cells (M1 and PMd pooled) using the Kalman filter (a) and the linear regression (b) (averaged over 20 different random subsets of cells data plotted as mean ± SEM). Each shade of gray depicts a different session. In the left column, there are two curves for each session, for the x- and y- components of the force.

of the forces had more temporal correlation (measured by the autocorrelation function) in the viscosity sessions (S9, S14 and S24) compared to the stiffness session (S20). The lag-one autocorrelation was around 0.9 for both the force components for S9, S14 and S24, while it was 0.8 and 0.83 for the x- and y- components, respectively, for S20. This could be one reason why the Kalman filter performs better for the former three sessions.

6.2.3 Predictive performance of M1 versus PMd

The primary motor cortex has traditionally been believed to be the area most involved in the production of forces, while PMd has been assigned a more planning role (Ashe, 1997; Kalaska et al., 1997). If that holds true, one would expect the cells from M1 to better predict the applied forces than those from PMd. To test this hypothesis, we repeated our analyses independently for sets of cells from M1 and PMd. We chose 20 different sets of 7 cells from each area and averaged the results over these sets (for session S20 we had only 7 neurons in PMd [Table 6.1], so to keep the number of neurons constant across sessions and areas we had to restrict our analysis to 7 neurons). A comparison of the decoding performance of the two areas is plotted in Fig. 6.4(a) for the Kalman filter and in Fig. 6.4(b) for the linear regression. As can be seen, neurons from both areas performed similarly overall in predicting the applied forces from the neural activity, with PMd neurons performing slightly better under some conditions. A more detailed

comparison of the decoding performance of the two areas would require data from more sessions, all with similar behavioral performance and force environments.

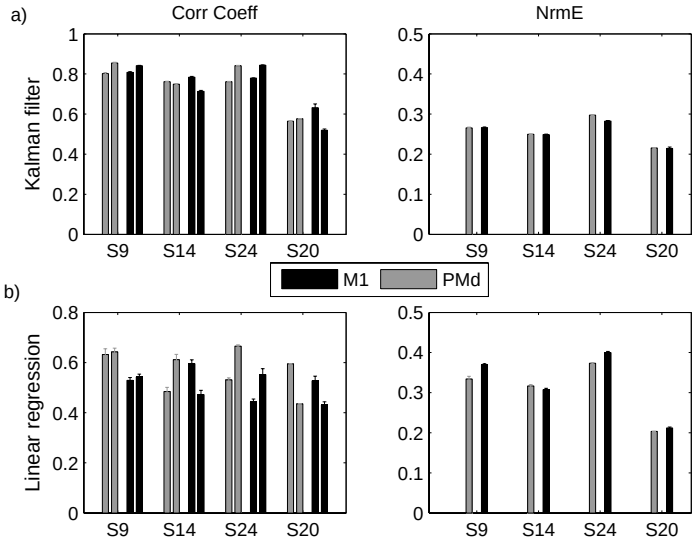

Figure 6.4: Comparison of the predictive performance of the same number of cells (n = 7) from M1 (*black*) and PMd (*gray*), using the Kalman filter (a) and the linear regression (b), for the four sessions (Table 6.1). In the left column, for each area, the right bar is for the x-component while the left bar is for the y- component of the force. Results are shown as mean $\pm$ SEM (the SEM in most cases is too small to be noticeable in the figure).

6.2.4 Generalization to novel force-fields

Since it is unreasonable to expect to be able to train the model with a human subject on all possible movement scenarios, it is important to check if the predictions made by the model generalize to previously un-practiced movements. For example, it would be desirable that a model built under one specific task condition would generalize to novel tasks. To see if this holds for the two methods discussed here, we built our model during a session in the viscous counter-clockwise force field (VCCW) and tested it on a session in the stiffness clockwise force field (SCW) performed on the same day (and vice versa). Note that this session in the viscous field (S19, 76 trials) was different from the three analyzed earlier, because none of those were on the same day as the session in the stiffness field. Fig. 6.5 (top and middle rows) plots the predicted force values overlaid on the actual force values for the x-component of the force, for both methods. The left column is for the case when the viscous field was used as the training data and the stiffness field as the test; the right column shows the opposite case. It can be seen that although the Kalman filter performs reasonably well, the performance of the linear regression is quite poor.

Given the poor performance, we wondered if it would help to update the model after

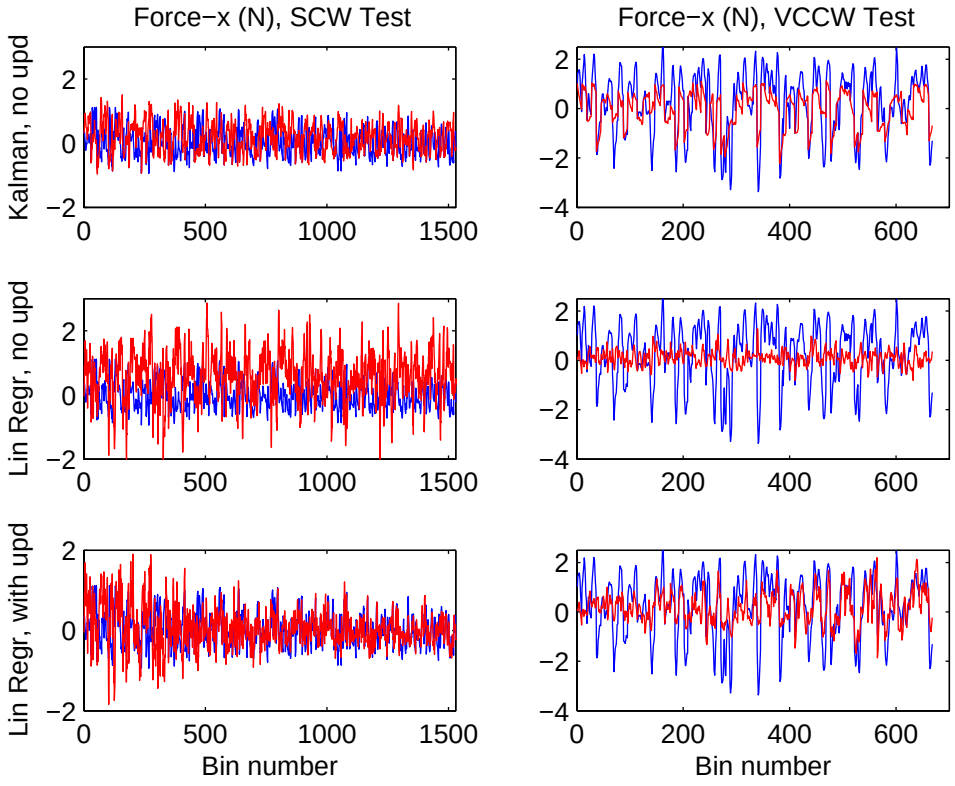

Figure 6.5: Generalization across force fields. The decoded values of the x-component of the force (*red*) overlaid on the actual values (*blue*) for the Kalman filter (*top row*) and the linear regression (*middle row*). All force values (ordinate) are in Newtons. The data in the left column are for the case when the model was trained on VCCW and tested on SCW. The right column plots the opposite case. Trials have been concatenated. The top two rows show data for the cases where the models were not updated; data in the lower row are for the case where the linear regression model was updated at the end of each trial.

every trial of the test set and then apply it to the next trial, which is a kind of crude adaptive method. Indeed, updating the models in this way improved the performance for both methods. As more and more trials are used to update the model, the new field becomes less and less novel, and the performance in the second half was found to be better than in the first. Fig. 6.5 (bottom row) supports these results by showing that although the actual and predicted values started off quite different, they gradually became similar. [Results are shown only for the linear regression method; similar, but smaller, effects were also observed for the Kalman filter.]

To summarize the performance, we evaluated the correlation coefficient and the normalized error for the first and the second half of the data. This is shown in Fig. 6.6(a); the columns 'No Upd' show the case when no updates were performed, while the columns 'With Upd' depict the case when we implemented a trial-by-trial update. The improvements in performance, especially for the linear regression, can be clearly seen from these plots. We also tested for generalization between the VCCW field (S15, 77 trials) and a null field (NF, no forces, S16, 92 trials) and obtained similar results (summarized in Fig. 6.6(b)).

6.2.5 Simultaneous prediction of the trajectory and the forces

For a patient to be able to operate a BMI, we need to be able to decode the desired trajectory of the device as well as the forces that the device will encounter during the motion. While we have shown that we can successfully predict the forces from neural activity, that is not in itself sufficient to allow a patient useful control over a prosthetic device. For that to be possible, we need to be able to predict the instantaneous position simultaneously with the instantaneous forces. We again used the linear regression and the Kalman filter methods to simultaneously predict all four variables from the recorded neural activity. As mentioned in the Introduction, one advantage of our approach is that this methodological and conceptual extension can be made without any change in the structure of the algorithms. Fig. 6.7(a) plots the actual and reconstructed values of the $x-$ and $y-$ positions using the Kalman filter method for part of the session S9 in the VCCW field. The reconstruction can be seen to be in close agreement with the actual values. Similar patterns were observed for the other sessions. As a measure of decoding accuracy, Fig. 6.7(b) shows the histograms of the Euclidean distance between the end-points of the reconstructed and actual trajectories for both the methods studied. The mean end-point errors for the four sessions using the Kalman filter were [2.7, 3.9, 3.8, 2.8] (cm) (for S9, S14, S24 and S20, respectively). The corresponding numbers for the linear regression were [4, 4.6, 4.9, 4.5] (cm) (significantly greater than for Kalman filter, $p < 0.001$, $n = 1217$, the total number of trials over all four sessions [see Discussion for possible explanations of the relatively large errors]).

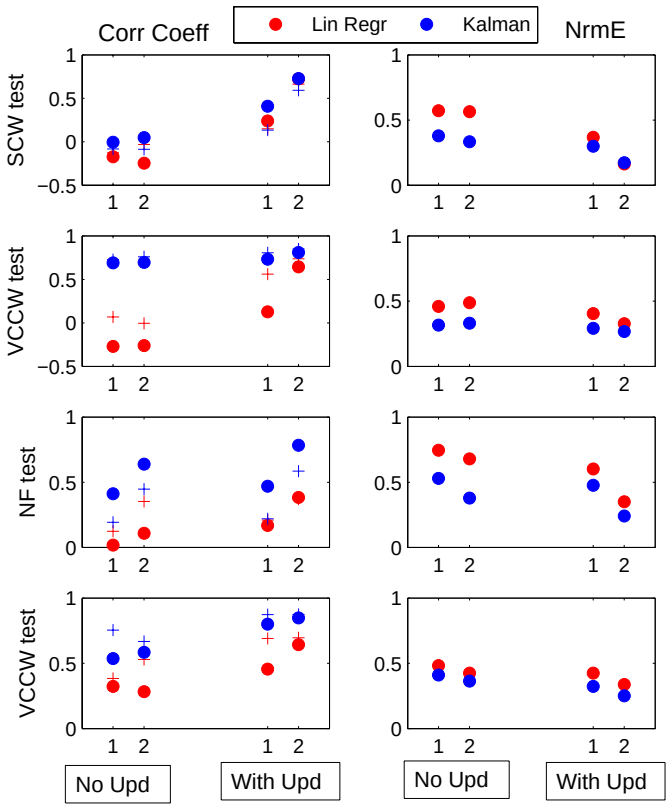

Figure 6.6: Performance evaluation metrics for the test of generalization between a viscous counter-clockwise field (VCCW) and the stiffness clockwise field (SCW) (a) and between a VCCW and a session without any forces (NF) (b). The field on which the algorithm was tested is mentioned on the far left of each row. *With Upd* refers to the case when the algorithm was updated after each trial in the test set, while *No Upd* refers to the case when no such update was performed. The columns with *1* and *2* show metrics calculated for the first and second half of the data, respectively. In the left column, the filled circles are for the x-component and the crosses are for the y-component of the force. Black markers are for linear regression, gray ones are for the Kalman filter.

Furthermore, the correlation coefficient and the NrmE also indicate good performance on average (Fig. 6.8, top row), with the Kalman filter performing better than the linear regression method. We also compared the fidelity of the prediction of forces under the two conditions prediction of only the forces ('Frc only') and simultaneous prediction of forces and position ('Frc simul') (Fig. 6.8, middle and bottom rows). Both algorithms can be seen to work equally well under both conditions. In fact, the Kalman filter shows better performance in the case of simultaneous prediction for the fourth data set (S20, stiffness field).

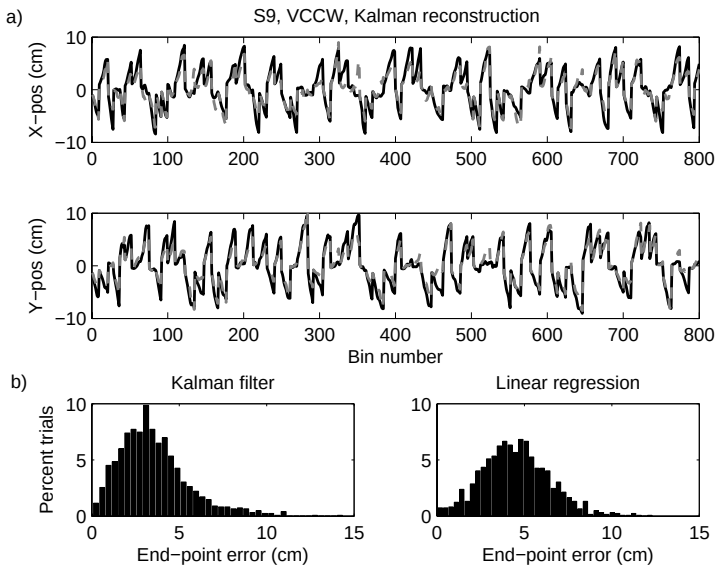

Figure 6.7: (a) Plots of the actual (*black solid*) and reconstructed (*gray dashed*) values of the x-position (*top*) and the y-position (*bottom*) using the Kalman filter for session S9 (trials concatenated). The reconstruction is in close agreement with the actual values. (b) Histograms of the Euclidean distance between the end-points of the actual and the reconstructed trajectories of all four data sets for the Kalman filter (*left*) and the linear regression (*right*.

6.2.6 Is it really kinetics or just scaled kinematics?

The forces we have used in our experiments are dependent on the kinematic properties of the movements, being either proportional to the position or to the velocity. Thus, it is natural to ask if the variable that we decode as 'force' really represents novel kinetics or whether it can be simply derived from the underlying kinematics. We would like to point out that the force variable we are decoding is not the force applied by the manipulandum on the monkey's hand, but rather the force that the monkey applies to control the manipulandum (as measured by the transducers). Therefore, there is no synthetically created correspondence between the force variable and the movement kinematics. Still, it is possible that there exists dependence between the measured kinetics and kinematics. To explore this issue further, we trained our models (linear regression and Kalman filter) to decode the two-dimensional forces, position and velocity during a session in which the monkey performed movements in the presence of a VCCW field (S15, 77 trials). We then tested them on a session performed immediately after, where we turned the forces off (S16, 92 trials). We compared the performance of this kinematic plus kinetic decoder with a decoder that decoded only kinematics (position and velocity). For our analysis, we used the only last fifty trials in the session in which the forces were turned off to avoid including trials that may have possible aftereffects from the previous session in the force field. Furthermore, to keep the number of trials consistent between the two sessions we also used

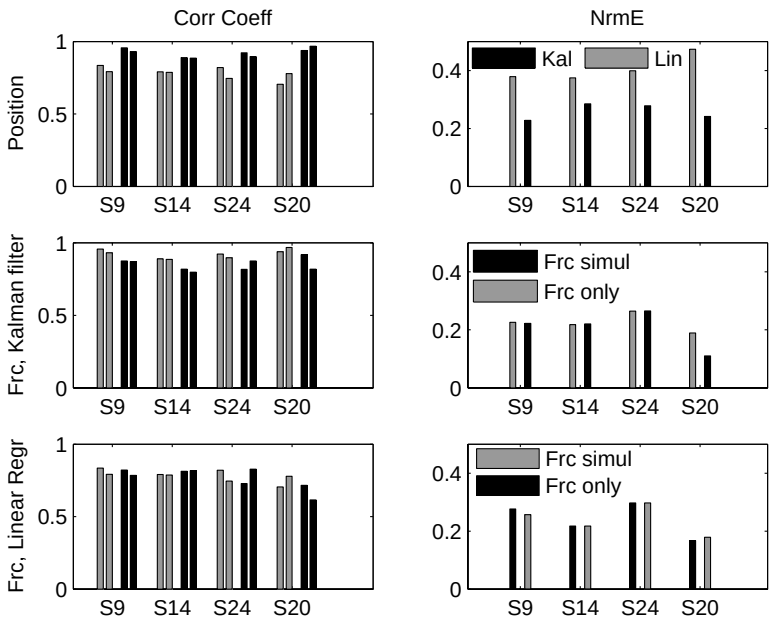

Figure 6.8: Summary of the performance evaluation metrics for the simultaneous decoding of position and force. The left and right columns plot the correlation coefficient and the NrmE, respectively, for position decoding (*top row*, Kalman filter in gray, linear regression in black), for force decoding using the Kalman filter (*middle row*) and for force decoding using the linear regression (*bottom row*). *Frc simul* simultaneous decoding of force and position, *Frc only* only force decoding (data same as in Table 6.2). In the left column of panels, for each color, the right bar is for the x-component of the force, while the left bar depicts the y-component.

only the last fifty trials of the force-field session. For the case of simultaneous decoding using the Kalman filter, the correlation coefficients between the actual and predicted values were 0.88, 0.81, 0.78, 0.64, 0.44 and 0.39 for the x- and y- position, velocity and force, respectively, while the NrmE was 0.26, 0.42 and 0.54. For the case of kinematic decoding, the correlations coefficients were 0.88, 0.81, 0.79 and 0.60 for the x- and y- position and velocity, while the NrmE was 0.28 and 0.42. Thus, it can be seen that a change in the force-field did not affect the decoding accuracy of the kinematics. In addition, we also calculated the quality of kinematic decoding for the session without the forces (S16) using trials from only that session (using cross-validation). The results (not shown) were found to be similar to the two cases discussed above. This suggests that the kinematics and kinetics are, to an extent, differentially represented in the neural signals and represent partially independent information.

6.3 Discussion

Brain-machine interfaces (BMIs) hold promise for restoring limb movements to human subjects with neurological disease or injury. In this chapter, we show that the neural activity recorded from the motor areas in a non human primate can be used to decode end-point forces successfully and with high fidelity, using only simple linear methods. We also show that the models exhibit limited generalizability to novel force environments. Finally, we demonstrate that forces and position can be predicted simultaneously without any degradation in decoding quality. Our results represent a useful extension of the current BMI technology. Below, we discuss various important issues and features of our approach

6.3.1 Decoding performance and choice of parameters

We found that linear methods perform the predictions reasonably well. If this performance level also turns out to be satisfactory for closed-loop BMI control, then it will be possible to keep the computations simple and fast by avoiding the use of non-linear methods. The literature on the decoding of hand kinematics has tried a number of non-linear alternatives and has, by and large, found that linear methods work almost as well as non-linear methods, and at times even outperform them (Averbeck et al., 2005; Kim et al., 2006). We have also demonstrated that accurate decoding did not usually require the use of a long data stream. For example, the useful information for decoding using the linear regression method could be obtained using data in as little as a 420ms time window (Fig. 6.2b). This suggests that one does not need to store a lot of past data when performing decoding in real-time. Furthermore, as expected, the performance of the prediction peaked when the time lag between the prediction point and the neural activity used for the prediction was small (Fig. 6.2a). However, the Kalman filter method did not exhibit a pronounced effect of the time lag on the performance, and even for the linear regression method, the "optimal" lag was not always zero; this is consistent with data showing that each cell may have its own "preferred lag" that may not be zero (e.g. Wu et al., 2002) and the fact that the activity of cells in the motor cortex has been found to usually precede the movement with different lags (Ashe and Georgopoulos, 1994). It is possible that aligning the different optimal lags of each cell may reveal a more pronounced tuning of performance with respect to the lags. Our results showed, as might be expected from previous work on decoding kinematics (Averbeck et al., 2005; Wessberg et al., 2000), that decoding accuracy increased with the number of cells used (Fig. 6.3). However, while the improvement was marked when we used the linear regression, the gains when using the Kalman filter were usually small. As we discussed in the Results section, this could be due to the already good overall level of performance of the Kalman filter. We were also able to integrate force decoding and trajectory reconstruction with little, if any,

degradation in the quality of the force decoding (Fig. 6.8), while simultaneously achieving a relatively good reconstruction of the $x-$ and $y-$ positions (Figs. 6.7 and 6.8). The end-point errors in position may seem large; however, we think that one reason for this could be short trial-times the median movement times for this subject were typically around 600ms (range 300ms to 1sec), which did not give us a lot of data points with 60ms bins. We expect the accuracy of the methods to increase if the trial time is longer (for example during continuous movements rather than discrete ballistic movements). Furthermore, in the context of BMI the decoding would be performed in a closed-loop setting and previous studies have shown a much better performance in closed-loop versus the open-loop case (Taylor, Tillery, and Schwartz, 2002; Carmena et al., 2003).

6.3.2 Decoding using different brain areas

A number of brain areas in the frontal cortex have direct corticospinal projections and contribute to the production and control of voluntary movement (see Porter and Lemon, 1995, for an overview). Classically, M1 has been found to have the densest projections, and is usually thought of as being the primary area involved in motor control, especially in the production of force (Ashe, 1997; Kalaska et al., 1997). This view has been changing recently and a number of studies have found substantial spinal projections from the premotor areas as well (Dum and Strick, 2005). Thus, it is interesting that we found that the cells in the dorsal premotor cortex performed the decoding of force as well as the cells in the primary motor cortex. This lends further support to the idea of distributed control of movement. Furthermore, it suggests that, in the context of force decoding, the exact placement of the electrode array and the exact composition of the cell ensemble may not be very critical when implementing the BMI in a clinical setting. To the best of our knowledge, none of the previous published studies have compared the performance of decoding dynamic end-point forces during reaching movements among cells in different motor areas. In the case of kinematic decoding there have been apparently contradictory results. For example, a study by the Nicolelis group found that although a number of cortical areas can provide signals for decoding position, velocity and the grip force, the neurons from the M1 contribute most to the decoding power (Carmena et al., 2003). Furthermore, Hatsopoulos and colleagues (Hatsopoulos, Joshi, and O'Leary, 2004) found that M1 activity is more suitable for reconstructing two-dimensional movement trajectories, whereas PMd neurons provide a better prediction of the position of discrete visual targets of reaching movements. In contrast, a different study by Nicolelis and colleagues (Wessberg et al., 2000) showed that, compared to M1, significantly fewer PMd neurons were required to achieve the same level of prediction accuracy of one-dimensional hand movements, suggesting that, on average, PMd neurons provide a higher contribution to the predictions (see Hatsopoulos, Joshi, and O'Leary, 2004 for a discussion of possible reasons for this

inconsistency).

6.3.3 Generalizability of the decoding algorithms

An extremely important feature of human motor behavior is its generalizability. When presented with an unfamiliar situation, we usually have some idea of how to perform the desired movement. This is important because we encounter new situations everyday and having to learn and store every situation encountered would be costly and inefficient. In the context of a BMI, it is not possible to train the algorithm with the subject performing movements under every conceivable condition or to build and store a separate model for each such condition. Therefore, ideally one would like the BMI decoding algorithm to generalize to novel task conditions. For example, can a model trained in one force field work well in another? Our results in Figs. 6.5 and 6.6 show that such generalization is reasonable with the Kalman filter, but less ideal using the linear regression. One reason for the better performance of the Kalman filter could be that, because of its iterative nature, it is able to extract and use some information about the new field even when using a model built under the previous force field. Since, linear regression cannot exploit any new information, it might be expected to do worse, especially if the temporal profiles of the applied forces are considerably different under the two conditions. The performance of both methods improves if the algorithm is updated at the end of each trial of the test set (Figs. 6.5 and 6.6). Furthermore, for the Kalman filter method, this regular updating does not cause any significant increase in computational time and thus it should be possible to do this online in the time interval between successive trials in a new force field. In addition, the updating procedure can be relatively brief as one can see improvement in performance in approximately 40-50 trials (Fig. 6.5) after which the updating can be stopped. We acknowledge that this number may represent a lot of trials when switching to a new task in a BMI setting. However, it must be noted that we implemented only a very crude way of adapting the model. Better adaptive methods may make the learning time much shorter (Sanchez et al., 2002; Wolpaw and McFarland, 2004).

The co-ordinate frame used for prediction may also affect the ability to generalize. For example, as an alternative to predicting end-point forces, one could consider predicting joint-torques. The coordinate frame in which movements are encoded in the motor areas of the brain is still a matter of debate, with evidence having been found for a variety of different representations (Kalaska et al., 1997). It is thus quite likely that it should be possible to decode shoulder and elbow joint angles in a manner similar to that for end-point forces. While, in general, we expect both approaches to work equally well under most conditions of operation of a prosthetic arm, the difference between end-point force control and joint-based torque control could be important when it comes to the generalizability of motor learning. Hand-based and joint-based learning have been shown

to have different generalization properties (Malfait, Gribble, and Ostry, 2005; Shadmehr and Moussavi, 2000) and further research is required to determine which is more applicable in the context of a BMI. We believe that another important factor in this regard would be the coordinate system in which the subjects are most comfortable imagining or thinking about their arm movements because that might enable them to more rapidly condition their brain activity associated with the intended movement to the actual movement of the device (Fetz, 2007).

In summary, our study and other recent research (Kim et al., 2007) represent a first step toward decoding applied forces from neural activity in real-time. Our results have a two-fold significance. First, real-time decoding of force and position simultaneously can be carried out as easily in the same algorithmic framework as for each one individually, without requiring additional assumptions or models. Second, simultaneous decoding of position and force does not degrade the quality of either decoded variable.

Chapter 7

Discussion

This concluding chapter carries an extended discussion of the results from our neurophysiological experiment. To begin, I discuss some of the main constraints and caveats of our experimental design. This is followed by a discussion of the behavioral results. Next, I discuss the results from the direction-tuning and the multiple regression analysis for single cells. Finally, I talk about our preliminary findings from the LFP data.

7.1 Methodological issues

One of the major differences between the design of our experiment and previous neural studies was that we examined motor learning as a continuous process over a period of a few weeks, whereas in other experiments each day is taken as an independent sample. While this allowed us an important and different perspective into the learning process, it also created some difficulties. Primary among these was the issue of *stability of the recorded single cells across days*. While there have been some attempts in the literature to develop methods to quantify recording stability across days, to the best of my knowledge very few research articles, if any, have based their analysis on this claim. It might be a few years until investigators begin to independently verify, and then gradually adopt, one or the other of the quantitative methods to show that single cells can be recorded over multiple days in a stable fashion. Therefore, the analyses presented in this thesis were based on the assumption that the cells recorded on different days might well be different. This constrained our single-cell analysis to be performed within a single recording day. As such, the analysis was focused on how the numbers and percentages of single cells showing a particular property changed across days. As I mentioned earlier, this stability constraint created difficulties for us when comparing the direction-tuning properties of single cells between different force-fields (Section 4.3; also see Section 7.3 below). However, the fact that we did have cells that were recorded under two different force conditions allowed us to study the dynamic switching of internal models of different force fields at the level of

single cells (Section 4.4).

The LFPs, on the other hand, are a little more forgiving as they represent aggregate signals from a local population of cells. Therefore, while one can't be sure that the spikes one detects on different days are from the same cell, one can be reasonably sure that the recorded field potentials are from the same region of the cortex. Part of the assurance comes from the fact that the chronically implanted arrays are free to move with the brain, thus minimizing (though not eliminating) relative motion. For the purposes of the analysis in this thesis, I assumed that the LFP signals from a particular channel across the recording days could be treated as a continuous record of the field potentials.

Our experimental paradigm was the same as the basic A-B-A paradigm used in the behavioral studies of motor interference, with a couple of important differences. The first was that we included several days of learning before the subjects experienced the first interference. While this allowed us to investigate the neural activity during the learning process, it also meant that *the monkeys were not as naïve as the humans* in the corresponding experiments. To balance these two issues (extended learning vs. risk of consolidation), we endeavored to introduce the first interference after the subject had demonstrated some behavioral improvement, but before they had apparently completed the "consolidation" of the learning. It is not possible to quantify how much more a subject can learn; therefore we can't be sure of his level of learning before the interference is introduced. However, it must be acknowledged that the human studies also suffer from the same problem.

Second, while the behavioral studies generally introduce just one interference, we introduced three different ones at regular intervals, while allowing the subjects a few sessions in between to "re-learn" the main force field. This approach can cause problems when analyzing the interferences subsequent to the first, as exemplified by the phenomenon called *learning-to-learn*. What this means for our experiment is that while the monkeys adapt to the first force field, they are learning more than just the specific field applied− they are also developing some level of skill in working with forces in general. Furthermore, when they are presented with the first interference, they also develop a general idea about the possible switching of force conditions. This might cause them to be less perturbed, and possibly better prepared, when the second interference is introduced, possibly leading to faster adaptation than if they had been naïve. This should not be problem when analyzing the data in the context of task switching, but it becomes important when analyzing learning and interference. Unfortunately, there does not seem to be a simple way around it, and this caveat must be kept in mind when interpreting our results.

Another potential concern regarding the behavior of the subjects could be a *lack of sufficient practice* in the interfering fields because only one session (and thus a limited number of trials) was presented under those conditions. Our results (Fig. 4.4) suggested

that this could be an issue mainly for the VCW field for the first subject, where the session gets terminated before the subject is able to approach the baseline performance levels. The amount of learning demonstrated by the subjects in the interfering fields is sufficient for the purposed of the studying the adaptation and switching aspects of the task, but it might become an issue when examining interference (beyond the scope of this thesis).

7.2 Behavioral evidence of learning and interference

This brings us to the learning and interference we observed in our subjects' behavior (Fig. 4.4). Our first observation was an increase in the magnitude of the subjects' hand path deviation when the forces were first introduced and for each of the subsequent switching of the force fields (from a familiar to an unfamiliar one, or *vice versa*), indicating that the performance was clearly disrupted by the fields. As expected, the increases were in the direction of the applied forces. Next, during the uninterrupted exposure to the main field (VCCW), the subjects demonstrated a continuing improvement in their behavioral performance (a little less clear for the second subject for reasons mentioned in Section 4.1). Importantly, the improvement was a continuous process with no big gaps between the days (as might have been expected if there was any overnight consolidation of learning). This is crucial because it tells us that it is unlikely that much task-related learning or consolidation happened during the periods when we were not observing the neural activity.

It can also be seen that, for all interfering sessions save one, the subjects were able to achieve baseline performance in a new force-field within just one session. This might seem at odds with the protracted learning observed after the first exposure to forces. Among the interfering fields, the fast learning during the NF 'interfering' session is not surprising, because the subjects were already adept at this condition. The SCW fields turned out to be much easier for the subjects because of its structure (the peak force was at the end of the movement) and also because the peak forces for SCW were less than those observed for VCCW. This was by design, keeping in mind that while the peak forces under VCCW are somewhat under the subjects' control, the same is not the case for SCW. However, the VCCW and VCW fields were identical in all respects except the direction, and indeed, the first subject could not achieve baseline performance by the end of the single session in the VCW force field. That the second subject could do so, could be because he was in general a fast learner. Or it could be due to the learning-to-learn phenomenon discussed in the previous section.

The interference part of our experiment was similar in design to the human behavioral studies dealing with the same issue, and therefore we can compare our results. The focus in the studies adopting the A-B-A paradigm is typically on the force field A on the second

day (call it A2), with the understanding (complemented by observations) that the subject would have "learned" the force fields A (call it A1) and B on the first day. In the three instances of interference in our experiments, we observed worse performance in A2 as compared to A1 (the A just before B). This was reflected not only in the initial increase in the hand-path deviations, but also in a further *gradual* decrease back to the baseline levels, indicating the onset of some 're-learning' (particularly so for the second subject). At first glance our results seem consistent with all the behavioral literature discussed in the introductory chapter (Section 1.5). However, if we look more closely, we realize that the force field A1 for the monkeys (VCCW) is not really the first exposure of the force field A as they have been performing in the same field for several previous days. Our results, then, are at odds with studies that claim complete consolidation after an uninterrupted period of 4-6 hrs after the first exposure to a new skill (Brashers-Krug, Shadmehr, and Bizzi, 1996; Shadmehr and Brashers-Krug, 1997). Instead, our results support one or both of the following hypotheses. First, the learning of force-fields never really gets consolidated to the point of being resistant to disruption. This is consistent with the results of Caithness et al. (2004), who provided evidence that interference occured even when exposures to the conflicting fields were separated by as much as one week. Furthermore, it was shown in that study that, in addition to oppositely-directed force fields, a session of performance without any forces also interfered with the subjects' learning. We also observed the same results after sessions in the null field (S16 for the first monkey and S25 for the second monkey). The second hypothesis is that, whether or not the learning has consolidated, performance in the same field 're-activates' the memory, bringing it into a labile state and thus making it susceptible to interference (Nader, 2003; Nader, Schafe, and LeDoux, 2000). The two hypotheses are tied to each other in a way, because if re-activation can make the memories susceptible again, can anything ever be called consolidated? Whichever of the two hypotheses holds true, it can be said that consolidation is not an absolute phenomenon but, rather, represents a continuous process of stabilization of memories, and is susceptible to interference.

It is also interesting to note that while each of the three conflicting fields disrupts the learning of the main field, the extent of disruption seems to decrease as time progresses (qualitative observation). Again, this could be due to a number of factors: differences in the level of the subjects' learning in the conflicting fields, differences in the characteristics (structure and/or strength) of the conflicting fields themselves, an increasing comfort level of the subjects in working under different forces, or, indeed, a very gradual improvement in the subjects' skill level in the main field (which can be called a kind of consolidation). While we did not attempt to distinguish between these alternatives in this thesis, I would like to remark that we can see some hints that support the last alternative. As I discussed at the end of Section 4.1, and exponential fit to the hand-path deviation data from the

main-field sessions of the first subject was found to be decreasing even towards the end of the experiment (see Fig. 4.6). This suggests that despite the interferences, the monkey kept on improving his skill in the main field throughout the experiment.

Finally, the issue could be just with the terminology more than anything else. In the light of our behavioral results, we are led to the following definitions. We would define interference as a partial degradation in the skill level of the subject in the field A (A1), due to a recent exposure to a conflicting field B, such that in an immediately subsequent re-exposure to A (A2), higher intial errors are observed and a period of re-learning is often required to regain pre-interference performance levels. We would define consolidation as a gradual process of skill learning in any new environment that essentially is never complete and is susceptible to transient disruptions by intervening conflicting environments. The possibility of a gradual decrease in the level of susceptibility with increasing time and practice seems a likely (and a practical) one, but in my opinion, still awaits conclusive evidence.

7.3 Lack of systematic changes in the direction-tuning properties of single cells

In the early 1980s, when Georgopoulos and colleagues (Georgopoulos et al., 1982; Georgopoulos, Schwartz, and Kettner, 1986) discovered the broad, but highly consistent, variations of the firing rates of single neurons in the motor cortex in relation to the direction of motion of the arm, the idea became so influential that for the next decade or more, many investigators believed that the direction of motion was all the motor cortex really cared about, notwithstanding the pioneering studies on motor cortex and production of force by Evarts more than a decade earlier (Evarts, 1968). Later work (for example, Ashe and Georgopoulos, 1994; see Ashe, 1997 for a review) revealed that the cells in the motor cortex also encoded velocity, position, acceleration and force and its derivatives (Georgopoulos et al., 1992; Taira et al., 1996), in addition to direction. Some other studies have found evidence of reprentation of single or groups of muscles and of joint torques in the motor cortex (Kakei, Hoffman, and Strick, 1999; Scott, 2003; Ajemian et al., 2008). The picture has become even more complex, with the cells in motor cortex having been found to encode abstract sequences (Lu and Ashe, 2005) as well as arbitrary color-movement associations that are behaviorally relevant (Zach et al., 2008).

In spite of that, it is still very difficult to find any neurophysiological study of reaching movements that does not talk about direction-tuning of single cells. Our experiment is no exception. While I describe the relation between the cells' firing rate and kinematic and kinetic variables in the next section, in this one I focus on the direction tuning of the cells we recorded. As I have mentioned before, the neural studies of force-field adaptation

by the Bizzi group (Li, Padoa-Schioppa, and Bizzi, 2001; Padoa-Schioppa, Li, and Bizzi, 2004) carried out a detailed examination of the tuning properties of single cells. While they found cells with varied patterns of changes in the preferred direction as the forces came on and off, as a population, the average shift in the preferred direction tended to be in the direction of the applied forces.

Our attempts to repeat that analysis exactly were significantly hampered by the fact that we could not establish the stability of the recordings of single cells over different days. As discussed earlier, one of the consequences of this was that we were limited to single cells recorded in at most two different force sessions on any particular recording day. Because we could not assume that any of the cells recorded over consecutive days were the same, we could not use the session in the familiar force field, after performance in the novel field, as a crucial control (cf. the no-force−force−no-force set-up in the Bizzi studies). This made it difficult for us to ascertain whether any changes that we may observe between the tuning under the two fields were actually task-related or were simply a consequence of the changes in the cells' properties over the course of the day. Furthermore, since we recorded signals throughout a continuous behavioral process, we did not have more than one set of cells that was recorded under identical behavioral conditions. Thus, we could not pool cells across days, and were left with the small numbers of cells recorded during any given day. This gave us very few cells that were tuned under both conditions, especially when we considered only the initial and final few trials (due to non-stationarity of the behavior). To maximize our numbers we divided each session into two halves and compared the tuning properties between them. We found that a large fraction of cells changed their tuning in most of the sessions, even the ones where the force fields did not change. Similar observations were also made in the Bizzi data (Rokni et al., 2007). Thus, we could not interpret these changes as being related to the adptation or switching processes. We also calculated the number of cells tuned under different conditions each day, but did not find any pattern across days that was consistent in both monkeys.

However, we did find some interesting patterns in the quality of fit of a cosine function to the direction-tuning curves. As Fig. 4.12 shows, the R^2 of the fit, on average, showed the most change from the start to the end of the days when the monkeys showed a big improvement in behavioral performance. This result was strongest in M1, but was also present to some extent in PMd. This suggests that the learning process correlates with an increase in the tendency of single-cell tuning to become more cosine-like.

In summary, in contrast to earlier studies, our results led us to the conclusion that changes in direction tuning of single cells do not strongly reflect neural correlates of motor learning and task switching.

7.4 Weighting of task parameters by single cells and their dynamic switching

Single cells in the motor cortex have been found to relate to a large number of motor parameters. We focused on four variables that were important for the performance of our task: direction, position, velocity and force. We adopted the method of Ashe and Georgopoulos (1994) and estimated the relative weight of a task variable from the magnitude of its regression coefficient in a standardized regression. Two interesting results came out of this analysis.

First, the number of cells that seemed to be actively engaged in coding for the force and velocity variables was modulated as a function of the novelty of the task. Thus the percentage of such cells increased whenever the subjects were performing in a new force field. Furthermore, as the subjects' behavioral deviation in the main field decreased, the percentages declined in a similar fashion. This suggests that the motor system may be coping with a new task by 'recruiting' more cells for the job. As the system then gradually acquires the skill, some of the cells are no longer needed and drop out. From the perspective of internal models, our results suggest that when learning a new skill, the motor system either increases the number of cells participating in the models currently being used, or that it simultaneously evaluates multiple candidate models (old or new), before settling down on one or a few. Our data do not permit us to distinguish between the two alternatives. That these patterns were observed only for force and velocity, and not for direction and position could be because, in our task, forces were the novelty and they were velocity-dependent (except SCW). The directional and positional features of the task stayed consistent throughout the experiment.

Second, the relative contribution of each variable toward the firing rate of single-cells was found to be dependent on the current force-field. Thus, the percentage of cells with the force as the most prominent variable (force-cells) was higher when the monkey was performing under the viscous force fields, relative to other fields. Similarly, the percentage of position-cells increased during performance in the stiffness field, while the percentage of velocity-cells, in general, was very low except for the sessions without any forces. The percentage of direction cells tended to be much higher than for the other variables and did not seem to change much. This is not surprising, since the changing force-fields should not have changed the importance of direction in the successful performance of the task. It should be kept in mind that on the days we changed the force fields, we recorded cells in the familiar as well as the novel condition. Our observations, then, suggest that when the force conditions change, some single cells change their relative weighting of the relevant task variables. Loosely speaking, one could think of it as paying more attention to the aspects of the task that are important to "get the job done". From the perspective of

internal models, this could indicate that either the cells switch their participation to a new model, or that the current model to which the cell contributes gets tweaked.

It should be noted that the two adaptation mechanisms, enhanced recruitment and changes in relative weights, described in the above two paragraphs are not mutually exclusive. However, the fact that we record from the same set of cells when force conditions change, allows us to make a stronger claim with respect to the second mechanism. Specifically, we can say that single cells show correlates of adaptation by changing their functional properties. Furthermore, this suggests that switching of internal models happens at the level of single-cells as well as in the population as a whole.

A point of comparison is with the work of (Gribble and Scott, 2002). In that study it was shown that some single cells participate in 'internal models' (suitably defined) of viscous fields applied at the elbow as well as internal models of viscous fields applied at the shoulder. Furthermore, changes in activity of individual neurons during multi-joint loads could be predicted (using vector addition) from their response to subordinate single-joint loads. Our results, while being consistent in showing significant overlap of internal models at the level of single cells, significantly extend the results of that study. First, we show that the overlap is very robust and extends beyond just the same field at different joints. Second, we demonstrate that the overlap in the models is likely manifested in the form of shared weighting of multiple task variables at the level of single cells. Finally, we provide evidence that the switching of the 'internal model of choice' of the single cell is achieved by the changing the relative weights of different task variables.

As discussed before, a wealth of behavioral data exists that is consistent with the theory of internal models. However, at present, the neural correlates of such models are not known. Specifically, it is not clear how the models could be represented at the level of single neurons. Our results suggest that some aspects of internal models can be manifested in terms of the weights of different motor variables in single cell's firing rates. In addition to the representation of internal models, it is also not known how the models are acquired and stored and how the controller (brain) switches between them when the task conditions change. Imaging studies have found that parts of the cerebellum, parietal cortex and frontal motor areas show and increase in the BOLD signal when subjects are learning new tasks (Imamizu et al., 2000), presumably via the acquiition of new internal models, or switching between multiple models (Imamizu and Kawato, 2008). However, not much has been said about the neural mechanisms behind adaptation and switching. Furthermore, no previous study has examined these processes in terms of the global representation of movement parameters at the level of single cells. Our results, for the first time, provide possible neural correlates of learning of new internal models and of switching between them by showing dynamic and rapid changes in the relative weights of different motor parameters at the level of single cells.

In the end, a note on our regression model. I used direction, position, velocity and force as the only kinematic and kinetic variables in the model. This seems appropriate as these are probably the most simple (i.e., least complex) and relevant variables of the task. I also tried the regressions after adding the first derivative of force, but the results were less clear (not to say that this was an inappropriate addition). Another factor that has been sometimes used is acceleration. However, instantaneous acceleration is often noisy and its relative importance found in the previous studies (Ashe and Georgopoulos, 1994) has not been very high. Furthermore, since acceleration did not seem to have any direct bearing on the performance in our task, I did not deem it appropriate to include it in the regression. Thus, although our model is likely not perfect, I believe we have been able to capture most of the relevant information.

7.5 Reflection of adaptation in the LFP signal

Local field potentials (LFPs) have gained importance over the last decade or so as a complementary source of information and computation in the brain. LFPs are thought to represent the aggregate synaptic *input* to the neurons, and have often been found to contain information independent of the concomitant *output* responses of single-cells [refs]. While the LFPs in the motor cortex have received a lot of attention in studies on movement kinematics, I do not know of any study that has examined LFP characteristics during reaching movements in force-fields, irrespective of whether the forces were novel or not. Therefore, while we can compare the general characteristics of our LFP signals with the kinematic studies, there is no baseline against which to verify our results in the presence of force-fields. I discuss some of the results and issues in the following.

One of the most striking characteristics that we observed in the power spectrum of the LFP signals was the elevated power levels in the beta band (centered close to 20 Hz) in all the three non-movement periods (center-hold, cue and memory delay) and a complete abolition of this in the movement period. This is consistent with what has been previously reported regarding the LFP signals in M1 as well as PMd (for example, see Rubino, Robbins, and Hatsopoulos, 2006]), as well as other brain areas and also with the vast literature on EEG recordings. The second interesting feature of the power spectra was the increased level of power in the higher-gamma band (70-200 Hz) in the movement period, relative to the power in the non-movement periods. This has also been previously observed in LFP studies of movements. These two features are sometimes referred to as the 'beta-ERD' and 'gamma-ERS', where ERD and ERS, stand for event-related desynchronization and synchronization, respectively.

Intriguingly, the basic shape of the LFP power spectra was, on average, remarkably well conserved across the different force conditions (including the absence of any forces).

This might imply that the force-related response of the motor cortices tends to be reflected more in the output of the areas (as measured via single-cell firing), rather than the input. In this thesis, I have been able to present only some preliminary results relating changes in power to the changes in the behavioral performance.

A different way of the looking at the LFP signals in the frequency domain is by examining the coherence spectra. The coherence spectrum of a pair of channels is defined as the absolute value of the normalized cross-spectrum of the two channels (Eq. 5.1). A high value of coherence at a particular frequency is indicative of a stable phase-locking of the two LFP signals at that frequency. We calculated the coherence spectra of all channel pairs in each area separately, and also for all channel pairs across the two areas (such that each channel of the pair belonged to a different area). The general features of the coherence were found to be similar to that of the power spectra (Fig. 5.4), with increased rest-period coherence in the beta-band and increased movement period coherence in the gamm band. Further, the coherence values tended to be higher for the M1 channel-pairs as compared to the PMd channel-pairs and the cross channel-pairs. And, even the coherence spectra tended to preserve its shape across the different force fields.

Thus, while the features of the power spectrum and coherence spectrum of our LFP data matched what has been observed in earlier studies of movements, there did not appear to be a clear correlate of force fields in the LFP signals. Our initial analysis of the average power of each channel in different frequency bands, further averaged over all trials in a session, and plotted across the sessions recorded, showed some hints of changes in the power levels for some channels in correspondence with the changes in the task conditions. However, those results were not very consistent and prompted us to look at the variation in single-trial power and the corresponding single-trial behavioral measure. As discussed in Section 5.3, results from this analysis were encouraging, but presented their own problems. This is an ongoing analyses at the moment and I cannot make any strong claims yet. Our preliminary results indicate that the power in the beta-band tends to increase gradually as the subject learns force fields for the first time, implicating this increase in power in the acquisition of novel motor skills. Furthermore, for the rest of the interferences, the power in the beta and gamma bands tends to show transient increases corresponding to the transient increases in the behavioral hand-path deviation.

7.6 Conclusions

In this dissertation, I presented our results from two experiments where we studied acquisition of multiple internal models of force fields and rapid switching between them. Our results from the behavioral experiment pointed out limitations in the motor system's ability to simulatneously acquire two conflicting models. We showed that the efficacy of

contextual cues and random presentation in enabling such acquisition does not extend to general conditions.

In our neurophysiological experiment, we investigated the neural mechanisms of adaptation and switching. Our main result was that internal models are acquired via changes in the relative weighting of motor parameter in single cells. Furthermore, rapid switching was accompanied by rapid and dramatic shifts in the parameter weights. On the other hand, we found little correlation between the changes in the direction tuning of single cells and the adaptation and switching processes. We also found systematic changes in the activity of the local fields potential associated with the acquisition and switching of models, though these data are preliminary.

References

Ajemian, R., A. Green, D. Bullock, L. Sergio, J. Kalaska, and S. Grossberg (2008). Assessing the function of motor cortex: single-neuron models of how neural response is modulated by limb biomechanics. *Neuron* 58(3): 414–28.

Ashe, J. (1997). Force and the motor cortex. *Behav Brain Res* 87(2): 255–69.

Ashe, J. and A. P. Georgopoulos (1994). Movement parameters and neural activity in motor cortex and area 5. *Cereb Cortex* 4(6): 590–600.

Averbeck, B. B., M. V. Chafee, D. A. Crowe, and A. P. Georgopoulos (2005). Parietal representation of hand velocity in a copy task. *J Neurophysiol* 93(1): 508–18.

Baker, S. N. (2007). Oscillatory interactions between sensorimotor cortex and the periphery. *Curr Opin Neurobiol* 17(6): 649–55.

Bartholow, R. (1874). Experimental investigations into the functions of the human brain. *Am J Med Sci* 67: 305–313.

Bays, P. M., J. R. Flanagan, and D. M. Wolpert (2005). Interference between velocity-dependent and position-dependent force-fields indicates that tasks depending on different kinematic parameters compete for motor working memory. *Exp Brain Res* 163(3): 400–5.

Bell, C. (1826). On the nervous circle which connects the voluntary muscles with the brain. *Philos Trans R Soc London* 116: 163–173.

Bernstein, N. (1967). *The co-ordination and regulation of movements*. Pergamon Press, Oxford.

Bock, O., S. Schneider, and J. Bloomberg (2001). Conditions for interference versus facilitation during sequential sensorimotor adaptation. *Exp Brain Res* 138(3): 359–65.

Brashers-Krug, T., R. Shadmehr, and E. Bizzi (1996). Consolidation in human motor memory. *Nature* 382(6588): 252–255.

Caithness, G., R. Osu, P. Bays, H. Chase, J. Klassen, M. Kawato, D. M. Wolpert, and J. R. Flanagan (2004). Failure to consolidate the consolidation theory of learning for sensorimotor adaptation tasks. *J Neurosci* 24(40): 8662–8671.

Carmena, J. M., M. A. Lebedev, R. E. Crist, J. E. O'Doherty, D. M. Santucci, D. F. Dimitrov, P. G. Patil, C. S. Henriquez, and M. A. L. Nicolelis (2003). Learning to control a brain-machine interface for reaching and grasping by primates. *PLoS Biol* 1(2): E42.

Cisek, P. and S. H. Scott (1999). An alternative interpretation of population vector rotation in macaque motor cortex. *Neurosci Lett* 272(1): 1–4.

Conditt, M. A., F. Gandolfo, and F. A. Mussa-Ivaldi (1997). The motor system does not learn the dynamics of the arm by rote memorization of past experience. *J Neurophysiol* 78(1): 554–560.

Conditt, M. A. and F. A. Mussa-Ivaldi (1999). Central representation of time during motor learning. *Proc Natl Acad Sci U S A* 96(20): 11625–11630.

Creed, R. S., D. Denny-Brown, J. C. Eccles, E. G. T. Liddell, and C. S. Sherrington (1932). *Reflex Activity of the Spinal Cord*. Clarendon, Oxford.

Criscimagna-Hemminger, S. E., O. Donchin, M. S. Gazzaniga, and R. Shadmehr (2003). Learned dynamics of reaching movements generalize from dominant to nondominant arm. *J Neurophysiol* 89(1): 168–176.

Donchin, O., J. T. Francis, and R. Shadmehr (2003). Quantifying generalization from trial-by-trial behavior of adaptive systems that learn with basis functions: theory and experiments in human motor control. *J Neurosci* 23(27): 9032–9045.

Duchenne, G. B. (1867). *Physiologie des Mouvements*. Bailliere, Paris. (Physiology of Motion, transl. by E. B. Kaplan. Philadelphia: Lippincott, 1949.).

Dum, R.P. and P.L. Strick (2005). Motor areas in the frontal lobe: The anatomical substrate for the central control of movement. In Riehle, A. and E. Vaadia, editors, *Motor Cortex in Voluntary Movements: A distributed system for distributed functions*, pp. 3–48. CRC Press, Boca Raton, FL.

Evarts, E. V. (1968). Relation of pyramidal tract activity to force exerted during voluntary movement. *J Neurophysiol* 31(1): 14–27.

Evarts, E. V. (1981). Role of motor cortex in voluntary movements in primates. In Brooks, V. B., editor, *Handbook of Physiology*, Vol. Sect 1, Vol 2, Part 2, pp. 1083–1120. American Physiological Society, Bethesda, Maryland.

Feldman, A. G., D. J. Ostry, M. F. Levin, P. L. Gribble, and A. B. Mitnitski (1998). Recent tests of the equilibrium-point hypothesis (lambda model). *Motor Control* 2(3): 189–205.

Ferrier, D. (1873). Experimental researches in cerebral physiology and pathology. *W. Riding Lunatics Asylum Med. Rep.* 3: 30–96.

Fetz, E.E. (2007). Volitional control of neural activity: implications for brain-computer interfaces. *J Physiol* 579(3): 571–79.

Flanagan, J. R., P. Vetter, R. S. Johansson, and D. M. Wolpert (2003). Prediction precedes control in motor learning. *Curr Biol* 13(2): 146–50.

Flanagan, J. R. and A. M. Wing (1997). The role of internal models in motion planning and control: evidence from grip force adjustments during movements of hand-held loads. *J Neurosci* 17(4): 1519–28.

Flook, J. P. and B. O. McGonigle (1977). Serial adaptation to conflicting prismatic rearrangement effects in monkey and man. *Perception* 6(1): 15–29.

Fritsch, G. and E. Hitzig (1870). Ueber die elektrische erregbarkeit des grosshirns. *Arch. Anat. Physiol. Wiss. Med* 37: 300–332. (Transl. by G. von Bonin. In: The Cerebral Cortex, edited by W. W. Nowinski. Springfield, IL: Thomas, 1960, p. 73-96.).

Fukushi, T. and J. Ashe (2003). Adaptation of arm trajectory during continuous drawing movements in different dynamic environments. *Exp Brain Res* 148(1): 95–104.

Gandolfo, F., C. Li, B. J. Benda, C. P. Schioppa, and E. Bizzi (2000). Cortical correlates of learning in monkeys adapting to a new dynamical environment. *Proc Natl Acad Sci U S A* 97(5): 2259–63.

Gandolfo, F., F. A. Mussa-Ivaldi, and E. Bizzi (1996). Motor learning by field approximation. *Proc Natl Acad Sci U S A* 93(9): 3843–3846.

Georgopoulos, A. P. (1995). Current issues in directional motor control. *Trends Neurosci* 18(11): 506–10.

Georgopoulos, A. P., J. Ashe, N. Smyrnis, and M. Taira (1992). The motor cortex and the coding of force. *Science* 256(5064): 1692–5.

Georgopoulos, A. P., J. F. Kalaska, R. Caminiti, and J. T. Massey (1982). On the relations between the direction of two-dimensional arm movements and cell discharge in primate motor cortex. *J Neurosci* 2(11): 1527–37.

Georgopoulos, A. P., J. F. Kalaska, R. Caminiti, and J. T. Massey (1983). Spatial coding of movement: a hypothesis concerning the coding of movement direction by motor cortical populations. *Exp Brain Res* Suppl. 7: 327–336.

Georgopoulos, A. P., R. E. Kettner, and A. B. Schwartz (1988). Primate motor cortex and free arm movements to visual targets in three-dimensional space. ii. coding of the direction of movement by a neuronal population. *J Neurosci* 8(8): 2928–37.

Georgopoulos, A. P., A. B. Schwartz, and R. E. Kettner (1986). Neuronal population coding of movement direction. *Science* 233(4771): 1416–9.

Goedert, K. M. and D. B. Willingham (2002). Patterns of interference in sequence learning and prism adaptation inconsistent with the consolidation hypothesis. *Learn Mem* 9(5): 279–92.

Goldscheider, A. (1898). *Gesammelte Abhandlungen II, Physiologie des Muskelsinnes*. Barth, Leipzig.

Granit, R. (1981). Comments on history of motor control. In Brooks, V. B., editor, *Handbook of Physiology*, Vol. Sect 1, Vol 2, Part 1, pp. 1–16. American Physiological Society, Bethesda, Maryland.

Gribble, P. L. and S. H. Scott (2002). Overlap of internal models in motor cortex for mechanical loads during reaching. *Nature* 417(6892): 938–941.

Gupta, R. and J. Ashe (2007). Lack of adaptation to random conflicting force fields of variable magnitude. *J Neurophysiol* 97(1): 738–45.

Hammond, C., H. Bergman, and P. Brown (2007). Pathological synchronization in Parkinson's disease: networks, models and treatments. *Trends Neurosci* 30(7): 357–64.

Haruno, M., D. M. Wolpert, and M. Kawato (2001). Mosaic model for sensorimotor learning and control. *Neural Comput* 13(10): 2201–2220.

Hatsopoulos, N., J. Joshi, and J. G. O'Leary (2004). Decoding continuous and discrete motor behaviors using motor and premotor cortical ensembles. *J Neurophysiol* 92(2): 1165–74.

Hochberg, L.R., M.D. Serruya, G.M. Friehs, J.A. Mukand, M. Saleh, A.H. Caplan, A. Branner, D. Chen, R.D. Penn, and J.P. Donoghue (2006). Neuronal ensemble control of prosthetic devices by a human with tetraplegia. *Nature* 442(7099): 164–71.

Hubel, D. H. (1959). Single unit activity in striate cortex of unrestrained cats. *J Physiol (Lond.)* 165: 559–568.

Hutchison, W. D., J. O. Dostrovsky, J. R. Walters, R. Courtemanche, T. Boraud, J. Goldberg, and P. Brown (2004). Neuronal oscillations in the basal ganglia and movement disorders: evidence from whole animal and human recordings. *J Neurosci* 24(42): 9240–3.

Imamizu, H. and M. Kawato (2008). Neural correlates of predictive and postdictive switching mechanisms for internal models. *J Neurosci* 28(42): 10751–65.

Imamizu, H, S Miyauchi, T Tamada, Y Sasaki, R Takino, B Putz, T Yoshioka, and M Kawato (2000). Human cerebellar activity reflecting an acquired internal model of a new tool. *Nature* 403(6766): 192–5.

Jackson, J. H. (1932). On the anatomical investigation of epilepsy and epileptiform convulsions. In Taylor, J., editor, *Selected Writings of John Hughlings Jackson*, Vol. 2, p. 113. Hodder and Stoughton, London.

Johansson, R. S. and K. J. Cole (1992). Sensory-motor coordination during grasping and manipulative actions. *Curr Opin Neurobiol* 2(6): 815–23.

Johansson, R. S., R. Riso, C. Hager, and L. Backstrom (1992). Somatosensory control of precision grip during unpredictable pulling loads. i. changes in load force amplitude. *Exp Brain Res* 89(1): 181–91.

Johansson, R. S. and G. Westling (1984). Roles of glabrous skin receptors and sensorimotor memory in automatic control of precision grip when lifting rougher or more slippery objects. *Exp Brain Res* 56(3): 550–64.

Kakei, S., D. S. Hoffman, and P. L. Strick (1999). Muscle and movement representations in the primary motor cortex. *Science* 285(5436): 2136–9.

Kalaska, J. F., S. H. Scott, P. Cisek, and L. E. Sergio (1997). Cortical control of reaching movements. *Curr Opin Neurobiol* 7(6): 849–59.

Kalisman, N., G. Silberberg, and H. Markram (2005). The neocortical microcircuit as a tabula rasa. *Proc Natl Acad Sci U S A* 102(3): 880–885.

Karniel, A. and F. A. Mussa-Ivaldi (2002). Does the motor control system use multiple models and context switching to cope with a variable environment? *Exp Brain Res* 143(4): 520–524.

Karniel, A. and F. A. Mussa-Ivaldi (2003). Sequence, time, or state representation: how does the motor control system adapt to variable environments? *Biol Cybern* 89(1): 10–21.

Kawato, M. (1999). Internal models for motor control and trajectory planning. *Curr Opin Neurobiol* 9(6): 718–727.

Kim, H.K., J.M. Carmena, S.J. Biggs, T.L. Hanson, M.A.L. Nicolelis, and M.A. Srinivasan (2007). The muscle activation method: An approach to impedance control of brain-machine interfaces through a musculoskeletal model of the arm. *Biomedical Engineering, IEEE Transactions on* 54(8): 1520–1529.

Kim, S.-P., J. C. Sanchez, Y. N. Rao, D. Erdogmus, J. M. Carmena, M. A. Lebedev, M. A. L. Nicolelis, and J. C. Principe (2006). A comparison of optimal MIMO linear and nonlinear models for brain-machine interfaces. *J Neural Eng* 3(2): 145–61.

Krakauer, J. W., C. Ghez, and M. F. Ghilardi (2005). Adaptation to visuomotor transformations: consolidation, interference, and forgetting. *J Neurosci* 25(2): 473–478.

Krakauer, J. W., M. F. Ghilardi, and C. Ghez (1999). Independent learning of internal models for kinematic and dynamic control of reaching. *Nat Neurosci* 2(11): 1026–1031.

Krakauer, J. W., Z. M. Pine, M. F. Ghilardi, and C. Ghez (2000). Learning of visuomotor transformations for vectorial planning of reaching trajectories. *J Neurosci* 20(23): 8916–24.

Krouchev, N. I. and J. F. Kalaska (2003). Context-dependent anticipation of different task dynamics: rapid recall of appropriate motor skills using visual cues. *J Neurophysiol* 89(2): 1165–1175.

Leyton, A. S. F. and C. S. Sherrington (1917). Observations on the excitable cortex of the chimpanzee, orang-utan and gorilla. *Q. J. Exp. Physiol.* 11: 135–222.

Li, C. S., C. Padoa-Schioppa, and E. Bizzi (2001). Neuronal correlates of motor performance and motor learning in the primary motor cortex of monkeys adapting to an external force field. *Neuron* 30(2): 593–607.

Liddell, E. G. T. (1960). *The Discovery of Reflexes*. Clarendon, Oxford.

Lu, X. and J. Ashe (2005). Anticipatory activity in primary motor cortex codes memorized movement sequences. *Neuron* 45(6): 967–73.

Malfait, N., P. L. Gribble, and D. J. Ostry (2005). Generalization of motor learning based on multiple field exposures and local adaptation. *J Neurophysiol* 93(6): 3327–38.

McGonigle, B. O. and J. Flook (1978). Long-term retention of single and multistate prismatic adaptation by humans. *Nature* 272(5651): 364–6.

Miall, R. C., N. Jenkinson, and K. Kulkarni (2004). Adaptation to rotated visual feedback: a re-examination of motor interference. *Exp Brain Res* 154(2): 201–210.

Miall, R. C. and D. M. Wolpert (1996). Forward models for physiological motor control. *Neural Netw* 9(8): 1265–1279.

Mitra, P. P. and B. Pesaran (1999). Analysis of dynamic brain imaging data. *Biophys J* 76(2): 691–708.

Morasso, P. (1981). Spatial control of arm movements. *Exp Brain Res* 42(2): 223–227.

Moritz, C. T., S. I. Perlmutter, and E. E. Fetz (2008). Direct control of paralysed muscles by cortical neurons. *Nature* [Oct 15; Epub ahead of print].

Mussa-Ivaldi, F. A. and E. Bizzi (2000). Motor learning through the combination of primitives. *Philos Trans R Soc Lond B Biol Sci* 355(1404): 1755–69.

Nader, K. (2003). Memory traces unbound. *Trends Neurosci* 26(2): 65–72.

Nader, K., G. E. Schafe, and J. E. LeDoux (2000). The labile nature of consolidation theory. *Nat Rev Neurosci* 1(3): 216–9.

Ojakangas, C. L., A. Shaikhouni, G. M. Friehs, A. H. Caplan, M. D. Serruya, M. Saleh, D. S. Morris, and J. P. Donoghue (2006). Decoding movement intent from human premotor cortex neurons for neural prosthetic applications. *J Clin Neurophysiol* 23(6): 577–84.

Omlor, W., L. Patino, M.-C. Hepp-Reymond, and R. Kristeva (2007). Gamma-range corticomuscular coherence during dynamic force output. *Neuroimage* 34(3): 1191–8.

Osu, R., S. Hirai, T. Yoshioka, and M. Kawato (2004). Random presentation enables subjects to adapt to two opposing forces on the hand. *Nat Neurosci* 7(2): 111–112.

Padoa-Schioppa, C., C. S. Li, and E. Bizzi (2002). Neuronal correlates of kinematics-to-dynamics transformation in the supplementary motor area. *Neuron* 36(4): 751–7865.

Padoa-Schioppa, C., C. S. Li, and E. Bizzi (2004). Neuronal activity in the supplementary motor area of monkeys adapting to a new dynamic environment. *J Neurophysiol* 91(1): 449–473.

Paninski, L., M. R. Fellows, N. G. Hatsopoulos, and J. P. Donoghue (2004). Spatiotemporal tuning of motor cortical neurons for hand position and velocity. *J Neurophysiol* 91(1): 515–32.

Patil, P. G., J. M. Carmena, M. A. L. Nicolelis, and D. A. Turner (2004). Ensemble recordings of human subcortical neurons as a source of motor control signals for a brain-machine interface. *Neurosurgery* 55(1): 27–35; discussion 35–8.

Percival, D.B. and A.T. Walden (1993). *Spectral Analysis for Physical Applications: Multitaper and Conventional Univariate Techniques*. Cambridge University Press, Cambridge, UK.

Phillips, C. G. and R. Porter (1977). *Corticospinal Neurones: Their Role in Movement*. Academic, London.

Porter, R. and R. Lemon (1995). *Corticospinal Function and Voluntary Movement*. Clarendon Press.

Rao, A. K. and R. Shadmehr (2001). Contextual cues facilitate learning of multiple models of arm dynamics. Number 302.4. Society of Neuroscience Abstr.

Ricci, G., B. Doane, and H. Jasper (1957). Microelectrode studies of conditioning: technique and preliminary results. In *Premier Congres International des Sciences Neurologiques*, pp. 401–415, Snoeck-Ducaju, Brussels.

Richardson, A. G., G. Lassi-Tucci, C. Padoa-Schioppa, and E. Bizzi (2008). Neuronal activity in the cingulate motor areas during adaptation to a new dynamic environment. *J Neurophysiol* 99(3): 1253–66.

Rokni, U., A. G. Richardson, E. Bizzi, and H. S. Seung (2007). Motor learning with unstable neural representations. *Neuron* 54(4): 653–66.

Roller, C. A., H. S. Cohen, K. T. Kimball, and J. J. Bloomberg (2001). Variable practice with lenses improves visuo-motor plasticity. *Brain Res Cogn Brain Res* 12(2): 341–52.

Rubino, D., K. A. Robbins, and N. G. Hatsopoulos (2006). Propagating waves mediate information transfer in the motor cortex. *Nat Neurosci* 9(12): 1549–57.

Saltzman, E. and J. A. Kelso (1987). Skilled actions: a task-dynamic approach. *Psychol Rev* 94(1): 84–106.

Sanchez, J.C., S.P. Kim, D. Erdogmus, Y.N. Rao, J.C. Principe, J. Wessberg, and M.A. Nicolelis (2002). Input-output mapping performance of linear and nonlinear models for estimating hand trajectories from cortical neuronal firing patterns. In *Proceedings of Neural Networks for Signal Processing*, Vol. 2, pp. 139–148.

Santhanam, G., S. I. Ryu, B. M. Yu, A. Afshar, and K. V. Shenoy (2006). A high-performance brain-computer interface. *Nature* 442(7099): 195–8.

Scheidt, R. A., J. B. Dingwell, and F. A. Mussa-Ivaldi (2001). Learning to move amid uncertainty. *J Neurophysiol* 86(2): 971–985.

Schoffelen, J.-M., R. Oostenveld, and P. Fries (2005). Neuronal coherence as a mechanism of effective corticospinal interaction. *Science* 308(5718): 111–3.

Schöner, G. (1990). A dynamic theory of coordination of discrete movement. *Biol Cybern* 63(4): 257–70.

Schwartz, A.B. (2004). Cortical neural prosthetics. *Annu Rev Neurosci* 27: 487–507.

Schwartz, A.B., X.T. Cui, D.J. Webner, and D.W. Moran (2006). Brain-controlled interfaces: movement restoration with neural prosthetics. *Neuron* 52(1): 205–20.

Scott, S. H. (2003). The role of primary motor cortex in goal-directed movements: insights from neurophysiological studies on non-human primates. *Curr Opin Neurobiol* 13(6): 671–7.

Scott, S. H., P. L. Gribble, K. M. Graham, and D. W. Cabel (2001). Dissociation between hand motion and population vectors from neural activity in motor cortex. *Nature* 413(6852): 161–165.

Sergio, L. E., C. Hamel-Paquet, and J. F. Kalaska (2005). Motor cortex neural correlates of output kinematics and kinetics during isometric-force and arm-reaching tasks. *J Neurophysiol* . (Epub).

Shadmehr, R. and T. Brashers-Krug (1997). Functional stages in the formation of human long-term motor memory. *J Neurosci* 17(1): 409–419.

Shadmehr, R., O. Donchin, E.J. Hwang, S.E. Hemminger, and A.K. Rao (2005). Learning dynamics of reaching. In Riehle, A. and E. Vaadia, editors, *Motor Cortex in Voluntary Movements: A distributed system for distributed functions*, pp. 297–328. CRC Press, Boca Raton, FL.

Shadmehr, R. and Z. M. Moussavi (2000). Spatial generalization from learning dynamics of reaching movements. *J Neurosci* 20(20): 7807–15.

Shadmehr, R. and F. A. Mussa-Ivaldi (1994). Adaptive representation of dynamics during learning of a motor task. *J Neurosci* 14(5 pt 2): 3208–3224.

Sherrington, C. S. (1939). *Selected Writings of Sir Charles Sherrington*. Hamish Hamilton, London.

Soechting, J. F. and M. Flanders (1992). Moving in three-dimensional space: frames of reference, vectors, and coordinate systems. *Annu Rev Neurosci* 15: 167–91.

Soechting, J. F. and M. Flanders (1995). Psychophysical approaches to motor control. *Curr Opin Neurobiol* 5(6): 742–8.

Stark, E. and M. Abeles (2005). Applying resampling methods to neurophysiological data. *J Neurosci Methods* 145(1-2): 133–44.

Taira, M., J. Boline, N. Smyrnis, A. P. Georgopoulos, and J. Ashe (1996). On the relations between single cell activity in the motor cortex and the direction and magnitude of three-dimensional static isometric force. *Exp Brain Res* 109(3): 367–76.

Takahashi, C. D., R. A. Scheidt, and D. J. Reinkensmeyer (2001). Impedance control and internal model formation when reaching in a randomly varying dynamical environment. *J Neurophysiol* 86(2): 1047–51.

Taylor, D.M., S.I. Tillery, and A.B. Schwartz (2002). Direct cortical control of 3d neuroprosthetic devices. *Science* 296(5574): 1829–32.

Thomson, D.J. (1982). Spectrum estimation and harmonic analysis. *Proceedings of the IEEE* 70(9): 1055–96.

Tong, C. and J. R. Flanagan (2003). Task-specific internal models for kinematic transformations. *J Neurophysiol* 90(2): 578–585.

Tong, C., D. M. Wolpert, and J. R. Flanagan (2002). Kinematics and dynamics are not represented independently in motor working memory: evidence from an interference study. *J Neurosci* 22(3): 1108–1113.

Velliste, M., S. Perel, M. C. Spalding, A. S. Whitford, and A. B. Schwartz (2008). Cortical control of a prosthetic arm for self-feeding. *Nature* 453(7198): 1098–101.

Wada, Y., Y. Kawabata, S. Kotosaka, K. Yamamoto, S. Kitazawa, and M. Kawato (2003). Acquisition and contextual switching of multiple internal models for different viscous force fields. *Neurosci Res* 46(3): 319–331.

Wainscott, S. K., O. Donchin, and R. Shadmehr (2005). Internal models and contextual cues: encoding serial order and direction of movement. *J Neurophysiol* 93(2): 786–800.

Wessberg, J., C. R. Stambaugh, J. D. Kralik, P. D. Beck, M. Laubach, J. K. Chapin, J. Kim, S. J. Biggs, M. A. Srinivasan, and M. A. Nicolelis (2000). Real-time prediction of hand trajectory by ensembles of cortical neurons in primates. *Nature* 408(6810): 361–5.

Wise, S. P., S. L. Moody, K. J. Blomstrom, and A. R. Mitz (1998). Changes in motor cortical activity during visuomotor adaptation. *Exp Brain Res* 121(3): 285–299.

Witney, A. G., S. J. Goodbody, and D. M. Wolpert (1999). Predictive motor learning of temporal delays. *J Neurophysiol* 82(5): 2039–48.

Witney, A. G., P. Vetter, and D. M. Wolpert (2001). The influence of previous experience on predictive motor control. *Neuroreport* 12(4): 649–53.

Witney, A. G. and D. M. Wolpert (2003). Spatial representation of predictive motor learning. *J Neurophysiol* 89(4): 1837–43.

Wolpaw, J. R and D. J. McFarland (2004). Control of a two-dimensional movement signal by a noninvasive brain-computer interface in humans. *Proc Natl Acad Sci U S A* 101(51): 17849–54.

Wolpert, D. M. and Z. Ghahramani (2000). Computational principles of movement neuroscience. *Nat Neurosci* 3 Suppl: 1212–1217.

Wolpert, D. M., Z. Ghahramani, and M. I. Jordan (1995). An internal model for sensorimotor integration. *Science* 269(5232): 1880–1882.

Wolpert, D. M. and M. Kawato (1998). Multiple paired forward and inverse models for motor control. *Neural Netw* 11(7-8): 1317–1329.

Wolpert, D. M., R. C. Miall, and M. Kawato (1998). Internal models in the cerebellum. *Trends in Cogn Sci* 2(9): 338–347.

Wu, W., M.J. Black, Y. Gao, E. Bienenstock, M. Serruya, and J.P. Donoghue (2002). Inferring hand motion from multi-cell recordings in motor cortex using a Kalman filter. In *SAB02-Workshop on Motor Control in Humans and Robots: On the Interplay of Real Brains and Artificial Devices*, pp. 66–73.

Wu, W., M.J. Black, Y. Gao, E. Bienenstock, M. Serruya, A. Shaikhouni, and J.P. Donoghue (2003). Neural Decoding of Cursor Motion using a Kalman Filter. In *Advances in Neural Information Processing Systems 15: Proceedings of the 2002 Conference*. MIT Press.

Wu, W., A. Shaikhouni, J.P. Donoghue, and M.J. Black (2004). Closed-loop neural control of cursor motion using a kalman filter. *Conf Proc IEEE Eng Med Biol Soc.* 6: 4126–9.

Xiao, J., C. Padoa-Schioppa, and E. Bizzi (2006). Neuronal correlates of movement dynamics in the dorsal and ventral premotor area in the monkey. *Exp Brain Res* 168(1-2): 106–19.

Zach, N., D. Inbar, Y. Grinvald, H. Bergman, and E. Vaadia (2008). Emergence of novel representations in primary motor cortex and premotor neurons during associative learning. *J Neurosci* 28(38): 9545–56.